Final Scientific/Technical Report

Project Title: Catalytic Upgrading of Thermochemical Intermediates to Hydrocarbons

Recipient: RTI International

Project Location: Research Triangle Park, NC 27709 and Lyngby, Denmark

Team Member: Haldor Topsøe A/S

Project Director/Principal Investigator: David C. Dayton

Acknowledgment: This material is based upon work supported by the Department of Energy's Office of Energy Efficiency and Renewable Energy Bioenergy Technologies Office, under Award Number DE-EE0005358.

Executive Summary

A lot of activity in catalytic pyrolysis and hydroprocessing occurred in the past 10-15 years with notable successes and failures; however, very little technical information is available in the open literature from pilot-scale studies such as those performed in this project. Besides, the next step along the technology commercialization pathway is to scale-up the catalytic biomass pyrolysis process, integrate this technology with a hydroprocessing unit, and demonstrate the long-term operation and performance of the integrated process; notably, these were achieved in this project.

RTI International has developed a single-step catalytic biomass pyrolysis process to produce a hydrocarbon-rich bio-crude intermediate. This bio-crude is more thermally stable and has lower oxygen content than conventional biomass fast pyrolysis oil, so it can be effectively and efficiently upgraded with traditional hydroprocessing technology to produce gasoline and diesel. Our partner, Haldor Topsøe, has developed a strategy for hydroprocessing bio-crude intermediates based on extensive catalyst and process development in support of converting vegetable oils and waste greases into high-quality diesel fuel. The goal of the originally proposed project was to demonstrate an advanced biofuels technology that integrates a catalytic biomass pyrolysis step and a hydroprocessing step to produce infrastructure-compatible biofuels. The specific technical goals of this project were 1) to optimize the catalytic biomass pyrolysis process to achieve high degree of deoxygenation, while maximizing the bio-crude production, 2) improve bio-crude thermal stability, 3) evaluate the impact of bio-crude quality in the hydroprocessing step, 4) minimize hydrogen demand of the integrated process, and 5) maximize biofuels yields.

This project showed that it is technically feasible to use non-zeolitic solid acid catalyst to consistently generate bio-crude with 20% oxygen content and that these liquids can be effectively hydrotreated into low oxygen fuel blendstocks. The reproducibility of the small-scale pyrolysis yields at the 1 tonne/day scale is an achievement worth noting and the effect of pyrolysis temperature on biocrude yields and quality was investigated at the pilot scale. Additionally, advanced analytical techniques were used to analyze bio-crude to investigate the effect of process conditions and feedstock on the concentration and speciation of oxygen-containing compounds. Insights into the impact of oxygen content and oxygen speciation on bio-crdue upgrading were also sought. Clearly, more successful upgrading correlated with bio-crudes with lower oxygen content. This was most evident when partially upgraded bio-crude with 55-90% less oxygen compared to the starting bio-crude was blended with straight run diesel and hydrotreated without any noticeable increase in pressure drop across the reactor or any measurable loss of hydrodenitrification (HDN) activity. Minimizing hydrogen demand while maximizing biofuels yield are the desired outcomes for the integrated process.

In summary, several technical challenges remain before catalytic biomass pyrolysis becomes a commercial reality, most notably bio-crude yields and quality still need to be improved. The integrated catalytic biomass pyrolysis hydroprocessing scheme being developed produces intermediates that can be refined for use as drop-in hydrocarbon replacement fuels. From a technology perspective, this advanced biofuel technology produces liquid transportation fuels that can leverage capital expenditures in the existing petroleum refining and distribution infrastructure. From a business perspective, this technology does not face potential market limitations as other nonhydrocarbon biofuels caused by oxygenated blending limitations and fuel certification for light-duty vehicle applications.

Table of Contents

List of Figures

List of Tables

Introduction

The demand for ethanol as an oxygenated blendstock in reformulated gasoline is currently being met with corn ethanol production. Consequently, additional lignocellulosic ethanol production would compete directly for market share with the existing corn ethanol industry unless the demand for fuel ethanol increases in the future. Increasing fuel ethanol consumption is inconsistent with improving vehicle fuel efficieny but can occur by increasing the number of flexfuel (E85) vehicles in the transportation fleet and increasing the ethanol content in reformulated gasoline. In January 2011, the U.S. Environmental Protection Agency (EPA) partially granted a waiver to increase the ethanol content of commerce gasoline to greater than 10 vol% and up to 15 vol% ethanol for use in model year 2001 and newer light-duty motor vehicles (http://www.epa.gov/otaq/regs/fuels/additive/e15/).

A more promising alternative is to develop conversion technologies that produce hydrocarbon-based biofuels that can be processed, blended, and distributed in the existing petroleum fuels infrastructure. Not only does this avoid the oxygenated blend limit for fuel ethanol, it also opens up additional markets beyond fuel for gasoline-powered light-duty vehicles that includes the diesel and jet fuel-powered segments of the transportation sector and the alternatives for petroleum-based products. This aligns with the U.S. Department of Energy's Bioenergy Technologies Office (DOE/BETO) goal of "developing cost-competitive biomass technologies to enable the production of biofuels nationwide and reduce dependence on oil through the creation of a new domestic bioenergy industry" [1].

Pyrolysis is a thermochemical processing option for producing liquid intermediates from biomass that can be upgraded into hydrocarbon fuels. Traditional biomass flash pyrolysis processes have demonstrated a roughly 70% liquid product yield; however, this pyrolysis oil product has limited use without significant upgrading or refining. Unfortunately, the physical and chemical properties of the current fast biomass pyrolysis oils make them unsuitable for integrating into the refinery. Adverse properties of conventional pyrolysis oil include (1) thermal instability and high fouling tendency, (2) corrosiveness due to high carboxylic acid content (pH 2.2 to 2.4, typically), (3) immiscibility with refinery feedstocks, and (4) metals (K, Na, and Ca) and nitrogen content, which foul or deactivate refinery catalysts. As a result, no commercial processes exist to convert these bio-oils into a transportation fuel.

Traditional hydroprocessing, including hydrocracking over solid acid catalysts and hydrodeoxygenation (HDO) in the presence of a catalyst and high-pressure hydrogen, can be adapted for biofuels production. Although both of these processes have the potential for producing hydrocarbon biofuels, it should be noted that both hydrocracking and hydroprocessing are accompanied by the loss of hydrogen (as H_2O) and carbon (as carbon dioxide [CO_2] or carbon monoxide [CO]) from the bio-oil [2, 3]. The relative contribution of HDO and decarboxylation needs to be balanced to optimize hydrocarbon yields while minimizing H_2 requirements. The status of bio-oil upgrading to fuels has recently been reviewed by Elliott [4].

HDO is carried out between 200°C and 450°C with hydroprocessing catalysts traditionally used in petroleum refining—sulfided forms of cobalt-molybdenum (Co-Mo) or nickel-molybdenum (Ni-Mo) on γ-alumina support [3, 5]. For raw bio-oils, the high oxygen content requires roughly 62 kg of H_2 (per dry ton of biomass) for hydroprocessing [4]. At typical process conditions with Co-Mo or Ni-Mo catalysts, however, coke formation during raw bio-oil hydroprocessing is severe, and product yields are quite low. As a result, a two-stage bio-oil upgrading process has been developed. A schematic of this bio-oil upgrading concept is shown

in Figure 1. In the first stage, the bio-oil is stabilized by catalytically removing oxygen at less severe process conditions (< 300°C) [2]. This stabilized oil is then converted into gasoline and diesel in a second, high-temperature stage using typical hydroprocessing process conditions.

Recent studies by UOP LLC, the National Renewable Energy Laboratory (NREL), and the Pacific Northwest National Laboratory (PNNL) have detailed the potential of catalytically upgrading condensed bio-oil into gasoline-range hydrocarbons [4]. UOP and Ensyn have formed a joint venture, Envergent Technologies, LLC, to commercialize a comparable biomass pyrolysis technology that produces renewable power, heat, and transportation fuels (http://www.envergenttech.com).

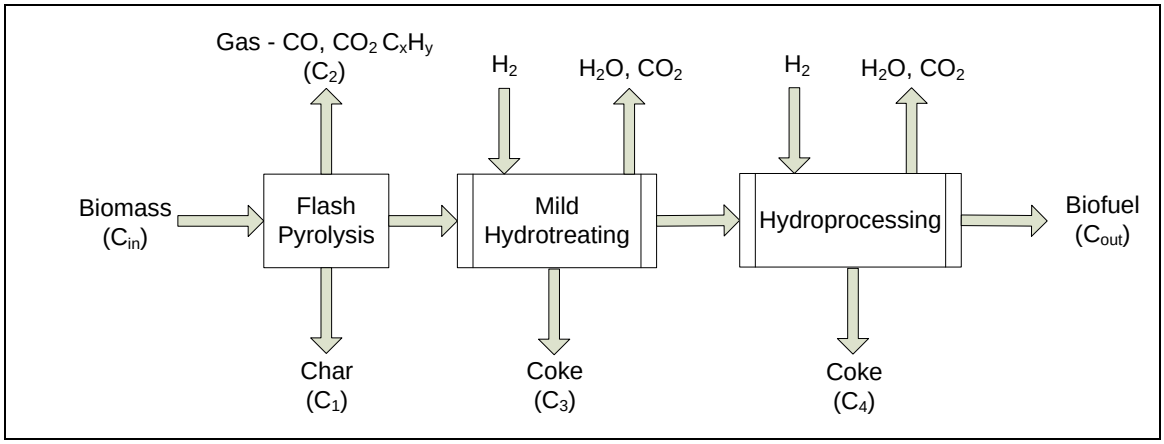

Figure 1: Current state of technology for bio-oil upgrading.

RTI is developing a catalytic biomass pyrolysis process to produce a hydrocarbon-rich intermediate that is more suitable for upgrading with traditional hydroprocessing technology and may potentially be co-processed in a traditional refinery. A block flow diagram of our proposed integrated catalytic biomass pyrolysis with bio-crude hydroprocessing is shown in Figure 2.

This process is similar to the technology demonstrated by KiOR, Inc. (http://www.kior.com) to produce a renewable crude from biomass. The technology is based on traditional fluid catalytic cracking catalysts and reactor designs to produce a deoxygenated hydrocarbon liquid from biomass. Several recent patent applications describe a three stage catalytic biomass pyrolysis process where the first stage "pretreats" the biomass, the second stage deoxygenates and cracks the products from the first stage, and the third stage upgrades the intermediate into fuels and chemicals [6, 7]. Few technical details about this process are publicly available so the conversion efficiencies and losses to coke are not known. Renewable crude yields are on the order of 10-20wt% as claimed in a recent patent [7].

The role of the catalyst in the process is to control the chemistry during biomass pyrolysis to produce a bio-crude that has lower oxygen content and is therefore more thermally stable than conventional biomass fast pyrolysis oil in a single step. This catalytic biomass pyrolysis has the potential to eliminate the need for a mild hydrotreating step or pretreatment to stabilize the liquid intermediate and, therefore, significantly reduce the overall process complexity and capital costs. In an optimized integrated process, the catalytic fast pyrolysis step and the hydroprocessing step need to be carefully balanced to produce a bio-crude intermediate with enough deoxygenation to allow efficient hydroprocessing but resulting in a finished product with higher overall energy recovery than hydroprocessing conventional biomass fast pyrolysis oil. In the current state of technology, bio-oil from fast pyrolysis contains > 40 wt% oxygen [8]. We have demonstrated

bio-crude production from catalytic fast pyrolysis with 40 to 50% less oxygen compared to traditional fast pyrolysis oils.

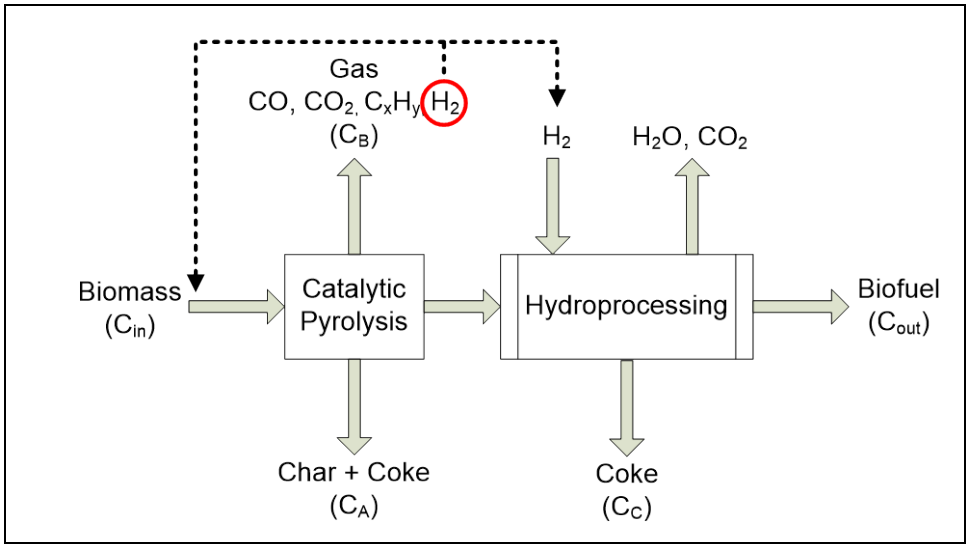

Figure 2: RTI's integrated catalytic pyrolysis process.

Complete deoxygenation can be achieved; however, the more oxygen that is removed the lower the bio-crude yield. Deoxygenation by CO and CO_2 removal (decarboxylation and decarbonylation) plus any carbon losses in the form of coke formation on the catalyst lead to lower hydrocarbon liquid yields and lower energy recovery in the thermochemical intermediate. Therefore, by itself, oxygen removal is not the ultimate goal. The objective is to produce a bio-crude intermediate that is thermally stable and recover as much biomass energy in the bio-crude as possible. The assumption is that bio-crude with lower oxygen content will be more stable because the more reactive oxygen functional groups that lead to re-polymerization will be removed. Any residual oxygen can be removed by HDO during hydroprocessing.

Bio-crude thermal stability is a key physical property because coke formation during hydroprocessing can be significant (~50% or more) [9]. Coke propensity tests and Conradson carbon residue (CCR) measurements (ASTM D 189) are known in petroleum refining and may have some merit in defining bio-oil "thermal stability" or "processability." The CCR measurement involves rapidly heating a weighted quantity of an oil sample and subjecting it to destructive distillation in an inert environment at flame temperatures. The key metric for processing any bio-derived oil is the ability to revaporize the liquid intermediate so it can be introduced into a hydroprocessing unit in a vapor form for upgrading to fuel. The inlet temperature for a typical hydroprocessing unit in a petroleum refinery is between 300 °C and 400 °C.

Material and energy balances were determined for the bio-oil processing scheme represented in Figure 1 and RTI's catalytic biomass pyrolysis scheme depicted in Figure 2. The product yields for the bio-oil upgrading scheme were taken from a PNNL Design Study [8], and the yields for the catalytic biomass pyrolysis process are based on bench-scale experimental results.

This analysis demonstrates that 50% of the input biomass energy can be recovered in the bio-crude from the catalytic pyrolysis process and the overall energy recovery (energy in biomass feed/energy in the finished HC fuel plus energy in hydrogen used in hydroprocessing) is

close to 40%. Energy in these calculations is based on the weight of oil or biomass multiplied by its heating value on the HHV basis. A similar analysis for the traditional fast pyrolysis scheme shown in Figure 1 can be performed. A conservative value of 35% coke formation during heating the bio-oil during hydroprocessing was assumed and the overall energy recovery from biomass to a finished HC fuel is about 20%. This 35% coke formation value is based on a number of experimental studies by Osama and co-workers [2, 3] and Wildschut et al. [10].

This preliminary analysis clearly highlights the importance of developing the catalytic biomass pyrolysis process and the hydroprocessing technology within the context of an integrated process. The integrated process objective is to demonstrate efficient hydroprocessing of the catalytic biomass pyrolysis bio-crude for gasoline and diesel production through optimizing the catalytic biomass pyrolysis process (catalyst formulation and process conditions) to improve the thermal stability of the bio-crude intermediate by removing as much of the oxygen as required for hydroprocessing and tailoring the hydroprocessing catalyst and conditions based on bio-crude properties for maximum biofuels production.

Statement of Project Objectives

Project Objectives

The goal of the project was to demonstrate an advanced biofuels technology that integrates a catalytic biomass pyrolysis step and a hydroprocessing step to produce infrastructure compatible biofuels. RTI International is developing a novel single-step catalytic biomass pyrolysis process to produce a hydrocarbon-rich bio-crude intermediate. This bio-crude intermediate is more thermally stable than conventional biomass fast pyrolysis oil. The project supported the scale-up of this catalytic biomass pyrolysis process to produce large enough quantities of bio-crude for hydroprocessing tests. Our partner, Haldor Topsoe, was able to leverage their extensive commercial experience to identify an optimal hydroprocessing catalyst and process to effectively and efficiently upgrade the hydrocarbon-rich bio-crude intermediate to produce gasoline and diesel hydrocarbon fuels.

The outcome of this project was engineering needed data to design and build a technically viable integrated catalytic biomass pyrolysis process with bio-crude hydroprocessing that maximizes hydrocarbon biofuel output and minimizes H_2 demand. The long term operation of this integrated bench-scale system within the project demonstrated long-term hydroprocessing catalyst stability as a function of biomass feedstock and intermediate bio-crude properties.

Project Scope

The technical goals of this project were 1) to optimize the catalytic biomass pyrolysis process to achieve high degree of deoxygenation, while maximizing the bio-crude production, 2) improve bio-crude thermal stability, 3) evaluate the impact of bio-crude quality in the hydroprocessing step, 4) minimize hydrogen demand of the integrated process, and 5) maximize biofuels yields.

Tasks Performed

Task 1.0: Pilot-scale Catalytic Biomass Pyrolysis

The main objective of this task was to continue the development of RTI's catalytic biomass pyrolysis process. This task supported commissioning of RTI's 1 ton/day (1TPD) catalytic biomass pyrolysis unit, coordination of sufficient quantities of high-impact biomass feedstock for the unit, and production of bio-crude to support the hydroprocessing development in Task 2.

Milestone 1.1 - Extensive physical and chemical characterizations were performed on each of these feedstocks. The analyses included: proximate and ultimate analysis; ash chemical analysis and carbohydrate and lignin compositions.

Milestone 1.2 – Complete 1TPD unit commissioning by demonstrating catalyst circulation under hot conditions, steady biomass feeding at a minimum of 100 lbs/hr, and steady-state catalytic biomass pyrolysis for a minimum of 4 hours.

Sub-Task 1.1: Feedstock Preparation

In year 2, five tons (dry basis) each of two materials, hybrid poplar and switchgrass, were to be prepared and delivered to RTI. The expectation was that the materials will be prepared to reliably and smoothly feed in RTI's feedstock handling and feeding systems. The materials were divided using a pilot-scale rotary splitter and shipped in super sacks such that at least three different subsets of each original whole sample will each be representative of their parent stock. 1,000 kg quantities of these samples were saved and split into representative subsamples for fast pyrolysis and upgrading tests to be conducted as part of BETO's research and development efforts over the next 3-5 years, starting in 2014. Additional quantities of these materials (up to 10 tons each) were sent to RTI upon request to support pilot plant activities in years 3 and 4. Schedule and budget permitting, blended feedstock would also be sent to RTI for catalytic biomass pyrolysis in the pilot plant.

Deliverable 1.1.1 – Five tons of 0.5" top size (minimum) hybrid poplar and switchgrass material with less than 20% moisture content.

Deliverable 1.1.2 – An additional 5-10 tons of 0.5" top size (minimum) hybrid poplar and switchgrass material with less than 20% moisture content to be delivered in Year 3, if needed.

Sub-Task 1.2: Pilot-scale Operation for Bio-crude Production

Commissioning of the 1 TPD catalytic biomass pyrolysis unit was completed so reliable bio-crude production could be achieved. Steady-state operation for continuous production of bio-crude over 12 hours was the initial target with 24/7 operation being the ultimate objective.

As part of the commissioning, temperature and catalyst to biomass ratio were evaluated to determine the balance between deoxygenation and energy recovery (yield) in catalytic biomass pyrolysis. Pyrolysis catalyst performance was monitored after multiple regeneration cycles to estimate catalyst activity loss due to coking, poisoning, and sintering and to determine catalyst attrition losses based on changes in particle size distribution.

The process conditions that produce the most stable bio-crudes with the most efficient energy recovery were identified and gallon quantities of bio-crude were generated for hydroprocessing tests as outlined in Task 2. Bio-crude physical properties such as pH, Total Acid Number (TAN), and viscosity were measured. The chemical composition of the bio-crude sample was also determined. Karl Fischer titration was used to determine water content and a

CHONS (ultimate) analysis was performed on each bio-crude and char sample to obtain mass and element balances. Chemical composition were determined from semi-quantitative GC/MS analysis of the bio-crude sample. Mass closures were determined by combining the solid and liquid compositions with the GC analysis of the permanent gases. The target mass balance was 95% for bio-crude production with less than 20 wt% oxygen.

Deliverable 1.2.1 - Catalytic pyrolysis of loblolly pine will be performed in the 1 TPD pilot plant to initially produce at least 25 gallons of bio-crude with less than 20 wt% oxygen for upgrading studies in Task 2.0. Subsequent samples will be produced as needed for upgrading in Task 2.0 and Task 4.0.

Deliverable 1.2.2 - Catalytic pyrolysis of hybrid poplar will be performed in the 1 TPD pilot plant to produce at least 25 gallons of bio-crude with less than 20 wt% oxygen for upgrading studies in Task 2.0 and Task 4.0.

Deliverable 1.2.3 - Catalytic pyrolysis of switchgrass will be performed in the 1 TPD pilot plant to produce at least 25 gallons of bio-crude with less than 20 wt% oxygen for upgrading studies in Task 2.0 and Task 4.0.

Task 2.0: Hydroprocessing Evaluation and Optimization

The feasibility of hydroprocessing bio-crude samples from the feedstocks selected for this project was assessed. Catalysts were screened to determine if hydroprocessing of these liquids is feasible with the existing catalysts. Hydroprocessing conditions were optimized for maximum carbon conversion efficiency while attempting to minimize pressure and hydrogen consumption. Product distribution between gasoline, naphtha, and heavy fractions was determined with a goal of maximizing diesel-range hydrocarbon production.

Milestone 2.1 – Developing upgrading strategy for RTI bio-crude samples including catalyst selection and initial process conditions.

Milestone 2.2 – Optimized bio-crude upgrading conditions based on long-term hydroprocessing of bio-crude samples from at least 3 different feedstocks.

Milestone 2.3 – Technical evaluation of strategies for co-processing bio-crude/refinery intermediate blends

Sub-Task 2.1 Bio-crude Upgrading and Analysis

A detailed physical and chemical analysis of the bio-crude samples produced at RTI was performed to help define the process operating conditions (T, P, SV, H_2 requirements) for selected hydroprocessing catalysts. The stabilized bio-crudes were analyzed by gas chromatography and for elemental content (C, H, N, S, and O) in addition to using standard methods developed by the American Society for Testing and Materials (ASTM) such as specific gravity (SG) 60/60 (D4052), simulated distillation (D2887), and distillation (D86).

Product quality was characterized by the suitability of the product as a final liquid transportation hydrocarbon fuel that can be blended at up to 30% by weight with ASTM petroleum fuels or as an upgraded bio-oil compatible with existing petroleum refining unit operations. The following analyses were done on the blends: SG 60/60 (D4052), simulated distillation (D2887), distillation (D86), flash point (D93), sulfur content (D5453), CCI (D4737 and D 76), oxidation stability (D2274 accelerated method), and middle-distillate fuel storage stability at 43°C/110°F (D 4625).

Sub-Task 2.2 Bio-crude Hydroprocessing Model Development

The data emerging from pilot testing of bio-crude upgrading and their blends with petroleum streams was to be evaluated through comprehensive modeling that aims at describing the yields, hydrogen consumption, and product properties as a function of catalyst type and process conditions for different types of bio-crudes. This modeling was to be based on a fundamental understanding of how the different groups of bio-crude molecules react under the relevant conditions. Prime objectives in this task were to determine which characteristics of the bio-crude facilitate hydroprocessing and to identify hydroprocessing conditions and catalysts that allow for stable and economical operation.

Task 3.0: Hydroprocessing Reactor Design and Fabrication for Integrated Process Development

The goal of this task was to complete the design, fabrication and installation of a bench-scale hydroprocessing unit for integrated bio-crude production and upgrading at RTI.

Milestone 3.1 – Complete hydroprocessing unit design package, including any modification based on findings from a process hazards analysis.

Go/NoGo Decision Point – Technical review of hydroprocessing unit design and cost analysis prior to start of fabrication.

Sub-Task 3.1: Hydroprocessing Unit Design

A design of a bench-scale (200-mL) hydroprocessing system was developed for installation and operation at RTI to upgrade bio-crude as it is produced in the 1 TPD pilot unit. Once the process flow diagram was finalized, the heat and material balances, vessel sizing, and equipment specifications were verified and detailed in a process design package. This process design package formed the basis of a detailed engineering design to include final reactor design, including a comprehensive equipment and instrument lists, piping and instrument diagrams (P&IDs), electrical wiring diagrams, utility needs, and a system layout. A process control system was also be designed to include all instrumentation and process alarms and safety interlocks identified during a comprehensive safety review of the design package.

Deliverable 3.1.1 – Complete hydroprocessing unit design basis

Sub-Task 3.2: Process Hazards Analysis

A comprehensive process hazards analysis of the hydroprocessing unit design was performed. A Design Hazard Review (DHR) was conducted by a team consisting of an independent facilitator and system design and operating personnel using selected guidewords (temperature, pressure, hydrogen partial pressure, etc.) and applying “What-if” failure scenarios to identify the most likely deviations or failure mode that could result in a potential hazard or operability problem. Only events and/or issues that resulted in a recommendation for an identified hazard or operability problem were recorded for further follow-up consideration by the project team.

Deliverable 3.2.1 – Complete process hazards analysis

Sub-Task 3.3: Fabrication and Installation

The approval for fabrication was granted once the design package was finalized and the Go/NoGo decision point had been passed. An outside vendor was selected for fabrication based on cost and schedule.

Deliverable 3.3.1 – Complete fabrication of hydroprocessing unit for delivery and installation at RTI.

Go/NoGo Decision Point – Commissioning hydroprocessing unit.

Task 4.0: Integrated Bio-crude Upgrading and Process Operation

The 200-mL hydroprocessing unit that was designed and fabricated in Task 3.0 was operated in conjunction with the 1TPD unit to determine advanced biofuel yields as a function of catalytic biomass pyrolysis conditions (process conditions and feedstock) and upgrading conditions. The impact of bio-crude quality (oxygen content, oxygen functionality, and thermal stability) on the hydroprocessing catalyst performance was evaluated. Long-term stability of the hydroprocessing catalyst under steady-state conditions was also investigated.

The bio-crude materials produced in Task 1 were used for upgrading in the hydroprocessing unit. Optimal process parameters (T, P, LHSV) identified during the catalyst evaluation were established, and the performance of the hydroprocessing catalysts identified in Task 2 were verified in the bench-scale reactor system. The duration of the long-term hydroprocessing tests were determined based on the steady-state catalyst performance. The upgrading tests were terminated if steady-state upgrading was achieved for at least 250 hours after an initial catalyst break in period or up to 1000 hours, whichever came first.

The throughput of the 1 TPD unit is sufficient to produce enough bio-crude in 100 hours to supply the hydroprocessing unit for 750-1000 hours. Bio-crude production in Task 1.0 met the demands of the long-term hydroprocessing tests. Additional material was produced as needed. At a maximum, six 100-hour continuous operation campaigns were planned to produce two bio-crude samples from each feedstock for upgrading at RTI and at our partner's facility.

Once this task was completed, bio-crude from three different biomass feedstocks would have been upgraded for a total of 2,000 hours of on-stream hydroprocessing. The overall performance of the integrated process was to be evaluated as a function of temperature, catalyst circulation rate, and biomass-to-catalyst ratio in the catalytic pyrolysis reactor and temperature, pressure, hydrogen partial pressure, and LHSV in the hydroprocessing unit. Additional upgrading of bio-crude blends with refinery intermediates was evaluated. Proof-of-concept tests with blends of bio-crude with refinery intermediates were performed.

Milestone 4.1 – Complete up to 1000 hours of upgrading with loblolly pine bio-crude. Document optimized process parameters for the unit operations in the integrated catalytic biomass pyrolysis/hydroprocessing process and determine biofuel yields and quality.

Milestone 4.2 – Complete up to 500 hours of upgrading with hybrid poplar bio-crude. Document optimized process parameters for the unit operations in the integrated catalytic biomass pyrolysis/hydroprocessing process and determine biofuel yields and quality.

Milestone 4.3 – Complete up to 500 hours of upgrading with switchgrass bio-crude. Document optimized process parameters for the unit operations in the integrated catalytic biomass pyrolysis/hydroprocessing process and determine biofuel yields and quality.

Task 5.0: Process Modeling and Refinery Integration

The goal of this task was to update heat and material balances for RTI's process models for an integrated catalytic biomass pyrolysis/hydroprocessing process with data collected in Task1, Task 2, and Task 4. This process model provides the basis for an economic analysis and life-cycle assessment of advanced biofuel production from this *in situ* direct liquefaction pathway. Measured bio-crude and upgraded product compositions inform refinery integration opportunities for commercial-scale units.

Milestone 5.1 – Design package for a 2000 tpd integrated catalytic biomass pyrolysis/hydroprocessing process.

Sub-Task 5.1: Process Modeling

RTI uses state-of-the-art computational tools, primarily Aspen Plus to develop heat and material balances, process design specifications, and comprehensive process design case studies, as well as to conduct sensitivity analyses and process optimization. The process modeling efforts built on the preliminary commercial-scale designs previously developed to track the economic impact of meeting the technical objectives for this project.

The cost and heat and material balance data generated from integrated Aspen models were used with Excel-based cash-flow models to calculate the cost of HC fuel production in terms $/gal. The integrated Aspen model will be continually updated using experimental data as the technology progresses from proof-of-concept stage to pilot-plant stage to commercial-demonstration stage.

Sub-Task 5.2: Life-Cycle Assessment

A life-cycle greenhouse gas (GHG) analysis and methodology were developed based on the GREET model. Over the course of the project, life-cycle GHG analysis was to be refined and improved. The data for the biofuels production stage was updated as new data became available from the bench-scale integrated process operation. This includes revised estimates for bio-crude yield, hydrogen demand, and finished product yields. In conjunction with our feedstock providers, revised estimates for feedstock production, collection, and transportation were to be incorporated into the life-cycle GHG analysis. In addition, potential opportunities were explored for further reduce life-cycle GHG emissions. This included more complete heat integration and using additional biomass for hydrogen production and renewable electricity generation to eliminate the need for natural gas and purchased power.

Sub-Task 5.3: Refinery Integration

In order to determine the best point to introduce bio-crude into an existing petroleum refinery, the consequences for the refinery operation and product properties must be investigated. This task integrated the results from the bench-scale hydroprocessing tests carried out in Task 2 and the modeling of these data. The model results were used in the techno-economic analysis.

Another objective of the modeling work proposed above was to provide a theoretical basis for evaluating different refinery integration options. The model should be able to give information on how the hydroprocessed bio-crudes compare with these specifications and how the blending with current refinery streams affect the product pool. The different refinery insertion points also give different process conditions under which the pyrolysis oil will be

hydrotreated, and the model should, therefore, also provide some input on the response to operating conditions or a window of conditions that allow for conversion to the desired product.

Milestone 5.2 – Economic analysis of the technical feasibility of co-processing bio-crude and hydrocarbon intermediate streams to define refinery integration options for catalytic biomass pyrolysis technology

Bio-crude Production

Installation and Commissioning of a 1 ton/day (1TPD) Catalytic Biomass Pyrolysis System

RTI designed a 1 ton/day catalytic biomass pyrolysis unit under a DOE/ARPA-E funded project. This project supported the development of the HMI and control system for the integrated unit which was delivered to RTI in April 2013.

The 1 TPD unit was assembled together and all mechanical interconnections between the skids (swagelock and pipe connections) were made. All power connections to the control cabinet were made and wiring for the interconnections between the cabinet and skid junction boxes were completed, checked, and verified. The control system commissioning started in June 2013 and communication was established with all instruments. The mass flow controllers, differential pressure transmitters, level transmitters, and pressure transmitters were also checked and calibrated. All connections were tested and verified in the control system. All pneumatically actuated and pressure control valves and heat tracing were tested and all thermocouples were validated. An example of the insulated piping and vessels is shown in Figure 3.

Figure 3: Example of completed insulation on regenerator bottom and critical flow orifice section (left) and air preheater and regenerator off-gas cooler

Testing and Calibration of the Biomass Feeder

Four tons of loblolly pine sawdust was procured from Iowa State University.The feed conveyer hopper was filled with the loblolly pine sawdust (0.125” top size) and the Flexicon system was tested and calibrated. The calibration results for the 0.125” top-size loblolly pine sawdust are shown in Figure 4. The screw conveyer can be controlled through the control system software and the screw speed was calibrated with the biomass feedrate. The maximum transfer rate is 600 lbs/hr at 100% motor speed. Feed system testing was also performed. The mechanical components of the biomass feeder functioned well and the feedrate was calibrated by varying the dosing screw and feed injector screw speeds independently. The calibration data for the 0.125” top-size loblolly pine sawdust is presented in Figure 5. The speed of the dosing screws and the feed screw were set to the same outputs. The testing showed that the speed of the feeder screw controls the actual feedrate. Also, the sawdust flowed very well so the dosing screws did not significantly affect the feedrate.

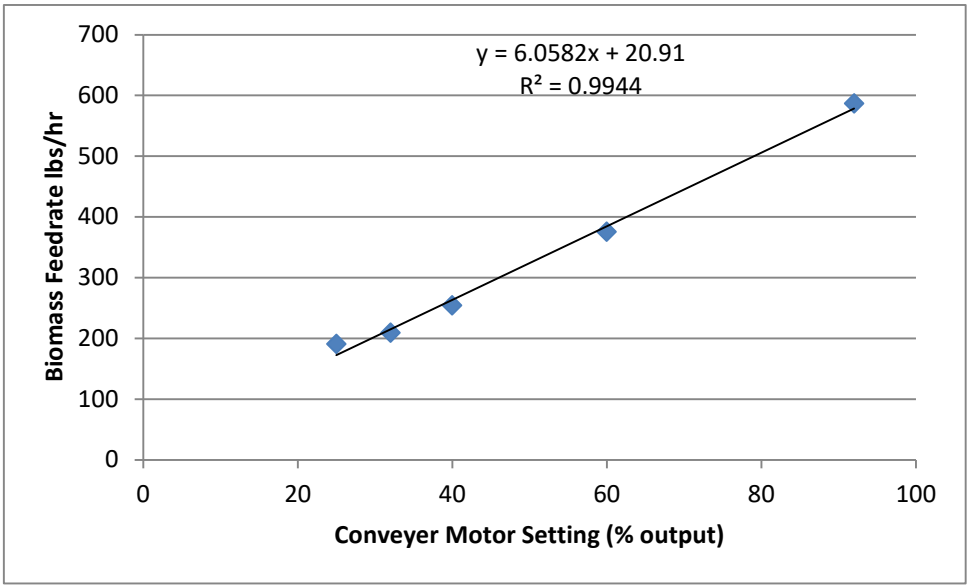

Figure 4: Conveyer Motor Calibration with 0.125" loblolly sawdust

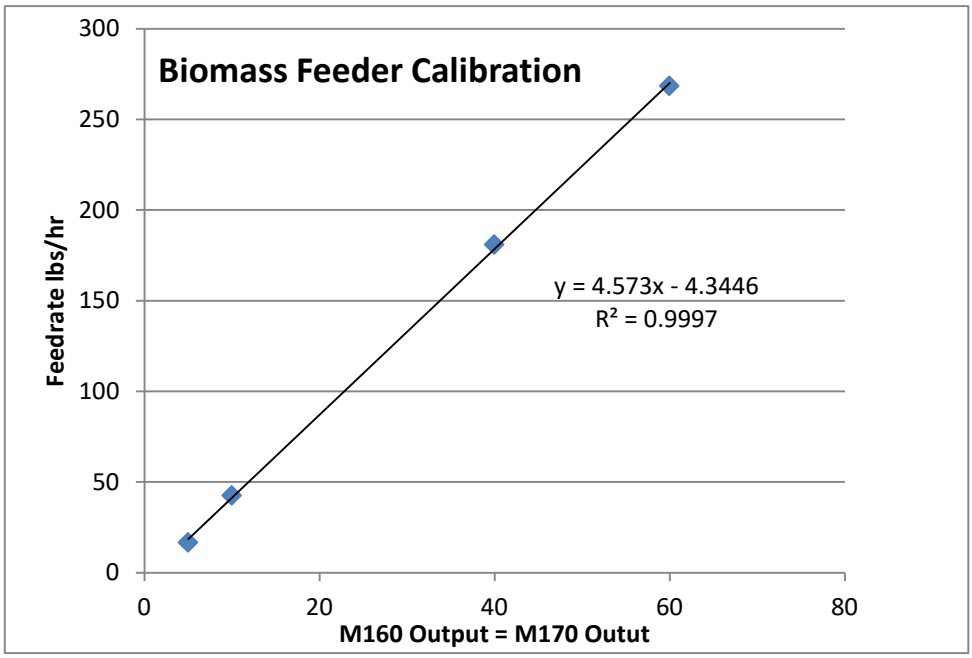

Figure 5: Biomass Feeder Calibration with the Dosing Screw (M160) Speed Equal to the Feed Screw (M170) Speed

Extensive feeder system testing and calibration were performed with hybrid poplar feedstock received from INL. The ground hybrid poplar material was much more fibrous in comparison with the loblolly pine sawdust and posed a greater challenge for continuous, reliable feeding. The material was ground to 0.25" top size and had a bulk density of 13 lbs/ft^3 with 10 wt% moisture. The physical properties of the hybrid poplar require that the dosing screw speed and the primary feeder screw speed are decoupled. With hybrid poplar, the primary feeder screw speed was set to 80% of the full output of the motor and the dosing screws speed was varied between 20% and 40% of the full motor output. A summary of the calibrated feedrates is shown in Figure 6. The data points are cumulative feed weights at a given time. The solid lines are linear fits to the data with the slope being the calibrated federate at a specific dosing screw rate.

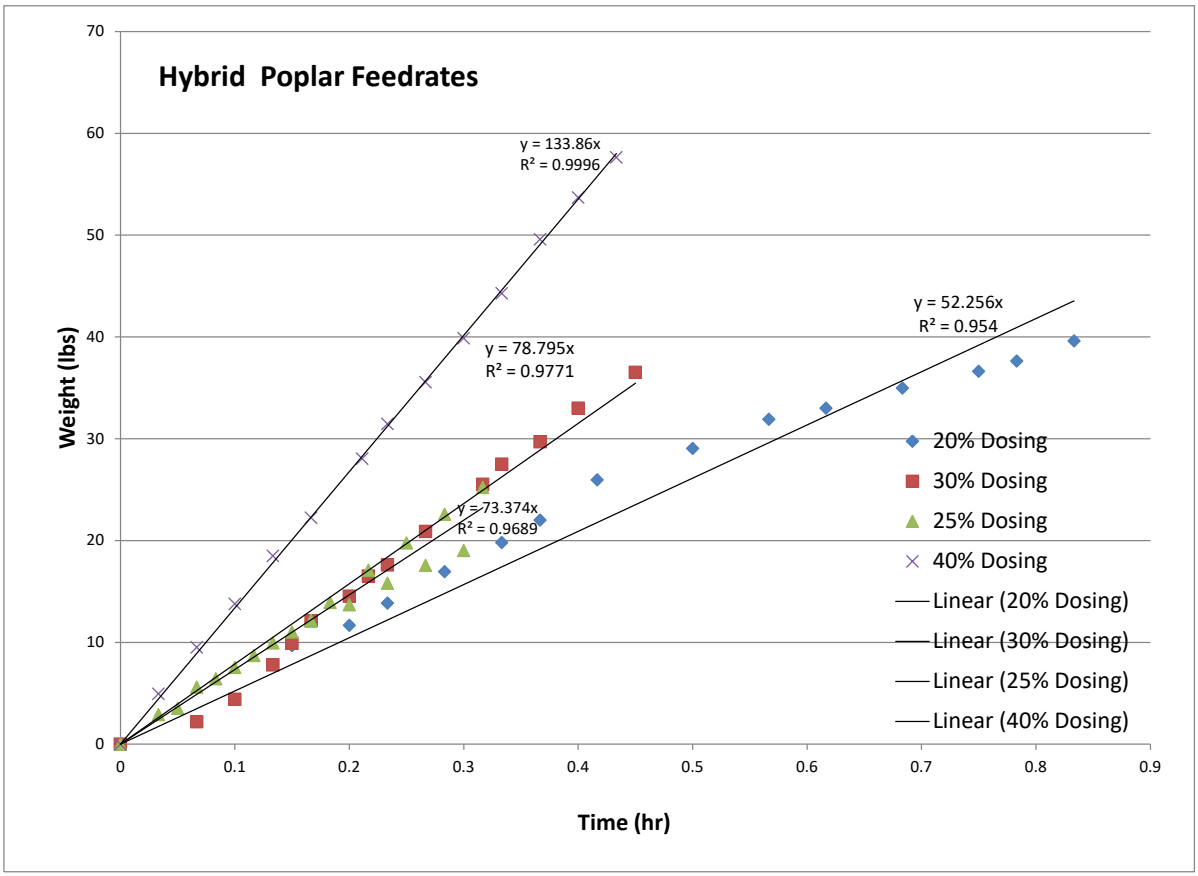

Figure 6: Hybrid Poplar Feedrate Calibrations. Primary feeder screw speed was held constant at 80% of the full motor output and dosing screw speed was varied between 20-40%. Solid lines are linear fits to the data and the slope of the lines represents the federate for a given dosing screws speed.

Cold Flow Catalyst Circulation Test

The objective of the cold flow tests was to validate the catalyst circulation and system operation at ambient temperature and pressure conditions using inert gases. The cold flow tests were also helpful in identifying process variables that can be used to change the rate of catalyst circulation. Some of these process variables are identified as below:

- Set point for differential pressure between regenerator and reactor effluent
- Conveying gas flow rate through mixing zone
- Aeration across orifice plate

A schematic of the catalyst circulation loop is shown in Figure 7. Air is fed to the regenerator to fluidize the catalyst and as the oxidizing medium during pyrolysis experiments. Fluidized catalyst from the regenerator is transferred to the reactor mixing zone through the orifice standpipe. Nitrogen is fed at the bottom of the mixing zone to maintain fluidization of the catalyst. In the absence of pyrolysis product vapors, additional nitrogen is added as lifting gas which conveys solids through the mixing zone and riser sections of the reactor and feeds into the reactor cyclone. The catalyst separated in the cyclone is returned to the regenerator through the loop seal. The catalyst in the orifice standpipe and loop seal legs is fluidized by adding aeration nitrogen, as shown by the green arrows in Figure 7. The circulation loop is sufficiently

instrumented with differential pressure transmitters. A list of these differential pressure transmitters, their ID, and high and low tap locations are given in Table 1. Reference to the high and low side tap locations is provided in Figure 7.

Table 1: List of pressure differential transmitters along with their process measurement and location on the catalyst circulation loop as shown in Figure 7

ID	Process Measurement	High Side	Low Side
PDT-201	Mixing zone gas distributor	1	2
PDT-202	Mixing zone bed	2	3
PDT-203	Riser bottom	3	4
PDT-204	Riser top elbow	5	6
PDT-205	Riser	4	6
PDT-206	Cyclone - Gas path	6	7
PDT-207	Cyclone - Solids path	6	8
PDT-210	Orifice bottom-Mixing zone	9	2
PDT-211	Orifice	10	9
PDT-230	Loop seal downleg	11	8
PDT-231	Loop seal upleg	11	12
PDT-300	Regenerator-Reactor gas outlet	17	7
PDT-301	Regenerator gas distributor	13	14
PDT-302	Orifice top-Regenerator	10	14
PDT-303	Regenerator bed	14	15
PDT-304	Loop seal top-Regenerator	12	15
PDT-305	Regenerator cyclone	15	17
PDT-306	Regenerator freeboard	15	16

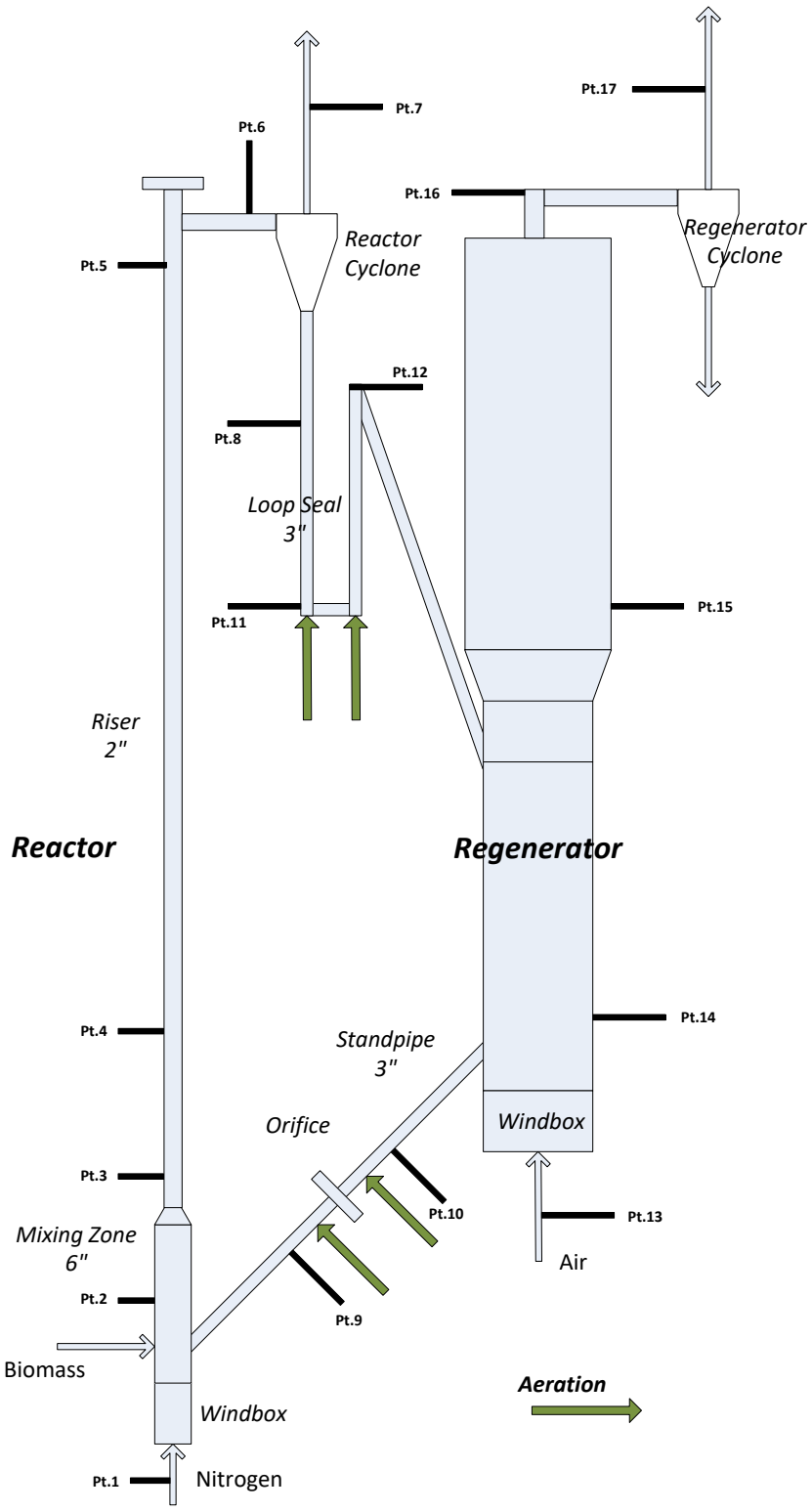

Figure 7: Schematic of the catalyst circulation loop along with pressure differential transmitter tap locations and aeration points

The cold flow test was conducted using fresh FCC catalyst. It has similar physical properties, namely appropriate particle density, particle size, and attrition resistance compared to our pyrolysis catalyst and it was readily available in larger quantities at RTI. About 160-kg of fresh FCC catalyst was added to the unit through the catalyst make-up bin and transferred to the regenerator vessel. Most of the catalyst inventory stays in the regenerator but some flows down through the orifice into the mixing zone. The bed height above the regenerator gas distributor is estimated using the pressure drop measured by pressure differential transmitter PDT-303. This measurement is a direct indicator of the solids inventory in the system. This differential pressure was at ~13 inches of water (in. H_2O) at the start of the test.

Qualitative measure of the catalyst circulation rate can be obtained using the pressure drop measured across the orifice plate (PDT-211). Prior to initiating catalyst circulation, the pressure drop across the orifice plate was approximately -10 in.H_2O. As catalyst circulation commences, the pressure drop across the orifice increases and the extent of increase in pressure drop is proportional to the rate of catalyst circulation. It is observed that PDT-211 pressure drop was -10 in.H_2O before and after the cold flow test when the catalyst was not circulating.

A plot of the feed and effluent gas flow rates measured during the cold flow tests is shown in Figure 8. The reactor effluent flow rate will always be higher than N_2 feed to the reactor due to the addition of purge gas through pressure taps and biomass feeder screw. The pressure drop (in.H_2O) measured by some of the pressure differential transmitters is shown in Figure 9.

Initial Start-up

During start-up, air feed to the regenerator and nitrogen feed to the reactor were increased while simultaneously increasing overall system pressure to 4 psig. The differential pressure set point between the reactor and regenerator effluent gases (shown as GasDP-SP in Figure 8) was set at -5 in.H_2O. At first, when air feed rate was increased an error on the air compressor caused the compressor to switch to standby mode which resulted in loss of air feed flow as well as instrument air and thus resulting in loss in communication with instruments. Once the compressor was brought online, air feed was steadily increased to 2835 scfh, equivalent to the superficial gas velocity of 0.86 ft/s through the catalyst bed and 0.38 ft/s through the freeboard. As nitrogen feed to the reactor was increased, catalyst circulation commenced when N_2 feed flow was above 425 scfh (equivalent to ~5 ft/s through the riser). The rate of catalyst circulation, as measured by an increase in pressure drop across the orifice plate, increased with increase in N_2 feed flow. Once the N_2 feed flow crossed 1100 scfh (equivalent to 12 ft/s through the riser), no further increase in circulation rate was observed. Nitrogen feed flow was further increased to 1250 scfh to ensure pneumatic conveying was not operating under choked flow mode, which tends to be erratic and difficult to control. As seen in Figure 3, the pressure drop across the orifice plate (PT-211) increased from -10 to -2.5 in.H_2O. During startup, N_2 aeration flow across the orifice was set at 10 scfh.

Performance

During the cold flow test, catalyst circulation was maintained for ~6 hours. For the entire runtime, except for the last 40 minutes, the solids inventory in the system (measured using regenerator bed pressure drop, shown in Figure 9 as RegenBed) stayed steady indicating minimal catalyst losses during the run through the reactor cyclone or due to catalyst entrainment out of the regenerator. During the initial 2.5 hours of catalyst circulation, aeration flow across the orifice plate was increased from 10 to 30 scfh. However, there was no effect on the catalyst

circulation rate. Similarly, aeration feed to the loop seal was also changed but did not affect the circulation rate.

Finally, the effect of changing the differential pressure set point was studied. The PDIC-300 set point was changed from -5 to -12 to -20 in.H_2O (in steps), As the differential pressure set point was lowered, the pressure drop across the orifice decreased which indicated a decrease in catalyst circulation rate. During this time, the pressure drop across the riser elbow, riser, and reactor cyclone also decreased. The decrease in catalyst circulation rate was expected as lowering the differential pressure set point lowers the pressure on the regenerator side relative to the reactor side. As the driving force for catalyst circulation is the pressure head on the regenerator side, lowering the pressure on the regenerator side reduced the driving force for catalyst circulation. Subsequently, the rate of catalyst circulation was increased by increasing the differential pressure set point from -20 to 0 in.H_2O. However, a sudden drop in regenerator bed pressure drop from 13 in.H_2O to 10 in.H_2O was observed indicating loss of catalyst. Further increase in differential pressure set point only increased the rate of loss of catalyst.

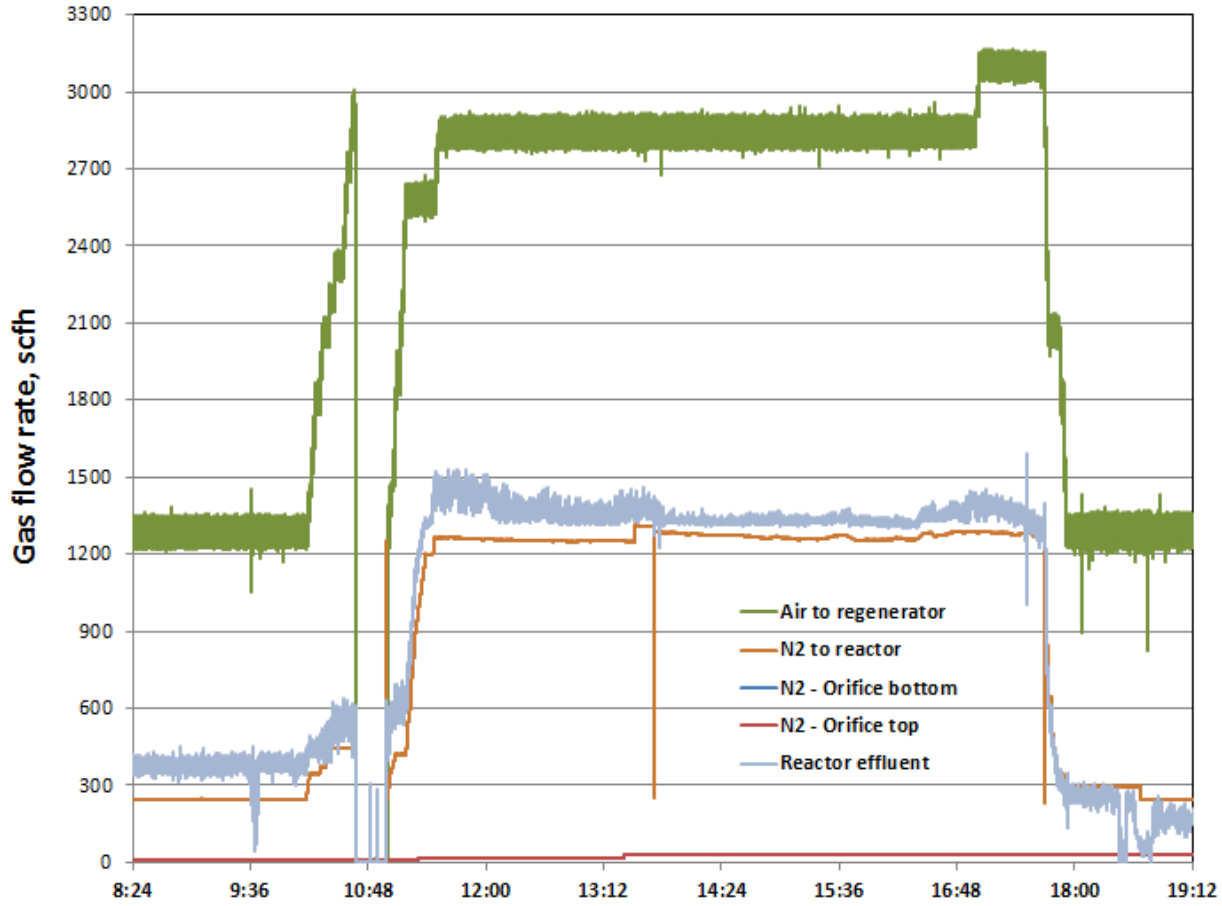

Figure 8: Feed and effluent gas flow rates during 07-16-2013 cold flow test

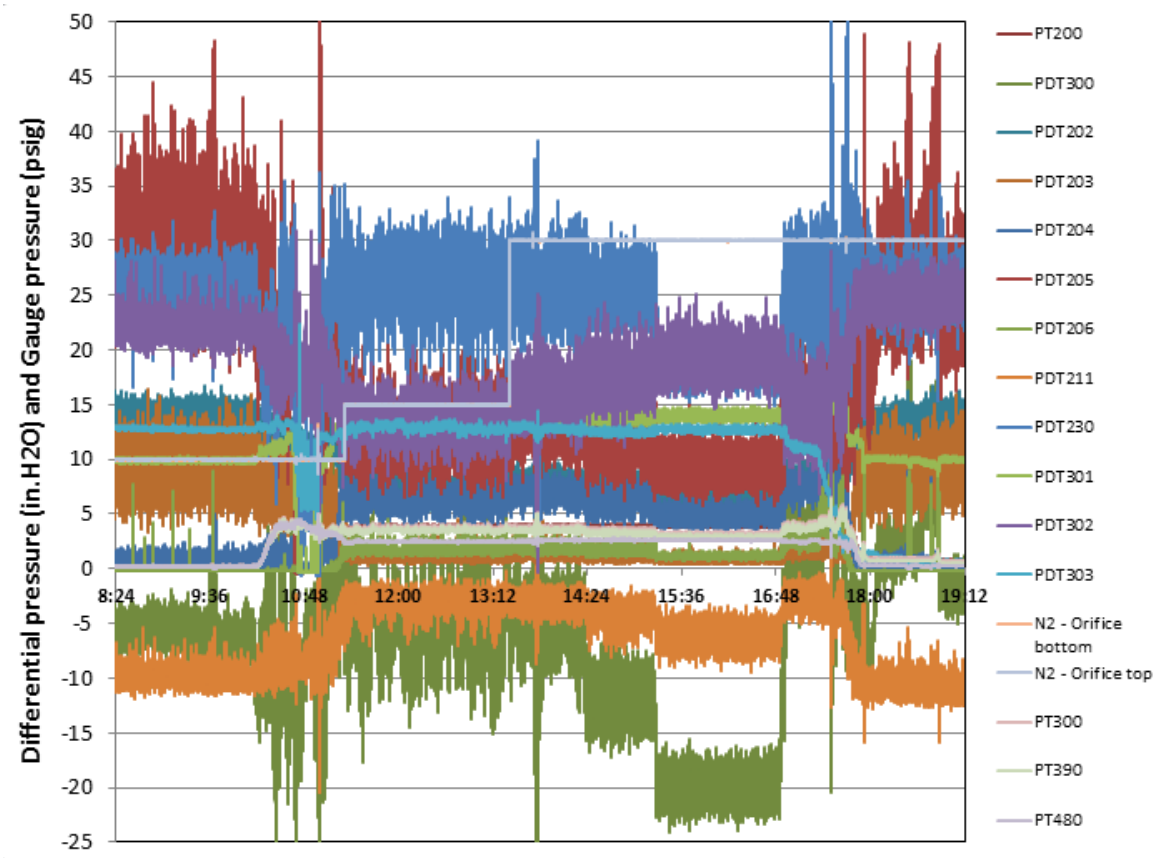

Figure 9: PDT and pressure transmitter readings during 07-16-2013 cold flow test

Toward the end of the cold flow test, the catalyst escaped the circulation loop through the reactor cyclone and ended up in the gas-liquid separator. The total amount of catalyst recovered from the separator vessel was ~56 kg (~35% of the catalyst inventory). Further investigation concluded that at higher differential pressure set point the solids height in the cyclone dipleg was very close to the cyclone bottom and fluctuations in the differential pressure led to solids backing up in the cyclone and adversely affecting its collection efficiency.

Hot Flow Testing and Catalytic Fast Pyrolysis with FCC catalyst

The FCC catalyst used for cold circulation testing was also used for catalytic fast pyrolysis testing to shakedown biomass addition under reaction conditions. These tests indicate of the behavior of product streams and were used to develop normal operation procedures.

The catalyst inventory in the system was refreshed to approximately 150-kg by adding additional fresh FCC to compensate for the losses in the cold flow tests. The entire system was electrically heated to between 250°C to 300°C with the heat tracing. Both the reactor and regenerator were operated as static bubbling fluid beds during the initial heating. The water was added to quench system through the spray nozzle at a rate of 10-13 gal/h. Gas flow rates and system pressure settings were adjusted to initiate catalyst circulation once desired temperatures were achieved.

Diesel fuel was injected into the regenerator once the catalyst was circulating through the system to increase the system temperature to achieve 500°C in the mixing zone. As diesel was injected into the regenerator, the coke deposition on the FCC catalyst increased quite substantially and created a large inventory of carbon in the regenerator as the system temperature increased. Consequently, as biomass was introduced into the system, the regenerator increased faster than expected to a higher temperature than anticipated. Water was added to the regenerator to limit and control the regenerator temperature. After biomass feeding was stopped, carbon oxidation continued in the regenerator for an additional 4 hours.

One of the key design concerns for such a small pilot plant was potentially excessive heat losses that would limit the conversion efficiency of the endothermic biomass pyrolysis process. This initial hot flow test demonstrated that the supplementary diesel fuel is not needed to maintain desired process temperatures and that there is more than enough energy in the char produced during the catalytic biomass pyrolysis process to provide all of the required process heat, and more. As a result, diesel addition during initial heating was deemed unnecessary. The revised startup procedure now uses only biomass to increase process temperatures.

Electrical heating is still used to increase the system temperature to 300°C but a single charge of biomass (1 ft^3 – or about 17 lbs of loblolly pine sawdust) is added to the mixing zone. The low pyrolysis temperature initially limits conversion of the biomass increasing the biomass solids to the regenerator where it is burned. The temperature slowly increases over 45 min until the regenerator temperature is 625°C. Water can be added to the regenerator to control the temperature in this range. The resulting pyrolysis temperature in the mixing zone is ~500°C. Pyrolysis temperature can be adjusted by changing the temperature in the regenerator and varying the biomass feed rate. Continuous biomass feeding starts after the temperatures are stabilized at the desired operating conditions.

Figure 10 shows the temperature profiles from the two sides of the reactor system for the length of a run with the FCC catalyst including the heating from biomass addition. For the duration of the test, 300 lbs. of biomass was fed over 5 hours with additional time for start-up and shutdown. Temperatures TE201 and TE202 are bed temperatures from the mixing zone of the pyrolysis reactor and TE300 and TE302 are bed temperatures from the regenerator. A 150°C temperature differential between the regenerator and pyrolysis sides of the reactor system was needed during sustained biomass feeding to achieve the desired pyrolysis temperature. The temperature differential between the two sides decreased when biomass feeding was stopped as the pyrolysis reactor temperature rose in the absence of the endothermic pyrolysis reactions.

Differential pressures are measured throughout the system to monitor solids circulation behavior. Figure 11 shows several key differential pressure measurements from catalytic fast pyrolysis with FCC. PDT 202 indicates the differential pressure across the riser of the pyrolysis reactor. The higher the differential pressure the higher the density of solids in the riser section. Under static conditions, the differential pressure is high at 17 in. H_2O and decreases as circulation begins. PDT207 is the differential pressure at the top of the down leg on the loop seal. PDT211 is the pressure drop across the orifice that is related to the catalyst circulation rate and PDT303 is the pressure drop in the regenerator bed that is related to the catalyst inventory.

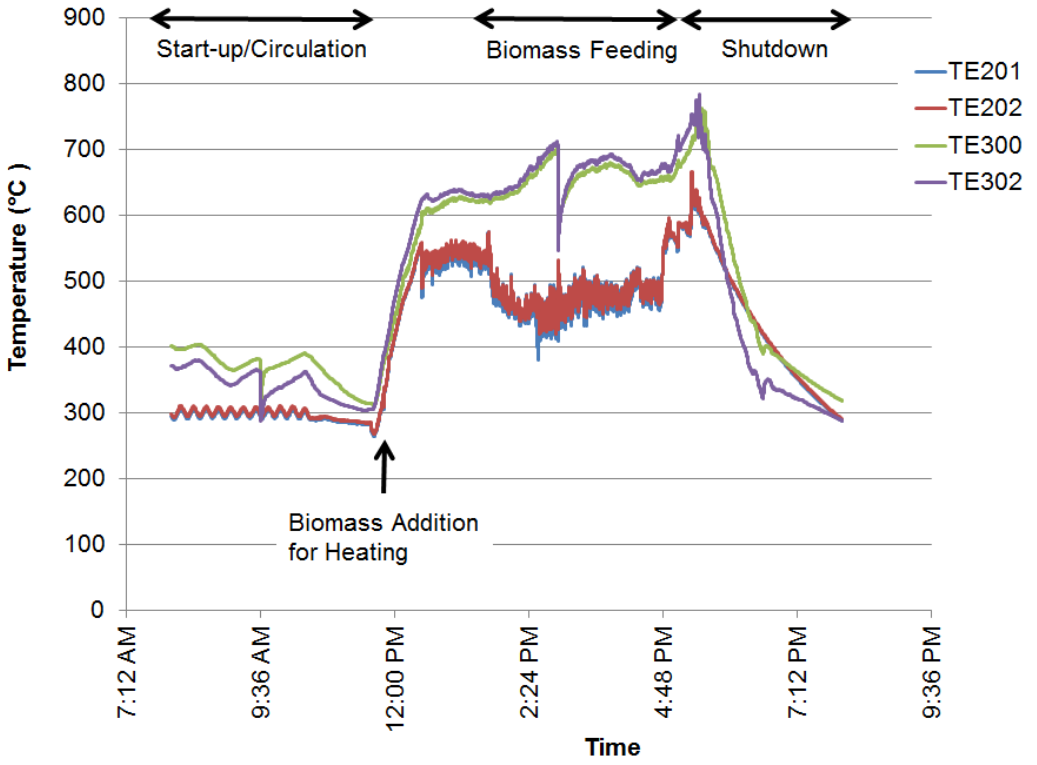

Figure 10. Temperature profiles from catalytic fast pyrolysis with FCC catalysts. TE 201 and TE 202 are pyrolysis reactor temperatures and TE 300 and TE 302 are regenerator bed temperatures.

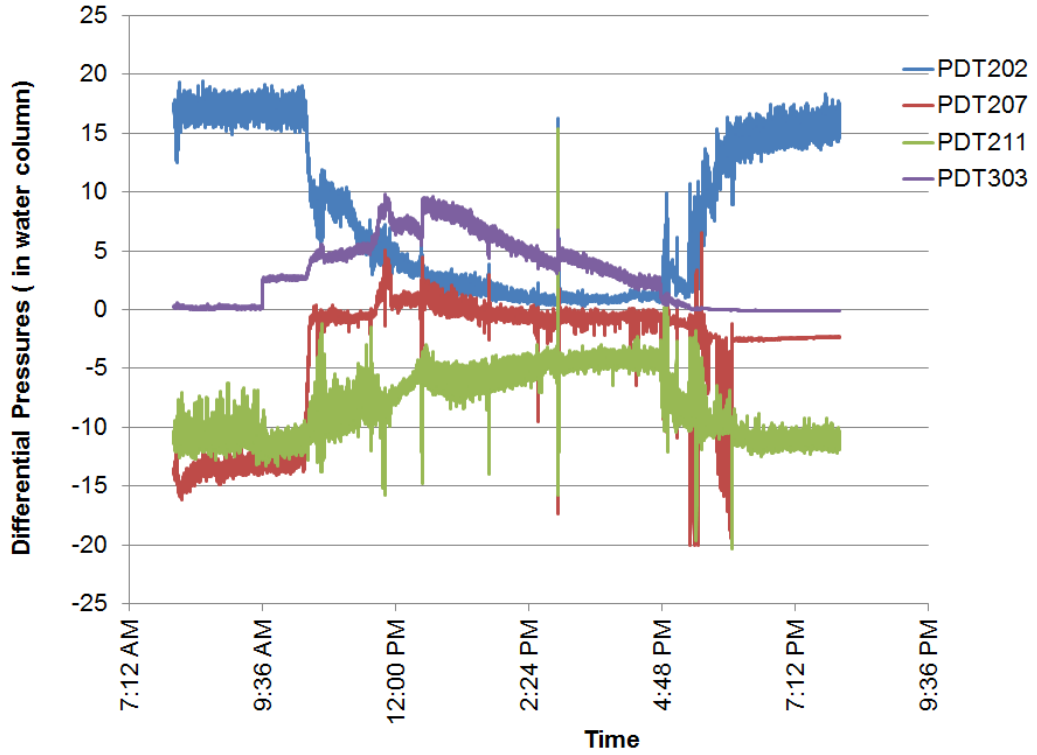

Figure 11. Differential pressure profiles from catalytic fast pyrolysis with FCC catalysts.

The material balance and the carbon closure for the catalytic biomass pyrolysis test with the FCC catalyst is shown in Table 2. The total inputs include biomass, water in the spray quench and the regenerator, and oxygen in the air into the regenerator. The initial charge of catalyst and nitrogen into the pyrolysis reactor are measured but not included in the mass balance calculation. The outputs include the bio-oil organic product, aqueous bio-oil fraction and water, char and catalyst fines from the regenerator cyclone, pyrolysis product gases that are treated in the thermal oxidizer, and regenerator off-gases produced during char oxidation. Catalyst fines collected from the regenerator cyclone are measured but not included in the mass balance calculation. For this experiment, the overall mass closure was 94% and the carbon balance was nearly 90%. The char content was determined by measuring the carbon content of the solids collected in the regenerator cyclone and assuming the remaining ash material was catalyst fines ejected from the regenerator. Pyrolysis product gas composition was measured with an on-line microGC and the regenerator CO and CO_2 products were monitored with a Continuous Gas Analyzer (NDIR).

Table 2: Mass and carbon balance from catalytic biomass pyrolysis in the 1 TPD pilot unit with FCC catalyst.

Inputs		**Outputs**		
Stream	Mass (lbs)	Stream	Mass (lbs)	% on input C
Pine	304	bio-oil/organics	33	15.8 %
Water	922	Water/aqueous	1044	7.6 %
Oxygen	169	char	41	18.1 %
		Pyrolysis Gases	48	13.3 %
		Regen Gases	147	34.6 %
Total	1395	Total	1313	
		Balance	94 %	89.5 %

Table 3. Bio-crude composition from operation of the pilot unit with FCC catalyst.

Bio-crude *Average Elemental Composition (dry basis)*	
C	71 wt%
H	7 wt%
O	22 wt%
Moisture Content	
Water Content	6 wt%

The pyrolysis product gas composition shown in Figure 12 is consistent with catalytic cracking of biomass pyrolysis vapors and is similar to the laboratory-scale catalytic biomass pyrolysis results measured in a 1”-diameter fluidized bed reactor. The most abundant pyrolysis product gas is CO followed by CO_2. A small amount of methane and higher hydrocarbons were also measured. The CO_2 and CO concentrations measured in the regenerator off-gas are shown in Figure 13. The elemental composition of the bio-oil product from catalytic biomass pyrolysis with the FCC catalyst is shown in Table 3. The oxygen content is quite a bit lower than conventional bio-oil from biomass fast pyrolysis but the yields are low, only about 11 wt% of the total biomass input. Excessive cracking of the biomass pyrolysis vapors with the FCC catalyst produced high char yields considering the solid char collected (13 wt%) and the high regenerator

off-gas yield (48 wt%). Nearly 50% of the carbon is lost through the regenerator side of the system and only 16% of the carbon is recovered in the bio-oil product.

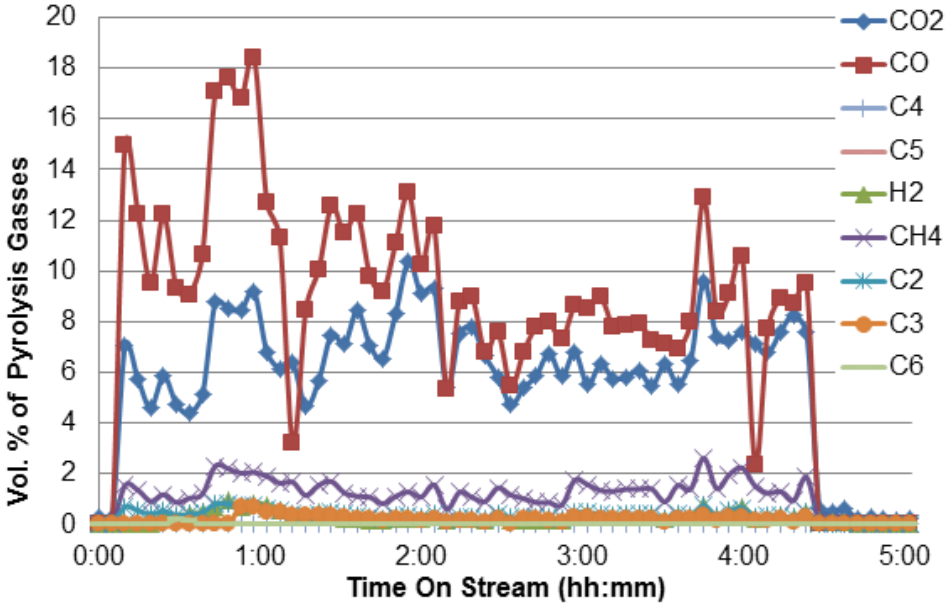

Figure 12. Product gas concentrations in the pyrolysis off-gas. (Volume percent of total off-gas including nitrogen.)

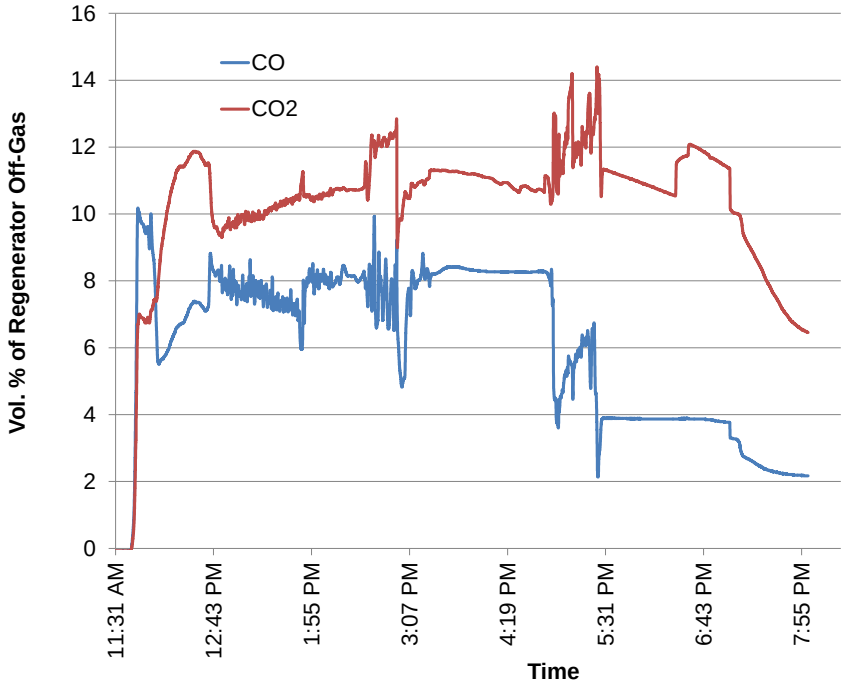

Figure 13. CO and CO_2 concentrations in the regenerator off-gas. (Volume percent of total off-gas including nitrogen.)

Improved system operability was realized through the first quench system modification, heating with the reactor system to pyrolysis temperatures with diesel instead of biomass to reduce cold introduction (below 300°C) of biomass, adjusting the spray nozzle flow, and increased air input to the regenerator to remove additional char. This operability was seen through 50% increases in the total amount of biomass fed in an individual trial and 100% increase in the bio-crude collected during those trials. Further optimization of the process conditions and quench system will increase these throughput and yield.

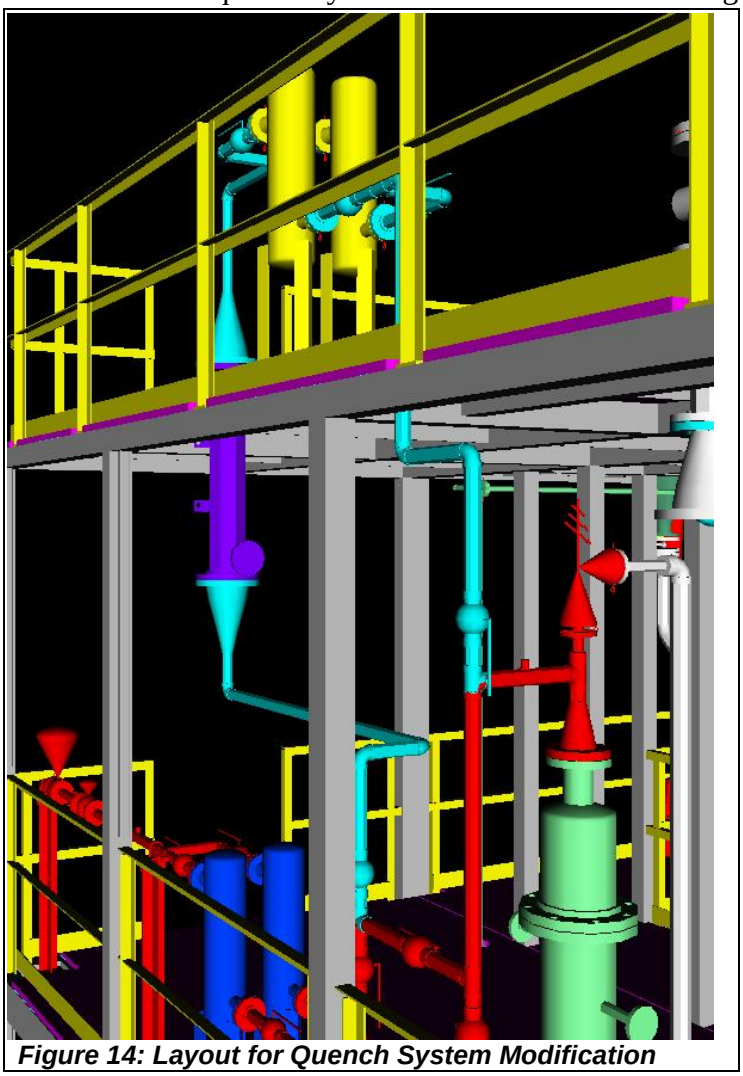

Figure 14: Layout for Quench System Modification

A second design modification for the quench system in the 1-TPD catalytic biomass pyrolysis unit was required to improve system operation. The first design modification removed the heat exchanger and replaced it with a water-jacketed pipe section. This change overcame the rapid pressure drop increases that occurred because of heat exchanger fouling by solids and heavy bio-crude product. However, product collection efficiency decreased because the temperature of the product vapors remained too high. Consequently, the second design modification includes a second set of parallel coalescing filters directly downstream of the gas liquid separator followed by the heat exchanger. The cooled gas stream from the heat exchanger will be introduced into the existing set of parallel coalescing filters before it exits the system through the pyrolysis gas control valve. A layout drawing of the quench system design modification is shown in Figure 14.

Catalytic Biomass Pyrolysis with non-zeolitic solid acid catalyst

An alternative pyrolysis catalyst (RTI-A10A) that is available in commercial quantities was identified for testing in the 1 TPD catalytic biomass pyrolysis reactor. The yield and oxygen content of the bio-crude produced with this catalyst in the 1”-diameter fluidized bed reactor system validated the catalytic biomass pyrolysis performance. 1000-kg were purchased and delivered and approximately 125 kg inventory was used to replace the FCC material in the 1 TPD reactor system. Additional catalyst is added after each run to maintain levels in the system.

The first bio-crude production with RTI-A10A was performed in the 1 TPD system in its original configuration with the heat exchanger installed as part of the quench system. On October

18, 2013, 6 hours of continuous operation were completed before the pressure drop across the heat exchanger forced a system shutdown. The system was electrically heated to 285°C before 18 cu. ft. of loblolly pine sawdust (bulk density of 17 lb/ft^3 and moisture content of ~10wt%) was fed into the pyrolysis mixing zone. The unconverted biomass and char circulated around the system into the regenerator where it was oxidized to provide heat to increase the solids temperature. Continuous biomass feeding started once the temperature in the regenerator reached 575°C. The average mixing zone temperature for the duration of the production run was 525°C.

As operational experience improved, a major limitation to the long-term operation was caused by fouling of the small diameter tubes that make up the heat exchanger. This caused the pressure drop across the heat exchanger to increase up to a point where the differential pressure across the reactor/regenerator loop could not be controlled and solids circulation decreased and ultimately stopped. As a result, the quench system was redesigned so the inlet to the gas/liquid separator is a water-cooled shrouded pipe with a 45° pyrolysis vapor inlet and a 45° transition into the gas/liquid separator instead of the heat exchanger with several 90° bends where solids tended to accumulate.

Another bio-crude production run with RTI-A10A was performed in December 2013 to test the modified quench system. The system was started up as before with electric heating to 300°C initially followed by biomass addition to increase the system temperature to 550°C. After the initial heat up, biomass was continuously fed at ~100 lbs/hr for approximately 6 hours. The system was shut down after 6 hours because the pressure drop on the pyrolysis side was prohibitively high; this was not a failure of the new quench design but the result of inconsistent biomass feeding and a higher than normal solids carryover during startup. The inconsistent feeding turned out to be caused by a broken motor shaft on the dosing screw assembly.

The average mixing zone (pyrolysis) temperature was 480°C. The pyrolysis temperature was lower than the previous run to determine the extent of cracking of the product vapors as a function of temperature.

The impinger train was installed to collect a slip-stream sample downstream of the gas/liquid separator during this production run to evaluate the product collection efficiency. Again, liquid samples were collected in the ice-cooled impinger, the dry-ice cooled impinger, and in the ESP. The elemental composition and the qualitative GC/MS analysis of the impinger samples indicate that the bio-crude sample and the impinger sample are similar products and there was no preferential loss of any product fraction.

A semi-quantitative GC/MS analysis was performed to provide a more detailed characterization of the bio-crude samples from the two production runs and the corresponding impinger train samples. The chemical composition was determined in terms of % of GC/MS signal area. The species were identified based on the hierarchy as the order listed in Figure 15 shows. Any species containing a benzene group is identified as a benzene derivative and any species with a phenol group is designated as a phenolic compound. The un-substituted aromatics are classified as PAHs. Any remaining compound with an acid functionally is labeled as an acid after the ketones are identified.

In general, as noted, the slip stream impinger samples were chemically similar to the bio-crude samples recovered from the quench system. The higher phenolic content of the 10/18 bio-crude sample compared to the slipstream is the anomaly and correlates with the lower fraction of benzene derivatives. One possible explanation for this result is that the water soluble phenolics in the slipstream sample concentrate in the aqueous fraction. There also appears to be a higher acid content in both the slip stream and bio-crude samples produced on 12/18/2013 compared to

10/18/2013. It is likely that the higher pyrolysis temperature established on 10/18/2013 favored a higher degree of deoxygenation via decarboxylation of the acidic components in the pyrolysis vapors.

In summary, 659 lbs of loblolly pine sawdust was converted into bio-crude during 2 production runs with a total of 12 hours continuous biomass feeding. A total of 61 lbs of organic bio-crude was produced. Solids carryover into the quench system limited the useable product to 2 gallons of sample that are suitable for upgrading. The bio-crude oxygen content was between 19 to 23 wt% as determined from various samples.

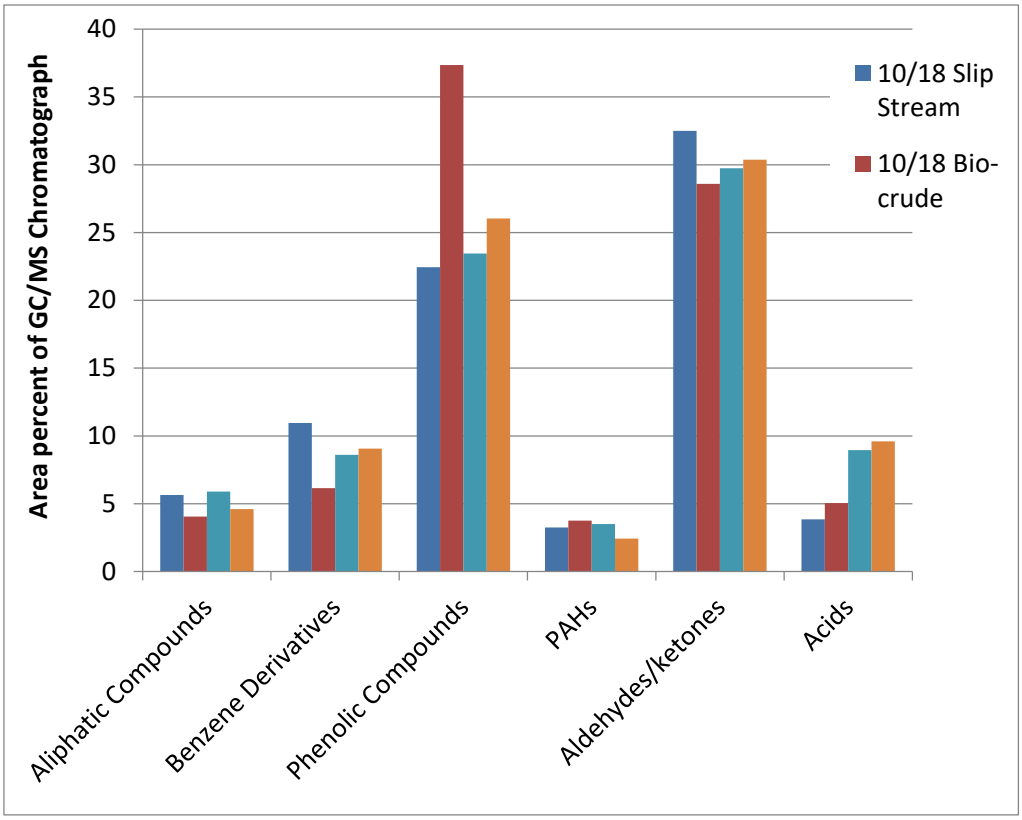

Figure 15: Qualitative GC/MS Analysis of bio-crude and slip stream samples from 10/8 and 12/18 runs with RTI-A10A

Operational Improvement Experiments

Bio-crude production with RTI-A10A continued in the 1 TPD system to generate sufficient quantities for upgrading testing at Haldor Topsoe. Six production runs were made with small variations on process conditions to continue to optimize system operability.

- Start-up heating with diesel continued to enhance operability by reducing carry-over of solid biomass to the quench system prior to the desire operation temperature being achieved.
- Increased air flow to the regeneration leg of the reactor increased char removal from the system and thus reduced char circulation and decreased shutdown time.
- A minimum nitrogen inlet flow rate was determined to maintain good mixing in the pyrolysis reactor mixing zone. Good mixing improves devolatilization of the biomass and dampens slugging in the system.

- Valve positioning to balance pressure drop on each side of the reactor was determined and it increased run length as well.
- Maintaining the temperature between 500°C and 525°C in the pyrolysis mixing zone appears to be optimal for minimizing carbon loss to the pyrolysis off-gasses or the regenerator products.

Additionally, catalytic biomass pyrolysis performance with RTI-A10A catalyst was validated in the bench-scale 1"-diameter fluidized bed reactor system. Loblolly pine sawdust (bulk density of 17 lb/ft^3 and moisture content of ~10wt%) was used. The test in the 1 TPD pilot unit with RTI-A10A lasted for 6.5 hours with continuous feeding totaling 550 lbs. of biomass. The system was electrically heated to 285°C before heating with diesel which was continued until the pyrolysis mixing zone reached 525°C. The average mixing zone temperature for the duration of the production run was 515°C.

The carbon balance for this production run is presented in Table 4 in comparison with the carbon balance observed in the 1" fluidized-bed bench-scale system. Table 4 also lists the elemental composition of the bio-crudes produced from each system and the water content of those bio-crudes. The 1TPD system had a lower bio-crude yield; however agreement in yields of other phases indicates that collection efficiency is likely still low and accounts for the lower observed yield. The GC/MS analyses of the bio-crude provide further evidence that lighter aliphatic molecules were not effectively captured contributing to the lower than expected yield and slight increase in bio-crude oxygen content. The 15% unrecovered carbon is expected to be uncollected bio-crude and some deposition in the system.

Table 5 details the pyrolysis off-gas composition (on a nitrogen free basis) for trials in each of the systems. Similar CO_2/CO ratios were observed in both systems; however, increased hydrogen and decreased C_2^+ yields were observed in the 1TPD system. The regenerator off-gas contained about 11 vol% CO_2 and 4 vol% CO during the run. The high levels of CO suggests incomplete combustion and possibly steam gasification of the char as water was added to the regenerator to control the temperature.

Table 4. Comparison of carbon yields and bio-crude composition between the bench-scale and pilot units.

	1" Fluid-Bed Reactor	**1 TPD Unit Operation**
Carbon Balance (wt. %)		
Organic Liquid Product	24.2	10.5
Aqueous Liquid Product	4.3	3.9
Pyrolysis Off-Gasses	17.6	20.1
Char & Regeneration Off-Gas	51.3	50.7
Total	*97.4*	*85.2*
Bio-crude Composition *(Slipstream values in parenthesis)*		
C (wt%.dry basis)	76.7	69.7 (72.8)
H (wt%, dry basis)	7.1	6.7 (6.9)
O (wt%, dry basis)	16.1	23.5 (20.3)
Water content (wt%)	12.4	9.5

Table 5. Comparison of pyrolysis off-gas compostion between the bench-scale and pilot units.

	1" Fluid-Bed Reactor	1 TPD Unit Operation
H_2 (vol. %, N_2 free basis)	1.9	5.0
CO (vol. %, N_2 free basis)	54.8	54.8
CO_2 (vol. %, N_2 free basis)	27.5	28.8
CH_4 (vol. %, N_2 free basis)	9.8	9.4
C_{2+} (vol. %, N_2 free basis)	6.2	2.0

Figure 16 shows the collected bio-crude from the coalescing filters as a function of the biomass fed during an experiment. Early tests produced little collection from the filters until almost 150lbs of biomass was fed. Additional increases in feed led to greater increases in collection. Increasing from 390 to 560 lbs. (a 40% increase) increased the bio-crude production from the filters from 1.5 gals to 3.6 gals (a 120% increase). Improved collection efficiency and increased run lengths are keys to demonstrating the anticipated bio-crude yields.

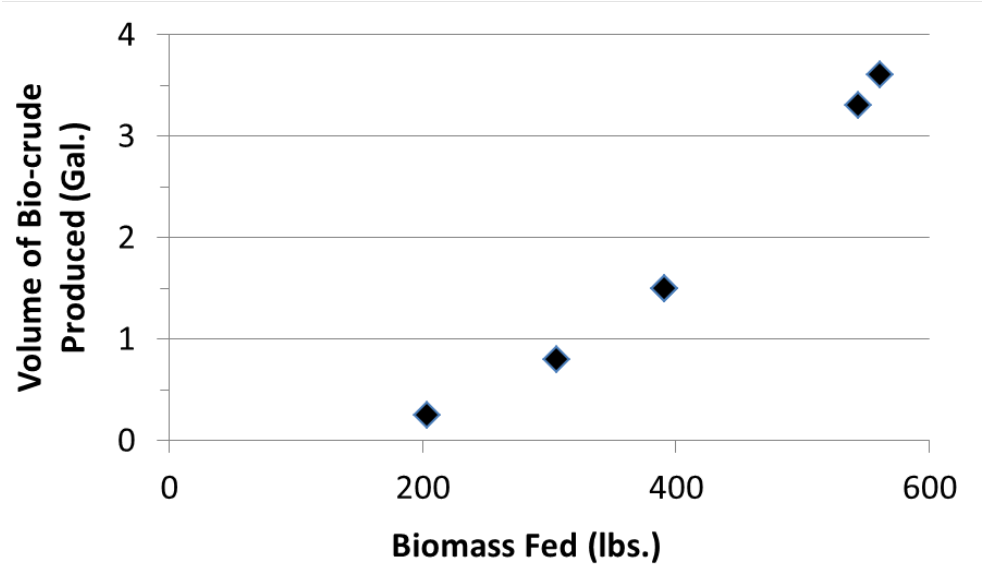

Figure 16: Bio-crude production as a function of biomass fed during a trial.

In several experiments, an impinger train was installed to pull a small slipstream (100 to 200 sccm) of product vapors from upstream of the heat exchanger to evaluate what fraction of the bio-crude product, if any, is not being collected. The impinger train consisted of an ice cooled impinger followed by a dry ice/acetone cooled impinger and an electrostatic precipitator (ESP). Liquids were collected out of each of these vessels and analyzed. The bio-crude collected with the impinger train had similar water content and slightly lower oxygen content compared to the bio-crude collected in the quench system. A semi-quantitative GC/MS analysis was performed to provide a more detailed characterization of the bio-crude samples from the quench system and the slipstream as shown in Figure 17. The qualitative GC/MS breakdown was also similar with more aliphatic compounds captured in the slipstream.

A closer look at the GC/MS results did suggest, however, that the collection efficiency of the lighter molecular weight products had to be improved. The quench system modifications

reduced pressure increases due to fouling in the heat exchanger but also increased the downstream temperatures through the collection system. In Figure 18 there is a higher percentage of species with shorter elution times on the GC Column for the slip stream samples compared to the bio-crude samples; suggesting that a smaller fraction of the lighter molecular weight species were captured in the quench system. Similarly, when the GC/MS data was viewed by compound type, the slipstream had a higher aliphatic content than the collected bio-crude. These basis's in collection efficiency by compound type and size likely account for the observed differences in the elemental composition between the bio-crude and slipstream bio-crude. Modification to the quench system to improve cooling was implemented.

In summary, 2400 lbs of loblolly pine sawdust was converted into bio-crude during 6 production runs with a total of 27.25 hours continuous biomass feeding. A total of 190 lbs of organic bio-crude was produced. Solids carryover into the quench system limited the useable product to 11 gallons of sample that is suitable for upgrading. The bio-crude oxygen content was between 19 to 23 wt% as determined from various samples. The results suggested that the pyrolysis temperature may have to be maintained above 500°C to improve devolatilization to increase yield and increase deoxygenation activity.

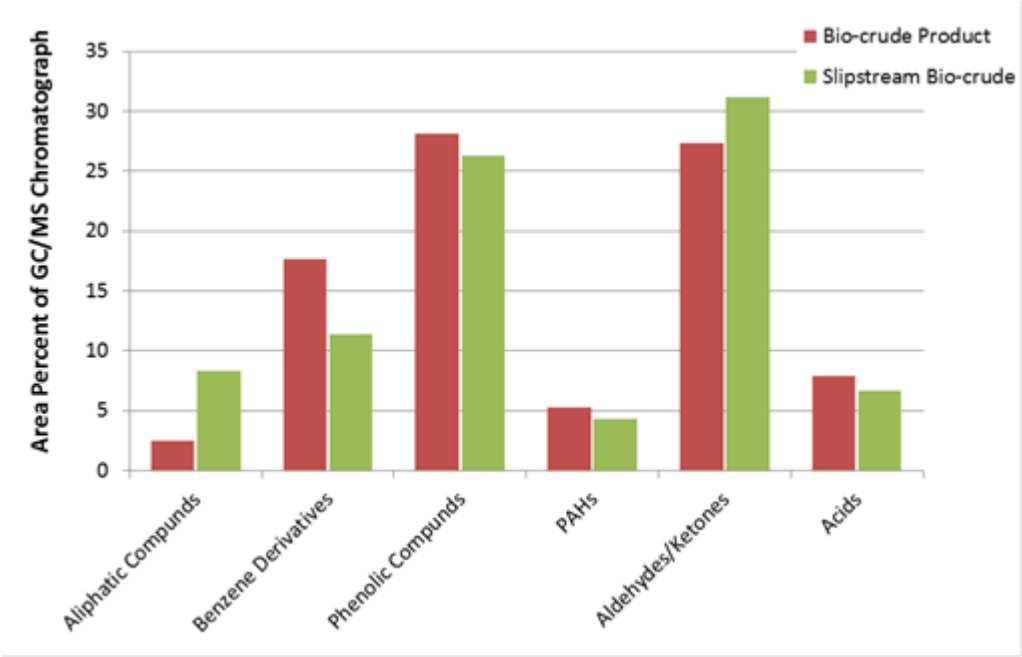

Figure 17: Qualitative GC/MS Analysis of bio-crude and slip stream samples from a run with RTI-A10A and system modifications.

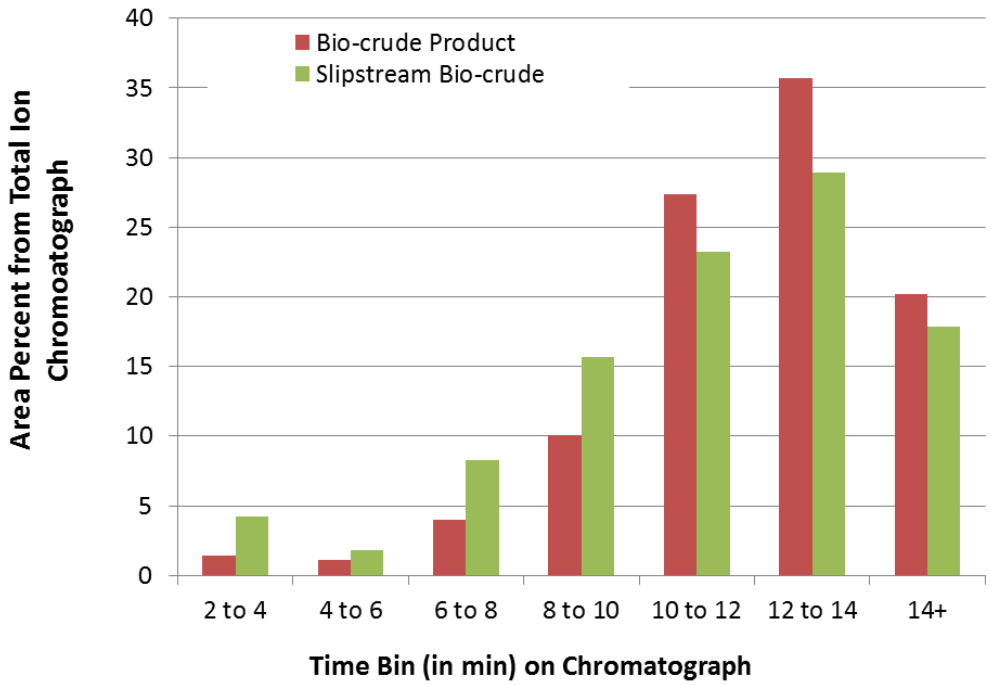

Figure 18: Qualitative GC/MS Analysis based on elution time from the GC column of bio-crude and slip stream samples from a run with RTI-A10A and system modifications.

Evaluation after System Improvement

In July 2014, over 1000 lbs of loblolly pine sawdust was fed in 15 hours, with 10 hours of continuous bio-crude production. The product yields (gas, bio-crude, aqueous, and solid) determined in the 1" fluidized bed laboratory reactor were effectively achieved in the pilot plant. The data collected during this steady state experimental campaign are compared to the laboratory data. The hybrid poplar did not successfully feed into the system and was not used.

System Start-up

The pyrolysis unit requires 250-300 lbs of fluidizable RTI-A10A catalyst for a full charge. Catalyst is loaded in the catalyst make-up bin and added to the regenerator. Before the system was heated, ambient temperature air was added to the regenerator to fluidize the catalyst. Fluidization was continued until the catalyst fines ejected from the regenerator was minimized based on the solids collected in the ash pot as a function of time.

After the size classification of the catalyst had equilibrated, the electric heat tracing was powered to begin heating the system. The system was electrically heated at a rate of about 1°C/minute until the temperature reaches 300°C. At this point, the nitrogen flow to the mixing zone and the air flow to the regenerator were increased while the control valves on the pyrolysis and regeneration sides of the loop were partially closed to initiate solids circulation. The control valves at the pyrolysis and regenerator outlets were then automatically controlled to maintain a constant total system pressure and differential pressure between the pyrolysis and regenerator sides of the loop, respectively. The total system pressure and differential pressure during start-up and catalytic biomass pyrolysis are shown in Figure 19. System pressure is measured in psig and differential pressure is measured in inches of water column (in H_2O).

Once solids circulation stabilized and the differential pressures across the system had equilibrated, the temperature of the system was increased by injecting diesel fuel into the bubbling catalyst bed in the regenerator. Figure 20 displays the temperatures measured in the mixing zone and in the regenerator as a function of time during system start-up and steady-state catalytic biomass pyrolysis. Diesel injection started at 1:20PM and continued until 3:00PM. During that period, the system pressure was maintained at 1.5 psig with the differential pressure controlled at 12 in H_2O. The rate of diesel injection was controlled to maintain a ~1°C/minute temperature increase in the system. Diesel injection was continued until the temperature in the mixing zone reached at least 525°C.

When the mixing zone temperature reached the desired biomass pyrolysis temperature, the diesel injection was terminated and biomass feeding was initiated. This occured at 3:00PM in Figure 19 and Figure 20. As biomass was fed into the mixing zone, the mixing zone temperature decreased due to injection of cold biomass and the endothermic biomass pyrolysis process. Biomass char and spent catalyst were circulated through the system to the regenerator providing fuel for combustion to reheat and regenerate the catalyst.

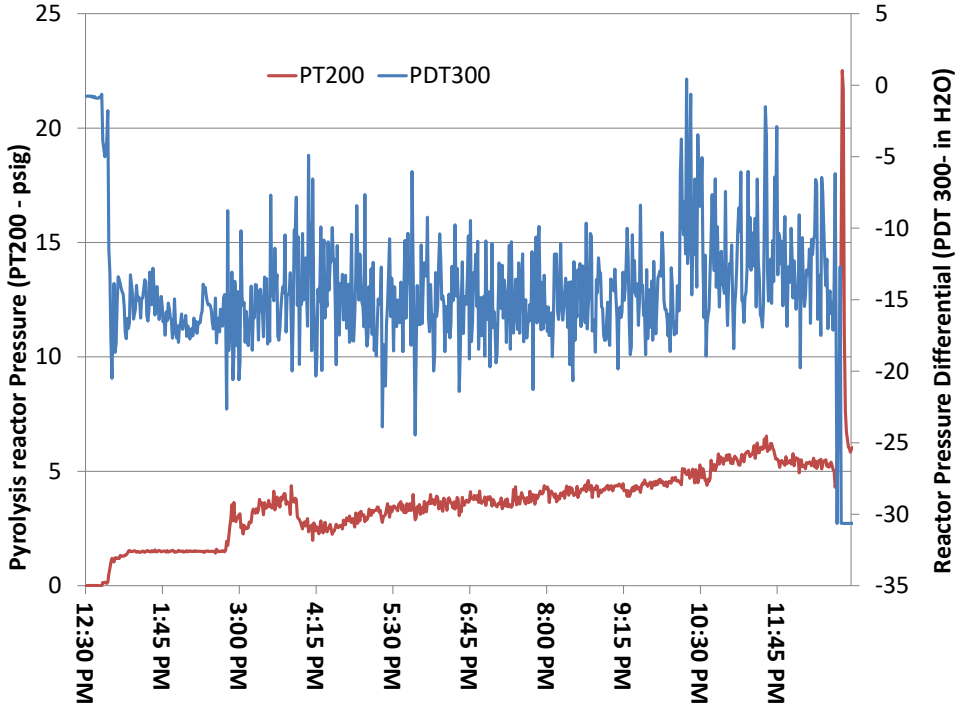

Figure 19: Total system pressure (PT200) and differential pressure (PDT300) between the pyrolysis and regnerator sides of the loop.

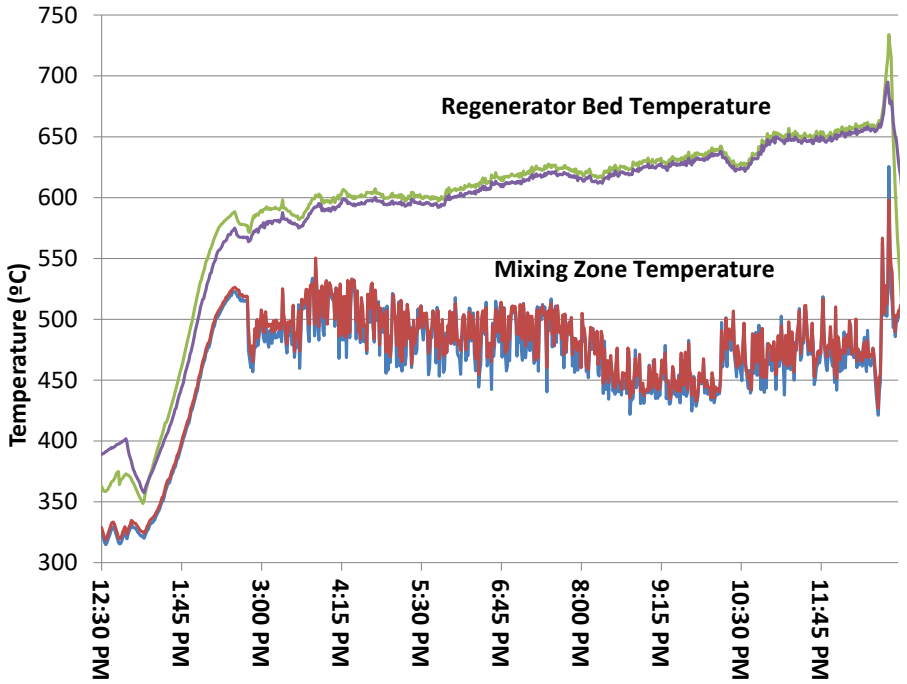

Figure 20: Biomass pyrolysis system temperatures during start-up and steady-state catalytic biomass pyrolysis.

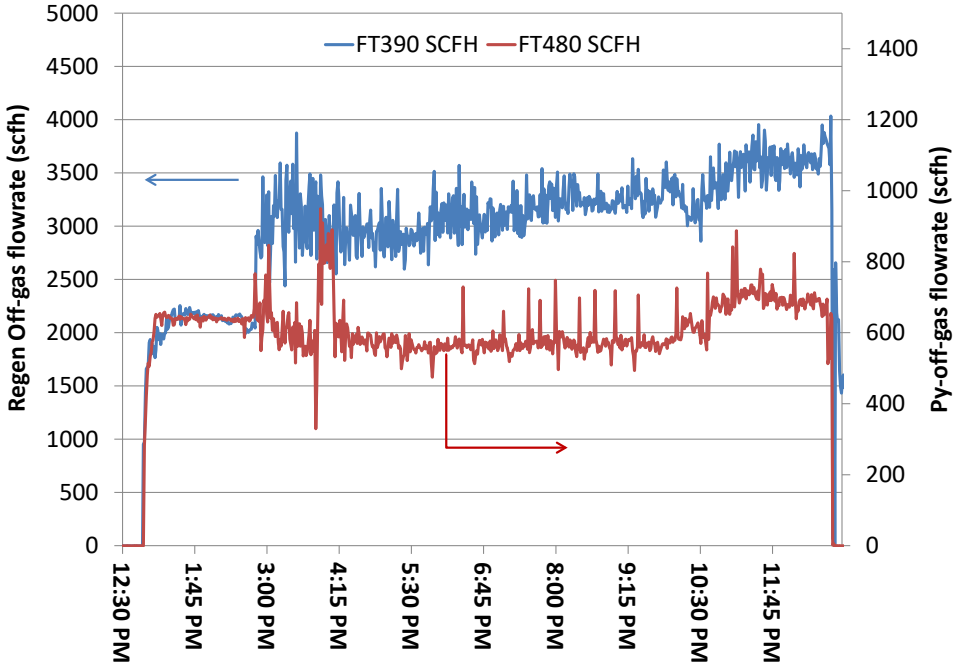

Figure 21: Product gas flow rates - Regenerator Product Gas (FT390) and Pyrolysis Product Gas (FT480)

As pyrolysis began, the nitrogen flow rate was decreased to compensate for the product gases and vapors generated during biomass pyrolysis and maintain a constant velocity through the riser. The product gas flow rates measured at the outlet of the pyrolysis reactor and regenerator are plotted in Figure 21. The system pressure also increased as the pressure drop across the coalescing filters increased due to the flow of more viscous pyrolysis vapors and gases

through the system. During catalytic biomass pyrolysis, the system pressure was controlled at 3.5 psig while the differential pressure control set point was not changed.

Continuous Catalytic Biomass Pyrolysis

Loblolly pine sawdust (0.25" and 0.125" tops size) was continuously fed into the mixing zone at an average rate of 126 lbs/hr. Approximately 500 scfh of nitrogen was added to the mixing zone to fluidize the hot, regenerated catalyst and approximately 2000 scfh of air was added to the regenerator to oxidize char and coke in the bubbling fluidized bed. Nitrogen and air were also added to a number of purge taps throughout the system, but these flows make up less than 10% of the total flow in the system. Water and air were added to the regenerator off-gas cooler to quench the flue gas from the regenerator. Water was also added at a rate of approximately 13 gal/hr in the quench system.

In total, 1120 lbs of biomass was fed into the system and 90 lbs of bio-crude was collected. The overall material balance, on a nitrogen free basis, is shown in Table 6. The water was input through the quench system and the oxygen input was from the air introduced into the regenerator for char combustion. The organic product was collected from the coalescing filters and the aqueous liquid product was the effluent from the gas/liquid separator. The flow rate of the pyrolysis gases was continuously measured and the gas composition determined from the on-line GC. The flow rate of the regenerator off-gas was also continuously measured and the composition determined from an on-line gas analyzer. Char was collected from the standpipe of the regenerator cyclone.

Table 6. Overall Material Balance for Loblolly Pine Catalytic Pyrolysis

Mass Balance			
Inputs		**Outputs**	
Biomass	1120 lbs	Organic Liquid Product	90 lbs
Water	1420 lbs	Aqueous Liquid Product	1830 lbs
Oxygen	430 lbs	Pyrolysis Off-Gas	100 lbs
		Regeneration Off-Gas	680 lbs
		Char	50 lbs
Total	*2960 lbs*	*Total*	*2750 lbs*
		Balance	*93%*

Of note is the apparently low organic product yield resulting from the fact that the system took several hours to reach equilibrium. The pyrolysis gas production rate and composition equilibrated very quickly after biomass feeding started. This was not the case with the liquid and solid production rates. As biomass is fed into the system, the water added for quenching and that produced from dehydration during pyrolysis became saturated with water soluble organic hydrocarbons as the pyrolysis vapors passed through the system. The coalescing filters was also saturated with bio-crude downstream of the gas/liquid separator. Consequently, very little bio-crude was collected during the first 2-3 hours of operation. As the system became saturated with carbon, the heavy bio-crude fraction was collected in the first coalescing filter and a water-rich light fraction was collected in the coalescing filter downstream of the heat exchanger.

During the equilibration period, very little organic product was collected. However, during the last two hours of the experiment, approximately 4.5 gallons of bio-crude was collected, accounting for ~18 wt% of the material balance during that time period. This is similar to the yields measured in the 1"-diameter laboratory fluidized bed reactor. Therefore, at the end of the

experiment, the bio-crude production rate was close to 42 gallons per ton of biomass. The average composition of the bio-crude product is 71 wt% C, 6.5 wt% H, and 22 wt% O, on a dry basis.

The carbon balance during the loblolly pine catalytic pyrolysis is shown in

Table 7. Half of the carbon exited out of the regenerator as either solid char or CO and CO_2 from char combustion. The aqueous fraction also contained a significant amount of carbon. However, the amount of carbon in the organic liquid product was expected to increase if bio-crude production had continued for a longer period.

Table 7. Overall Carbon Balance for Loblolly Pine Catalytic Pyrolysis

Carbon Balance				
Inputs		**Outputs**		
Biomass	500 lbs	Organic Liquid Product	51 lbs	10 %
		Aqueous Liquid Product	86 lbs	17 %
		Pyrolysis Off-Gasses	34 lbs	7 %
		Regeneration Off-Gas	210 lbs	41 %
		Char	39 lbs	8 %
Total	*500 lbs*	*Total*	*416 lbs*	*83 %*

The product gas measured at the outlet of the pyrolysis side of the system as a function of time on stream during biomass feeding is shown in Figure 22 on a dry, nitrogen-free basis. The primary gas phase pyrolysis products were CO_2 and CO, as expected, with lesser amounts of hydrogen, methane, and other hydrocarbons. The average pyrolysis gas composition, on a nitrogen free basis is presented in Table 8.

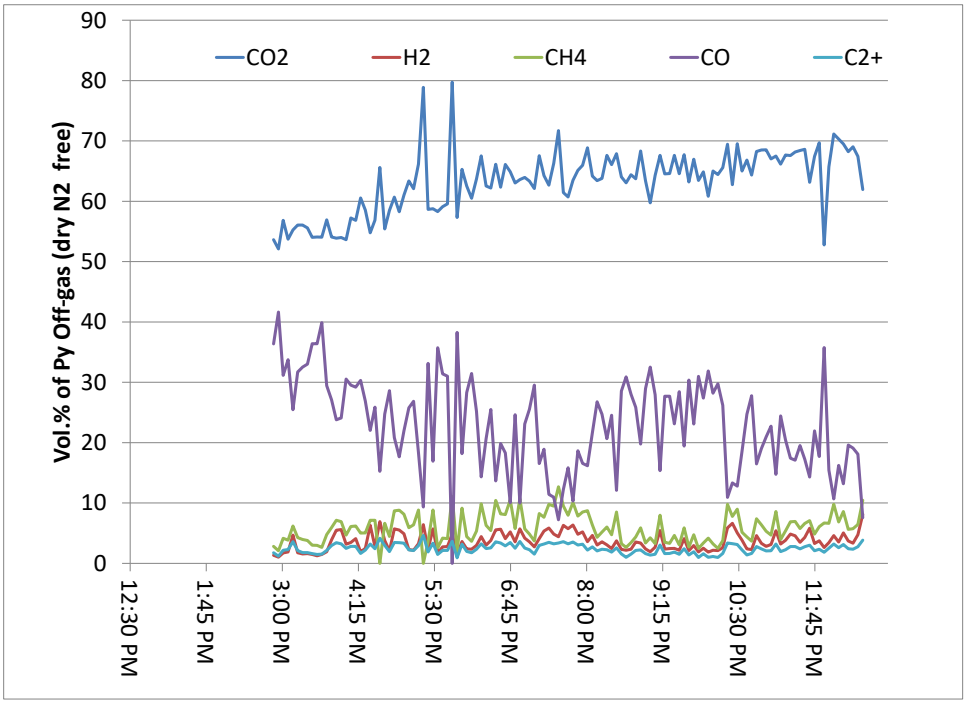

Figure 22: Pyrolysis product gas composition in Volume % of a dry, nitrogen-free basis

Table 8. Average Gas Phase Pyrolysis Product Composition (vol%, N_2 free)

Product	Volume %, N_2 free
CO	23
CO_2	62
H_2	3
CH_4	6
C_2+	2

Additionally, as the system reached equilibrium, the composition and characteristics of the solids circulating in the reactor also equilibrated. Fine catalyst particles were entrained out of the regenerator and the char concentration in the regenerator began to increase. At first, all of the char was burned to provide process heat. But the rate of char accumulation was greater than the rate of char consumption and an excess of char builds up in the regenerator. Pressure differential measurements of the regenerator indicated minimal change in the bed height but also a decrease in the bed density that was indicative of the increasing char concentration. Excess char that was not consumed was entrained by the flue gas and collected in the standpipe of the regenerator cyclone.

Figure 23 shows the solids collection rate as a function of time on stream. A sample of the total amount of solids collected at a given time was put in an oven and heated to combust any char or coke in the sample. The loss of weight after combustion was the percentage of char in the sample. The ash content of the loblolly pine was 0.6 wt% so ash accumulation during this relatively short experiment was negligible.

The first sample collected was almost entirely catalyst solids. Analysis of the particle sizes indicates that the material entrained out of the regenerator in the first sample was primarily smaller than 40 microns. The relative amount of catalyst fines collected during this trial decreased as the relative amount of char increased. The particle size distribution was measured for each of the solid samples collected after the char was burned off. These are presented in Figure 24 along with the particle size distributions for the fresh catalyst (red line) and a sample of the catalyst remaining in the regenerator after the experiment was completed (burgundy line). The first solid samples contain a high fraction of very fine material (less than 40 microns). As the catalyst fines were removed from the system, the mean particle size of the collected samples increased. Later samples also contained an increased number of very small particulate likely from the ash remaining after char combustion since these samples contained mainly char. The final bed material had a mean particle diameter of nearly 100 microns compared to 61 microns for the fresh catalyst.

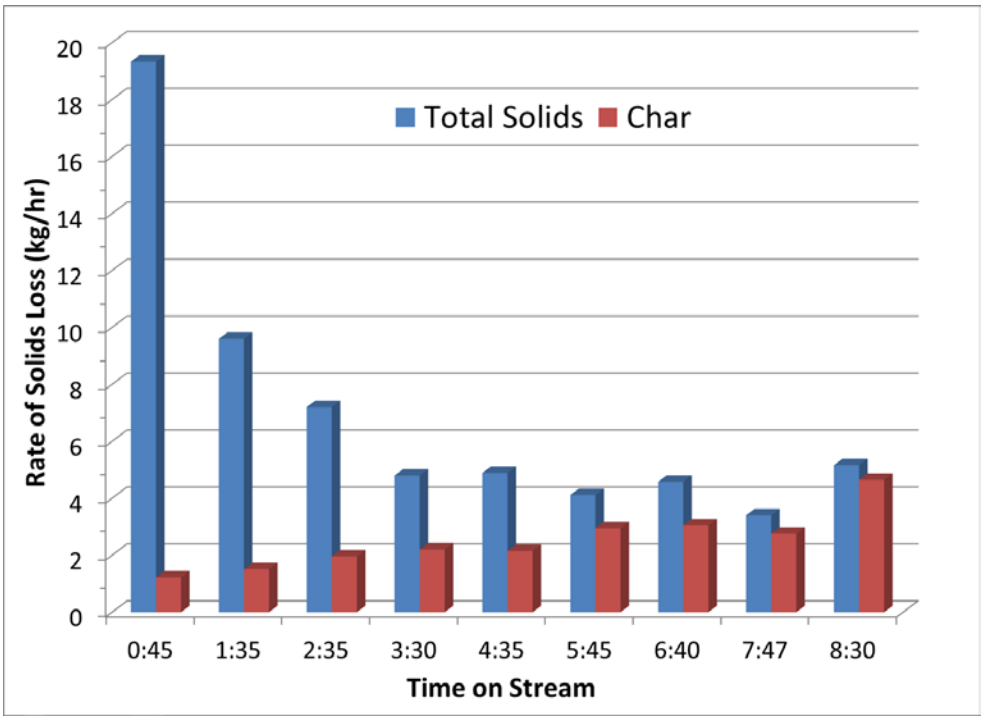

Figure 23: Distribution of catalyst fines and biomass char collected with the regenerator cyclone as s function of time during catalytic biomass pyrolysis. Char content is determined from the residual losses after the sample is heated in air to oxidize the carbon.

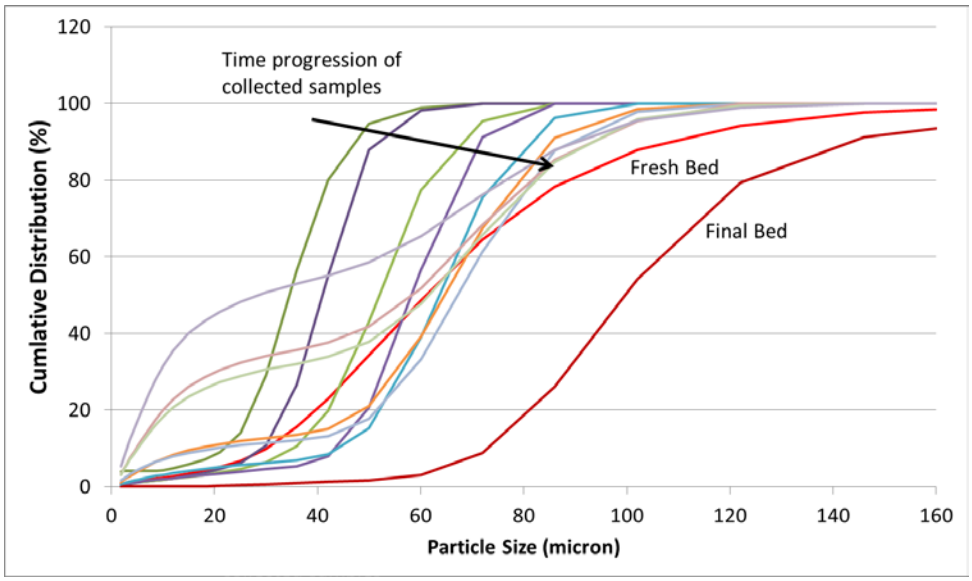

Figure 24: Particle size distribution of solids collected with the regenerator cyclone (after char combustion) over time during catalytic biomass pyrolysis.

Evaluation of Different Biomass Feedstocks

Several feedstocks were tested in the 1TPD system. A hybrid poplar meal that was first pelletized and then re-ground was tested unsuccessfully. Corn stover received from a previous project (NABC, Iowa State University) was also tested. The bulk density of the corn stover

(~7.34 lbs/ft^3) is very similar to the ground hybrid poplar (~ 8 lbs/ft^3). This material did not not feed well into the system and bridged quite severely in the hopper.

At the other extreme, hardwood pellets from a local supplier were sourced for testing. The pellets had a bulk density of 42 lbs/ft^3 and flowed very well in the feed system. Unfortunately, the pellets feed too well and it was hard to control the feedrate below 150 lbs/hr. Two CFP experiments were attempted with the hardwood pellets and at both times the pyrolysis side of the reactor plugged. This was caused by either too much pellets flooding into the mixing zone or a slug of pellets being injected into the riser tube.

When the hardwood pellets were fed into the system, the pyrolysis temperature in the mixing zone equilibrated at ~600°C. This was attributed to poor conversion of the pellets resulting in 1) a lower heat demand to drive the endothermic pyrolysis process in the mixing zone or 2) higher heat release in the regenerator caused by a higher carbon loading from incomplete conversion. In fact, sounds from the pellets hitting the top of the riser could be heard, indicating that the pellets were barley devolatized even in the mixing zone andthe integrity of the pellets were .

Closing the mass balance was not practical based on the short time on stream and the operational problems encountered with feeding the hardwood pellets; but, bio-crude and aqueous phase samples were collected. Hydrocarbon liquid product was collected from both the high temperature coalescing filter directly upstream of the gas-liquid separator and the low temperature coalescing filter downstream of the heat exchanger. The “hot filter” product was collected at 90°C while the “cold filter” product was collected at ambient temperature after passing through the heat exchanger cooled to 7°C.

The elemental composition was determined and a semi-quantitative GC/MS analysis of each sample was performed. The “hot filter” sample was considerably more viscous than the “cold filter” sample and it was difficult to remove a small sample for CHON analysis. This sample also did not dissolve in the titrant used for Karl-Fischer water analysis and did not dissolve in methanol used as a solvent for the GC/MS analysis.. The “cold filter” sample was successfully analyzed and the results are present in Table 9.

Of note is that the water content was quite low indicating very good phase separation and the oxygen content was only 7.12 wt%. The semi-quantitative GC/MS analysis had many peaks that were unidentified or had poor match quality but the low oxygen content is consistent with the relatively low sugar, acid, and phenol content. During this campaign the pyrolysis temperature was maintained between 500-550°C. Pine feedstock that was found to feed well was also tested; but in this experiment, the main feed screw kept binding and causing the feed to stop. Attempts were made to correct this problem but ultimately the feed screw bound completely and would not turn. The “hot filter” and “cold filter” samples of the loblolly pine bio-crude were collected as described earlier. The elemental analysis and semi-quantitative GC/MS composition of the samples is compared to a “whole” pine bio-crude sample as shown in Table 9. The oxygen content of the heavy “hot filter” bio-crude fraction was 30.5 wt% with a comparatively high phenol, and acid content. The oxygen content of the “cold filter” light product was much lower (12.9 wt%). This correlated with a lower phenol and acid content compared to the heavy fraction. The PAH content was also significantly higher.

Table 9. Bio-crude Sample Analyses

	Pine Whole Oil	**Pine Light**	**Pine Heavy**	**Hardwood Light**	**Hardwood Heavy**
GC/MS (area %)					
Other	15.5	6.3	9.6	55.7	Sample did no dissolve in selected solvent
Aliphatic	0.6	8.5	11.2	1.7	
Aldehyde/Ketone	11.2	17.2	16.3	19.8	
Acid	4.5	0.0	5.1	1.9	
Total Aromatic	65.6	68.0	57.7	20.9	
Benzene	2.7	12.9	2.3	1.9	
PAH	8.4	42.3	17.4	17.5	
Phenol	54.6	12.8	38.0	1.5	
Sugar	2.6	0.0	0.0	0.0	
TOTAL	100.0	100.0	100.0	100.0	
Karl-Fischer					
water content (%)	14.44	1.86	20.85	0.70	Sample did not dissolve in KF titrant
Elemental (wt.%)					
C	58.03	78.75	61.91	83.68	27.72
H	7.24	8.39	7.58	9.04	10.15
O	34.11	12.86	30.51	7.12	62.13
N	0.62	0	0	0.16	0

Evaluation of the System for Extended Period

Pine feedstock was pyrolyzed with RTI-A10A catalyst for an extended period of 30 hours. The locally sourced loblolly pine was used as-received; particle size of 2 mm top size, average moisture content of 15 wt%, and the carbon (C), oxygen (O) and hydrogen (H) contents were respectively 47.4 wt%, 46.2 wt%, and 6.5 wt%. The average pyrolysis temperature was 520 °C and a total of 1130 kg of loblolly pine was reacted with the catalyst at a feed rate of 38 kg/h. The catalyst loading was about 120 kg and the catalyst-to-biomass ratio was approximately 2. Fluidization in the reactor was maintained with an average nitrogen flow 280 scfh; the established apparent residence times in the mixing zone and the riser were 1.48 s and 1.36 s respectively. The regenerator was maintained between 610-630 °C and air volumetric flow rate of approximately 1130 scfh was used to oxidize char and coke in the bubbling fluidized bed regenerator during the run. Water and additional air were added to the off-gas cooler to quench the flue gas from the regenerator. Approximately, a total of 28 L/h of water was utilized in the quench/separator system, the regenerator, and the regenerator off-gas cooler. The system pressure was stable between 4-5 psig throughout the campaign.

Figure 25 shows the temperature profile for the reactor mixing zone and the regenerator. The mixing zone temperature was between 500 °C and 530°C.The regenerator temperature was 100 °C higher than the reactor temperature due to the combustion of char and catalyst coke; and as such, provided the necessary heat for the endothermic biomass pyrolysis process. Figure 26

shows the steady-state operation gas flow profile for the system. It is worth mentioning that the experiment was briefly paused after 7.5 hours to remove char particles mixed with some organics (referred herein as tar-char) that had accumulated in the separator. The pilot-scale unit was run continuously afterward without any major operational issues until the 30-hour period.

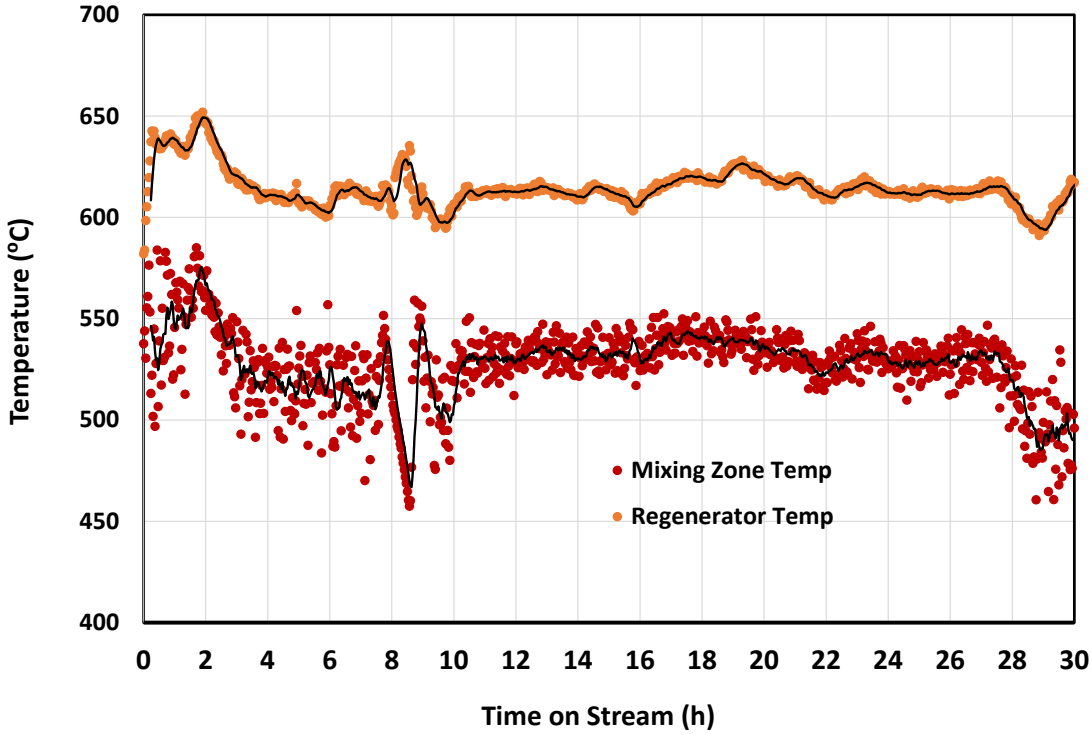

Figure 25. Pilot-scale CFP experiment temperature profile

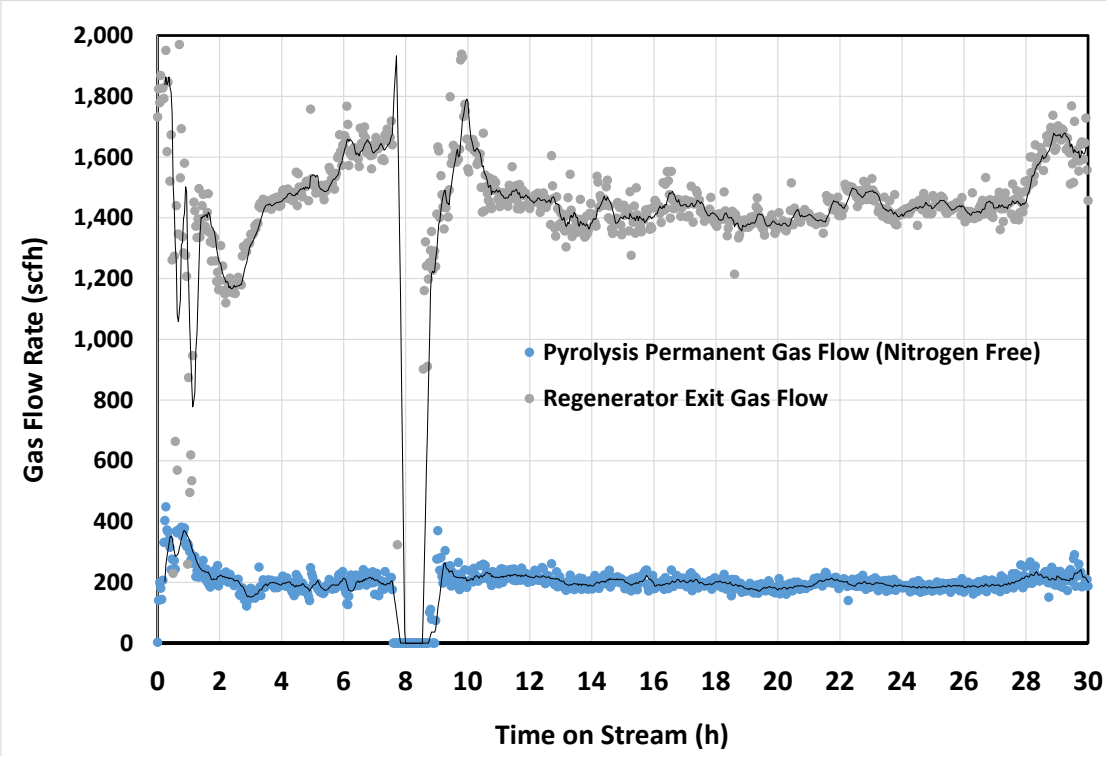

Figure 26. Pilot-scale CFP experiment gas flows profile

The pyrolysis products: organic liquid phase; aqueous phase; char/catalyst coke; and gases were analyzed to evaluate the process. With approximately 1130 kg of loblolly pine processed, a total of 109 litters (~ 29 gallons) of organic liquid product (biocrude) was collected representing 10.9wt% of the biomass. Specifically, 9.5 liters of light-organic liquid with KF moisture of about 4.9 wt%, 61.7 liters of heavy-organic liquid with a KF moisture of 11.2%, and 37.8 liters of another organic phase (termed as "indeterminate phase") with KF moisture between 45-55% were collected. The organic liquid was collected in two separate points in the process at different temperatures. The heavy organic product was collected with a coalescing filter downstream of the gas liquid separator and at a higher temperature (at ~ 90°C) than the light organic product that was collected in a coalescing filter downstream of the hot filters and a heat exchanger. The aqueous phase was also collected from the low temperature coalescing filter downstream of the heat exchanger. As shown in Table 10, the organic liquid phase accounted for 11.5% of the carbon balance and the aqueous liquid product also represented 13% of the biomass carbon. Overall, a total of 24.5% of the biomass carbon was recovered in the liquid products. About 50% of the biomass carbon end up in the gas phase (pyrolysis permanent gasses and regenerator flue gas). The carbon in the char and tar-char products accounted 23.6% of the biomass carbon. The lower carbon yield for the liquid products in this run is partly because some of the organic vapors condensed together with fine char/catalysts particles which escaped to the condensation train and formed this tarry product referred in this report as "tar-char". Minimization of this carbon loss to the tar/char product and the off-gases could increase the overall liquid carbon.

Table 10. Carbon Balance

Inputs		**Outputs**		
Biomass	1196 lbs	Heavy Organic Liquid Product	97 lbs	8 %
		Light Organic Liquid Product	16 lbs	1 %
		Aqueous Liquid Product	138 lbs	11 %
		Indeterminate Phase Product	27 lbs	2 %
		Pyrolysis Off-Gasses	261 lbs	21 %
		Regeneration Off-Gas	343 lbs	28 %
		Tar/Char at Separator	254 lbs	21 %
		Ash pot Char	54 lbs	4 %
Total	*1196 lbs*	*Total*	*1190 lbs*	
		Balance		*99.5%*

The KF moisture, density, and viscosity of the light biocrude were 4.9 wt%, 1.018 g/cm^3, and 4.1 cSt respectively while that of the heavy biocrude were 11.4 wt%, 1.162 g/cm^3, and 154 cSt respectively. As indicated by the results and implied by their descriptive names; the heavy biocrude was denser and viscous than the light biocrude. Additionally, the organic elemental analysis on dry-basis indicated that the light organic fraction had an average carbon content of 78.4% and oxygen content of 13.6.0%. In contrast, the heavy biocrude had an average carbon content of 69.2% and the average oxygen content was 24.2.0%. The combined bio-crude product (light and heavy) would have 70.2 wt% carbon and 23.1 wt% oxygen on dry basis Clearly, the light biocrude was less oxygenated, which partly explains why it was less dense and viscous. Further analysis of the biocrude by simulated distillation (ASTM-D7213-C) confirms that the light contained higher amount of lower boiling point components than the heavy biocrude. For example, the gasoline range fraction (<216°C) in the light biocrude was 50wt% and that of the

heavy biocrude was about 25wt%. Based on GC/MS and ^{13}C-NMR analyses, the light fraction was found to be rich in mono-aromatic hydrocarbons, aliphatic hydrocarbons, monofuctional phenolics, and some ketones. The heavy fraction was found to contain mainly methoxylated and multi-functional phenolics. Other chemical species identified in the heavy fraction include poly-aromatic hydrocarbons, furans and hydroxyl-carbonyls (See Figure 27).

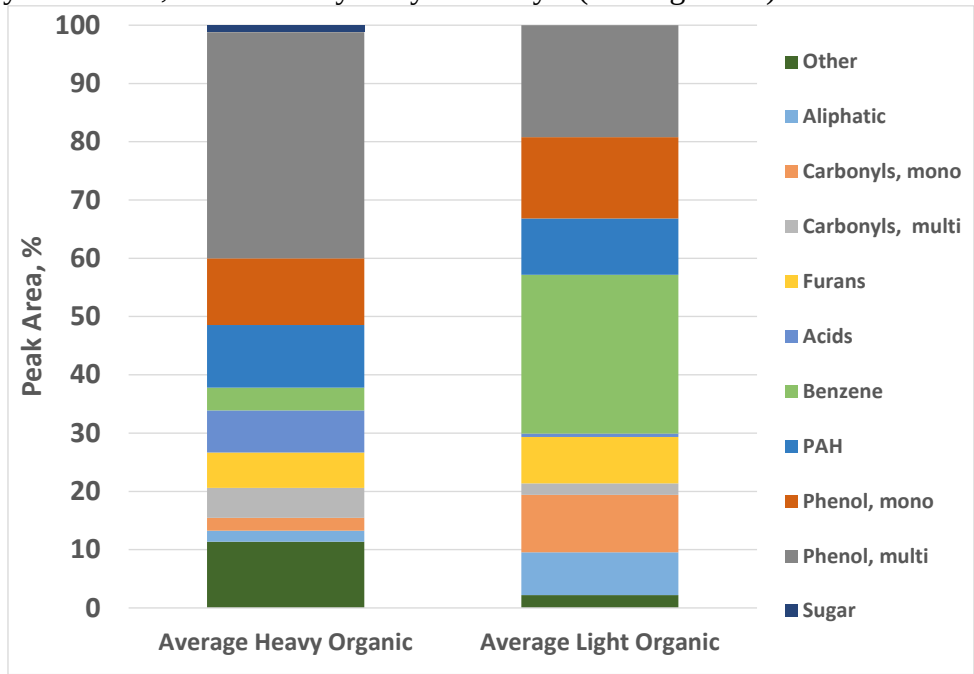

Figure 27: Distribution of various functional groups based on GC/MS analysis present in the organic liquid fractions collected during the 30-hour campaign.

Parametric Studies: The Effect of Temperature

The effect of temperature on the pyrolysis product distribution and the operability of the 1TPD system was investigated. Locally sourced loblolly pine (with a moisture content about 12-15 wt%.) and RTI-A10A catalyst were used for the study. The distribution of hydrocarbons (light phenolics through heavy PAHs) in the bio-crude can have a direct impact on the operability of the 1TPD unit. Specifically, the accumulation of high molecular weight tars in the quench system causes lower bio-crude yields and operational problems over time. The yield of higher molecular weight hydrocarbons is thought to be a function of temperature. The process temperatures investigated were 425°C, 465°C, 485°C, 520°C, and 575°C. All the experiments were performed at a feed rate between 60-70 kg/h over fresh solid acid catalyst each time. In most cases, the experiments were allowed to run for at least 12 hours before they were purposely terminated. Overall, the 1TPD unit was run for a cumulative period of at least 68 hours. Steady-state operations were achieved for all tests except for one of the experiments at 520 °C and the experiment at 575 °C that lasted for 4 and 7 hours respectively. The cause for the unplanned shutdowns in each case was a plug, at different points in the process, that resulted in an increased system pressure. For the experiment at 575 °C, the plug was caused by higher molecular weight (HMW) tarry oil mixed with char particles that accumulated in the quench just upstream of the separator. For the experiment at 520 °C, a leak through the side of the main feed screw in the mixing zone was identified. As the leak was sealed, the feedrate rapidly increased which unfortunately injected large volume of biomass feed into the pyrolysis side/riser tube causing a

plug. Thus, mass and carbon balances were only performed for the experiments with at least 6 run hours. Nonetheless, all the pyrolysis products: organic liquid phase; aqueous phase; char/catalyst solids; and permanent gases were analyzed to evaluate the process. In some of the experiments, bio-crude samples were collected at different time intervals to determine yield and composition changes as a function of time on stream. The first sample was usually collected after 4 hours and the subsequent samples were collected every 2 hours until shut down. The collection of the bio-crude at different time intervals enable stead-state yield analysis to be performed.

Effect of temperature on the liquid products

Figure 28 below shows the effect of temperature on the carbon yields of bio-crude and aqueous fractions. Detailed carbon balances for the experiment at 465 °C and 575 °C are presented in Table 11 and Table 12 respectively for comparison. In general, the total liquid carbon yield increased as temperature increased from 425°C through a maximum at 465°C before it decreased gradually at 575°C. The total carbon yield for bio-crude and aqueous fraction at 465°C was 41.05 % with 17.2% in the organic phase and 23.13% in the aqueous phase. On the other hand, at 575 °C, a total of 16.7% of the biomass carbon was recovered in the liquid product with 7.8% in the organic phase and 9% in the aqueous phase. Also, at 520 °C the carbon recovery in the liquid product equaled 24.5% with 11.5% in the organic phase and 13% in the aqueous phase. Overall, the highest bio-crude carbon yield was 17.2 wt% and the lowest was 7.78wt%. Steady-state bio-crude yields (Figure 29) based on dry biomass feedrate for CFP temperatures of 425°C, 465°C, and 485°C would result in average steady state yields of 40 gallons per dry ton, 48 gallons per dry ton, and 38 gallons per dry ton, respectively. These results suggest that perhaps devolatilization at the lower temperatures was not complete while over-cracking at the higher temperatures reduced bio-crude yield. Specifically, the relatively higher carbon recovery to the liquid product for the run at 465°C could be attributed to the fact that devolatilization was more complete and thermal cracking was less severe at that condition. This probably explains why the aqueous fractions at 465°C was significantly higher than 425°C. In contrast, the decrease in the liquid yields with temperature increase could be attributed to extensive cracking of the primary vapors into non-condensable gases and coke. Therefore, at 575 °C, the reaction severity was high and extensive cracking of the vapors was favored, hence the organic liquid yield was lower. It is also worth pointing out that the lower yield at 575 °C could be due to unaccounted losses since the run had operational issues. In a nutshell, moderate temperatures ($450 \leq T < 500$) would be appropriate in producing high yields of bio-crude based on the current findings with loblolly pine feedstock.

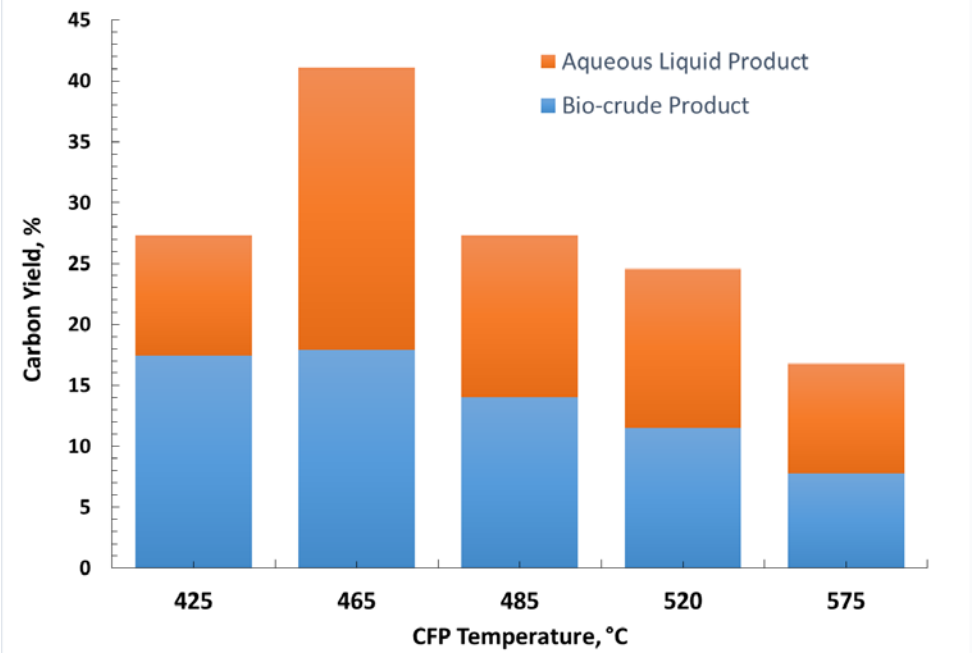

Figure 28: Effect of CFP temperature on the yields of bio-crude and aqueous liquid.

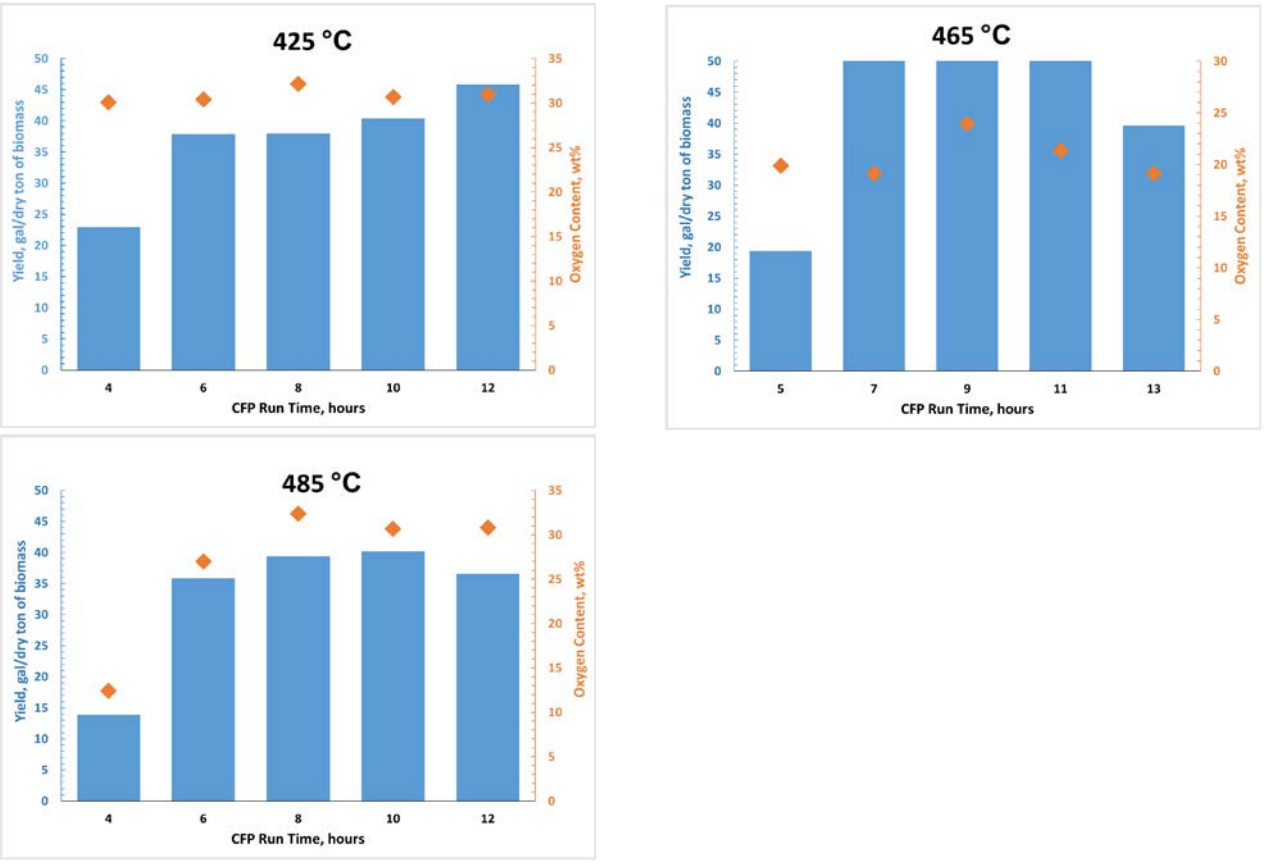

Figure 29: Bio-crude yields in gallons per dry ton of biomass showing the effect of CFP temperature.

Table 11. Carbon Balance for Experiment at 465 °C

Inputs		**Outputs**		
Biomass	388 kg	Heavy Organic Liquid Product	69.54 kg	17.92%
		Light Organic Liquid Product		
		Aqueous Liquid Product	89.74 kg	23.13 %
		Pyrolysis Off-Gasses	46.0 kg	11.16 %
		Regeneration Off-Gas	112.7 kg	29.03%
		Tar/Char at Separator	62.71 kg	16.16 %
		Ash pot Char	30.60 kg	7.88 %
Total	*388* kg	*Total*	*411.3* kg	
		Balance		*105%*

Effect of temperature on the product gas

The effect of temperature on the composition of product gas is provided in Figure 30. It can be seen from the chart that the concentration of hydrogen, methane, and C_2^+ light hydrocarbons increases with increasing temperature while the carbon dioxide concentration decreases with increasing temperature. Interestingly, the concentration of carbon monoxide did not appear to be influenced at the temperatures investigated. Typically, higher temperatures tend to result in higher concentration of CO since studies have reported that the formation of CO is highly influenced by secondary reactions (decarbonylation) of low molecular weight products (ring-opened intermediates).

Table 12. Carbon Balance for Experiment at 575 °C

Inputs		**Outputs**		
Biomass	195 kg	Heavy Organic Liquid Product	14.4 kg	7.4%
		Light Organic Liquid Product	0.70 l kg	0.36 %
		Aqueous Liquid Product	17.5 kg	8.97 %
		Pyrolysis Off-Gasses	26.86 kg	13.78 %
		Regeneration Off-Gas	47.3 kg	24.29%
		Tar/Char at Separator	13.45 kg	6.9 %
		Ash pot Char	15.10 kg	7.75 %
Total	*195* kg	*Total*	*135.36* kg	
		Balance		*69.45.5%*

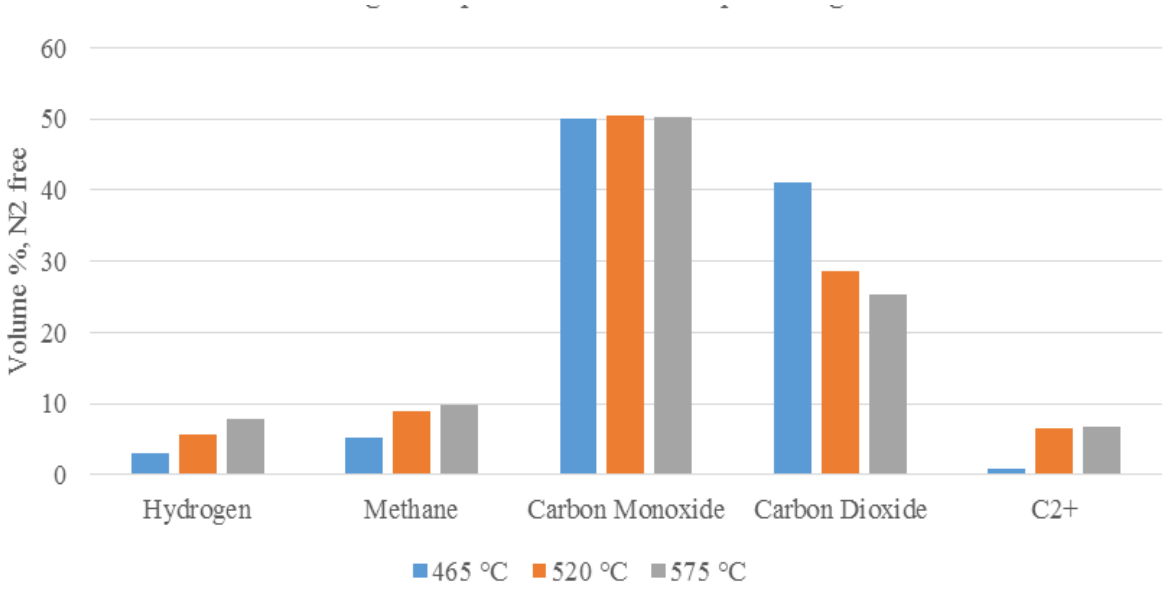

Figure 30: Effect of temperature on the composition of the CFP product gas

Effect of temperature on the composition of bio-crude.

Figure 31 shows the effect of temperature on the oxygen and carbon contents of the bio-crude fractions. As expected, the oxygen content of the bio-crude generally decreased with temperature. However, it is important to point out that the effect was not significant for temperatures between 465°C and 575°C. The CHON analysis indicated that the bio-crude produced at 425°C was the least deoxygenated with an oxygen content of 30.85wt%. The most deoxygenated bio-crude was produced at 575°C with an oxygen content of 21.16wt%. Interestingly, the bio-crude produced at 465°C had comparable oxygen content with the bio-crude at 575°C. This further suggests that the use of high CFP temperature was not advantageous in terms of both liquid yield and degree of deoxygenation.

The effect of temperature on the bio-crude chemical composition is shown in Figure 32. The GC/MS analysis indicates that compounds such as anhydrosugars, methoxylated phenolics, and PAHs were influenced by the CFP temperature. Bio-crudes produced at temperatures below 500 °C had measurable amount of levoglucosan and a significant amount of methoxylated phenolics whereas bio-crudes produced at temperatures above 500 °C had a higher amount of mono-functional phenolics and PAHs. In fact, the experiment at 575 °C produced a significant yield of PAHs. For carboxylic acids and other carbonyl compounds, the CFP temperature does not seem to have a considerable effect.

It can be inferred from the compositional analysis of the bio-crudes that reactions such as dehydration and dehydrogenation were enhanced at higher CFP temperatures which explain the formation of PAHs. However, reactions such as decarboxylation and decarbonylation were not influenced by temperature, which could also explain why the carbonyl functionalities were not significantly affected. These observations suggest that deoxygenation reactions are more influenced by the catalyst than operating conditions such as temperature.

Also, the effect of temperature on other physicochemical properties (see Table 13) such as density, viscosity, and distillation characteristics wasn't straightforward. In general, the effect of temperature on the physicochemical properties of the bio-crudes appear to be subtle.

Overall, the most significant effect of temperature in the CFP process appear to be on the yield of the products and operability of the system. As realized in the high temperature run, the carbon recovery in the liquid product is lower and the production of HMW compounds could cause operation problems in the condensation train.

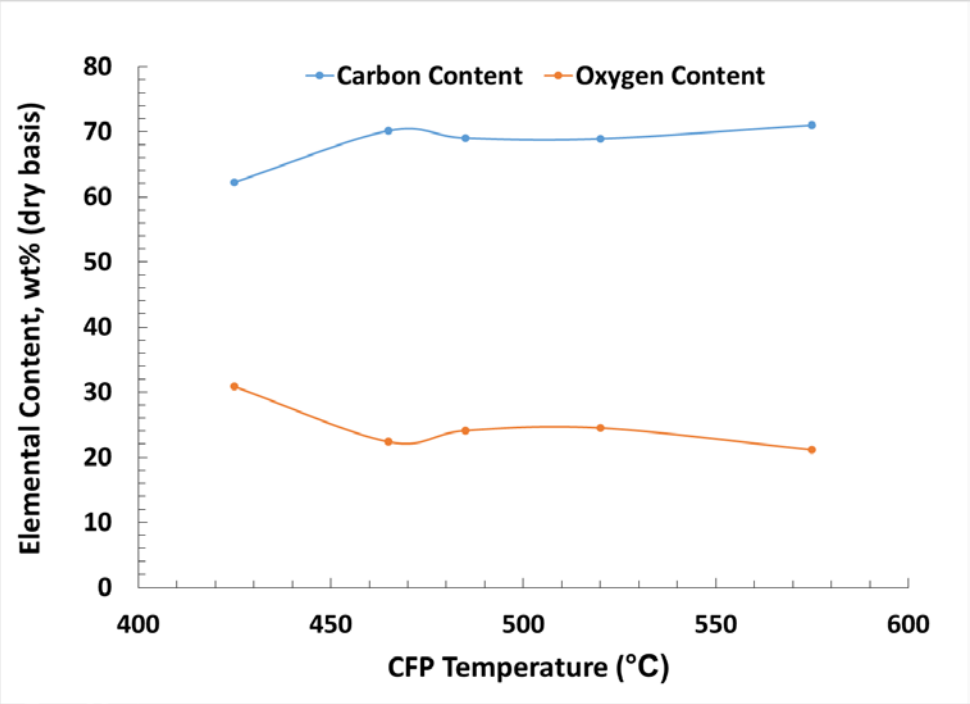

Figure 31: Effect of temperature of the oxygen and carbon contents of the bio-crude fractions.

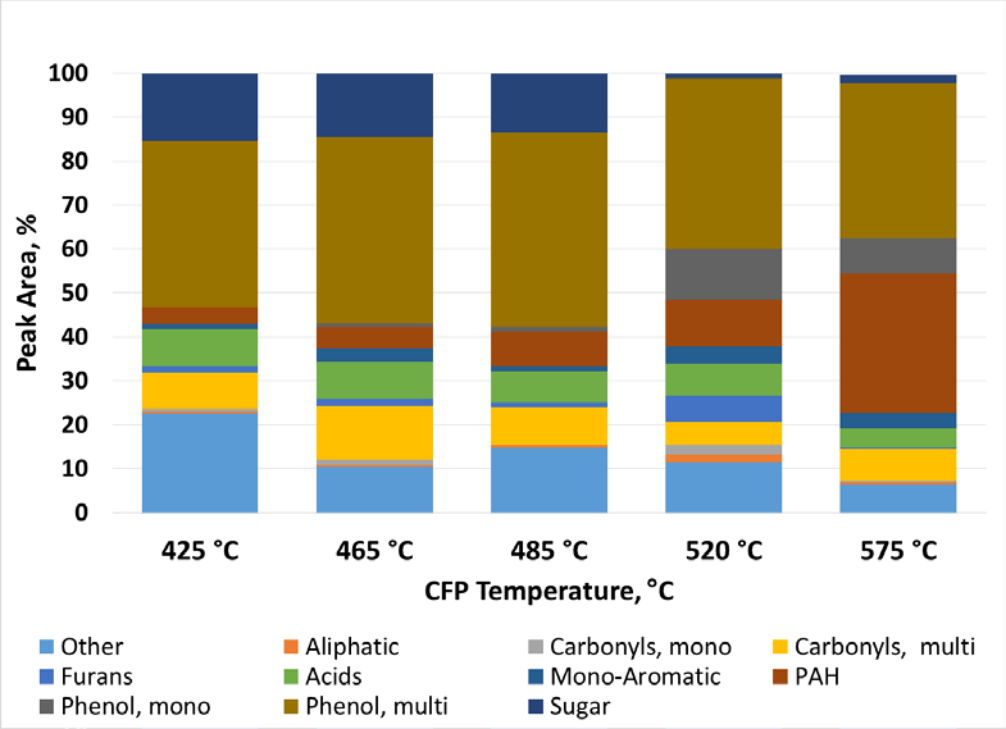

Figure 32: Effect of CFP temperature on the composition of bio-crude

Table 13. Elemental and physical property analysis

Elemental, wt.%(dry basis)	Heavy Organic Fraction		
	465 °C	520 °C	575 °C
C	70.15	68.91	71.01
H	7.21	6.58	7.32
N	0.32	0.00	0.51
O*	22.37	24.50	21.16
Density, g/cm^3 (ASTM D4052)	1.218	1.154	1.194
Kinematic Viscosity, cSt (ASTM D445)	294	154.35	205.1
Distillation (ASTM D1160)			
IBP, °C	107.3	101.1	105.7
10% (T10), °C	110.9	109.1	110.0
20% (T20), °C	153.4	171.1	186.6
30% (T30), °C	202.4	217.9	241.1
40% (T40), °C	246.7	248.4	265.2
50% (T50), °C	284.4	284.9	301.0
60% (T60), °C	331.2	315.6	327.1
70% (T70), °C	335.9	351.0	

*By difference

Effect of Gas flow rate on the CFP product distribution

A 20-hour steady state experiment in the 1TPD system was performed with loblolly pine to examine the impact of gas flow rate on the CFP product distribution. This experiment adds another process variable to the parametric studies that evaluated the effect of CFP temperature (425°C, 465°C, 485°C, 520°C).

The experiment was conducted at an average process temperature of 460°C. The loblolly pine used had a moisture content of about 15 wt% and 1230 kg of biomass was processed at an average feed rate of 63 kg/h. The catalyst was RTI-A10A with a mean particle size of approximately 70 µm. The regenerator temperature was maintained at 600 °C. The average N_2 flow rate into the pyrolysis mixing zone was 525 scfh and the average air flow rate into the generator was 1670 scfh. As shown in Figure 33 the N_2 flow rate was 600 scfh for the first 11 hours, was changed to 400 scfh for 6 hours, and increased back to 600 scfh for the remainder of the run.

The experiment continuously ran without any major process upsets, plugs, or pressure excursions and was purposely terminated after about 20 hours of biomass feeding. All the pyrolysis products: organic liquid phase; aqueous phase; char/catalyst solids; and permanent gases were analyzed. The bio-crude samples were collected at different time intervals to determine yield and composition changes as a function of time on stream. The collection of the bio-crude at different time intervals enabled steady-state yield analysis to be performed.

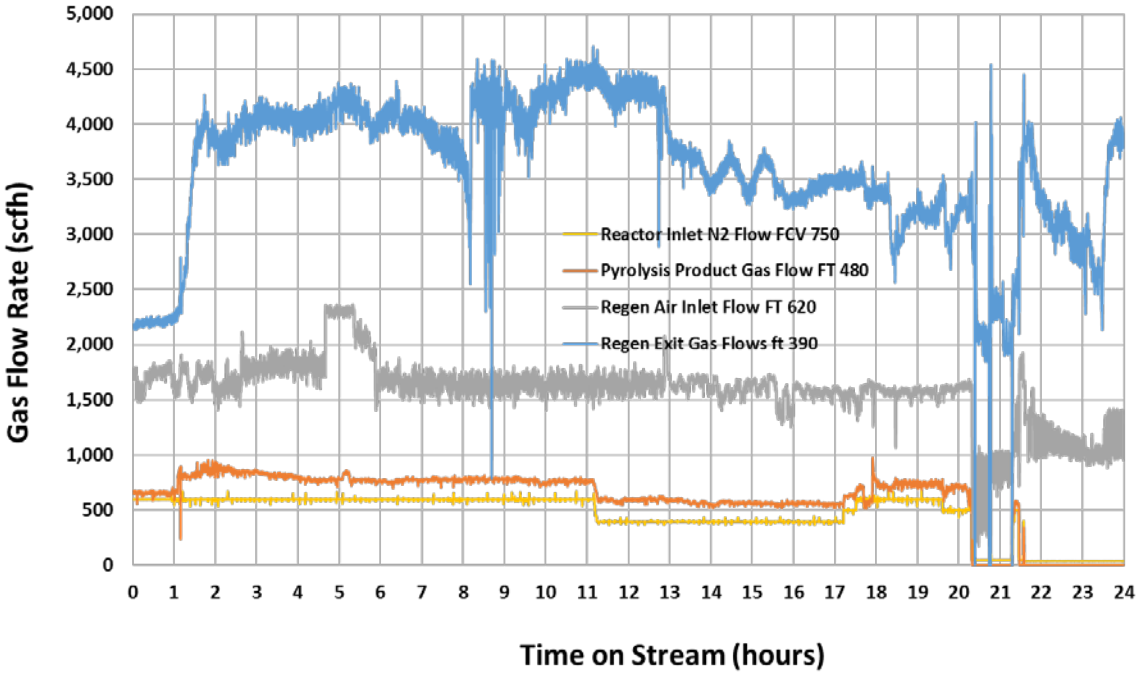

Figure 33: Reactor and Regenerator Gas Flows

Table 14 shows the carbon distribution for the catalytic pyrolysis products. The carbon balance was 76%. Unaccounted tar-char product not recovered from the gas-liquid separator likely reduced the carbon closure. The total carbon yield for bio-crude and aqueous fractions were 6.7 % and 10.2 % respectively. The pyrolysis permanent gas and the regeneration off-gas accounted for 3.7% and the 42.5% of the biomass carbon. Clearly, the conditions used in this experiment reduced the pyrolysis liquid yields. A comparison of the results from a previous run at similar temperatures (460 °C) and biomass feed rate (65 kg/h) suggest that the higher nitrogen flow rate reduced the devolatilization efficiency during catalytic pyrolysis (Figure 34).

It is well known that the fluidizing gas flow into the reactor influences the pyrolysis vapor contact time with the catalyst and the overall apparent residence time in the mixing zone and the riser. Higher N_2 flow rate leads to shorter residence times. At 460 °C, a gas flow rate of 450 scfh and 600 scfh establishes a total apparent residence time of approximately 1.0 s and 0.75 s respectively in the mixing zone. The difference doesn't seem significant. Nevertheless, in the absence of other data points, the results in Figure 34 suggest that for process temperature around 460 °C, gas flows higher than 450 scfh negatively impacts the liquid yields. Based on the low pyrolysis gas yield (3.7%), it can be inferred that, the use of 600 scfh with biomass feed rate of 65 kg/h decreased the contact time for the biomass particles in the mixing zone and probably, as a result complete devolatilization and efficient primary cracking of the pyrolysis vapors was not established. Also, the high yield of regenerator off gas (42.5%) suggest that char particles that transferred from the riser may not have undergone complete devolatilization. The composition of the pyrolysis gas supports this interpretation.

CO_2 was the most abundant pyrolysis gas as shown in Figure 35 while the concentration of CO was lower. Typically, fast pyrolysis of woody biomass yields equal concentration of CO and CO_2 while catalytic fast pyrolysis in general tend to form more CO than CO_2 due to catalytic cracking. Also, past studies with the same catalyst and biomass feedstock at the same pyrolysis

temperature have shown higher concentration of CO than CO_2. Therefore, the minimal formation of CO at high gas flow rate supports the notion that devolatilization and efficient primary cracking of the pyrolysis vapors was not complete at the higher nitrogen flow rates. Ultimately, a future studies at various gas flow rates and temperatures may reveal the effect of the residence time with some level of certainty.

Table 14. Carbon distribution for pyrolysis products

Carbon Balance				
Inputs, kg		**Outputs, kg**		
Biomass	582.9	Heavy Organic Liquid Product	39.0	6.7 %
		Aqueous Liquid Product	59.4	10.2 %
		Pyrolysis Off-Gasses	21.6	3.7 %
		Regeneration Off-Gas	247.9	42.5 %
		Tar/Char at Separator	39.7	6.8 %
		Ash pot Char	35.7	6.1 %
Total	582.9	Total	443.4	
		Balance		76.0%

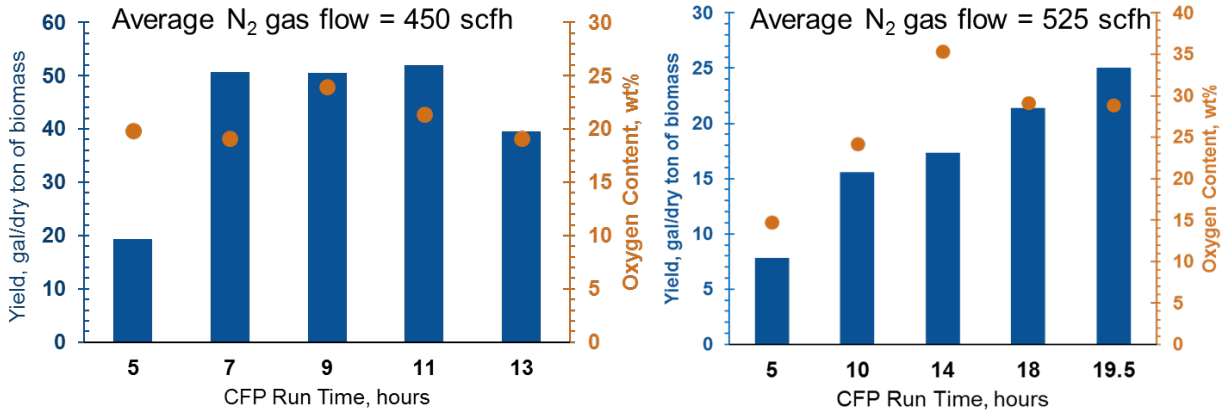

Figure 34: Potential effect of N_2 gas flow rates

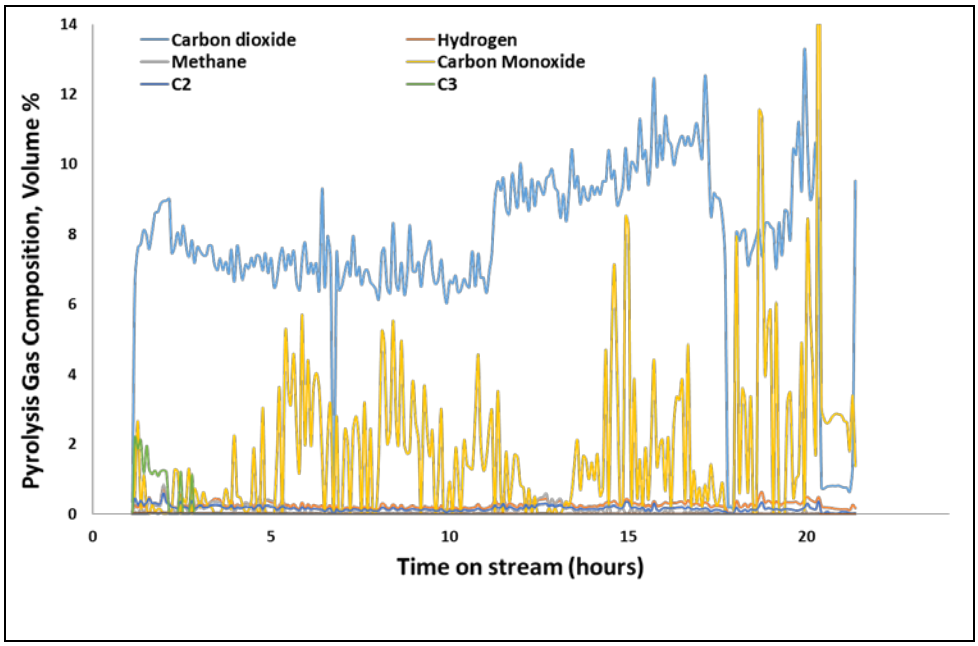

Figure 35: CFP product gas composition in N_2

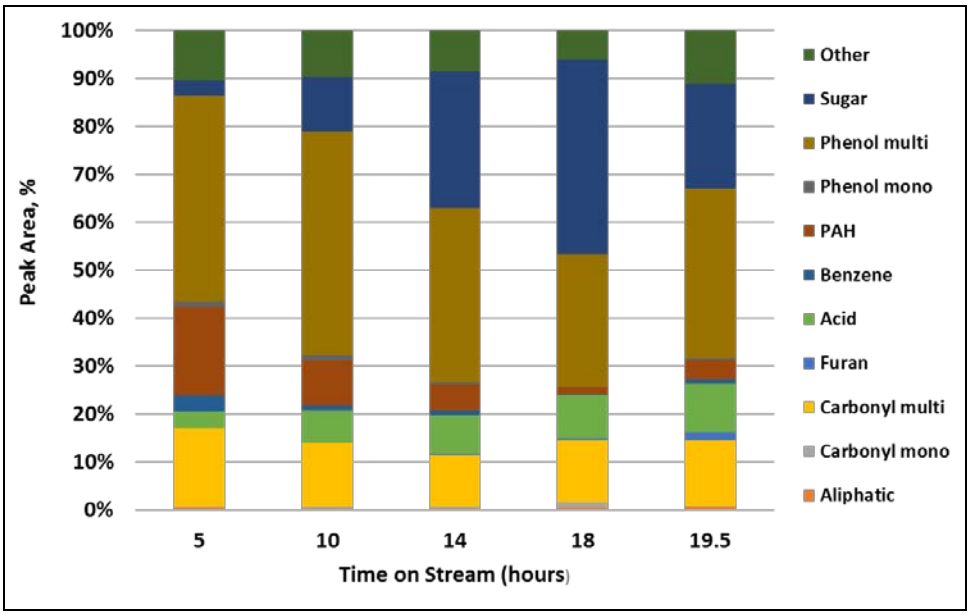

Figure 36: Change in the chemical composition of the produced bio-crude with time-on-stream

The composition of the bio-crude collected seems to have been affected as well. Overall, the average oxygen content was 26.46 wt%, a bit higher than typically measured at this pyrolysis temperature. The bio-crude oil collected between 10-14 hours on stream had high oxygen content (35.35 wt%). This means that effective deoxygenation did not occur at higher gas flow rate. Furthermore, the chemical composition by GC/MS analysis shown in Figure 36 indicates that multifunctional carbonyls, anhydrosugars, and methoxylated phenolics were the most abundant groups of compounds present. The amount of PAHs was high in the biocrude collected within the first 5 hours of the run; but as time went on, the amount decreased and this may be attributed

to catalyst deactivation or loss. On the contrary, the amount of anhydrosugars and acidic groups increased with time-on-stream. Clearly, the bio-crude oil from this run contained higher amount of oxygenated compounds. Again, this substantiates the other notion that the pyrolysis vapors also did not have sufficient residence time to undergo deoxygenation at higher gas flow rates.

Catalytic Pyrolysis of Red-Oak

The effect of gas flow rate into the reactor was further studied with red-oak. Three experiments were conducted with a non-zeolite alumina based catalyst.The red oak was sourced from Iowa State University and was used as-received; particle size was less than 2 mm, average moisture content was10 wt%, and the carbon (C), oxygen (O), hydrogen (H), and nitrogen (N) contents on wet-basis were respectively 45.5 wt%, 47.7 wt%, 6.4 wt%, and 0.4 wt%. Table 15 summarizes the conditions used in each experiment. The flow of N_2 into the mixing zone and the riser section of the reactor for fluidization was the primary parameter that varied. Operationally, experiment 1was interrupted intermittently due to malfunctioning of the thermal oxidizer and as a consequence, biomass feeding into the reactor was inconsistent; thus the experiment was terminated after 7 hours of run time. In experiments 2 and 3, the biomass unit operated very smoothly for the first 5 hours. Nonetheless, operational issues such as biomass bridging in the feeding system resulted in unplanned shutdowns in each case. Specifically for experiment 2, the bridging of the biomass caused pressure excursions which blew catalyst out of the loop seal.

Table 15. Red Oak CFP Experimental Conditions

Conditions	Experiment 1	Experiment 2	Experiment 3
Average mixing zone temperature, °C	519	521	502
Average riser temperature, °C	494	495	493
Average regenerator temperature, °C	631	636	626
Average fluidization gas flow rate, mixing zone section, scfh	531(0.8s)	50(8.3s)	463(0.9s)
Average fluidization gas flow rate, riser section, scfh	731(0.5 s)	530(0.7s)	563(0.7s)
Average biomass feed rate, kg/h	40	71	74
Run Time, h	7	6	7

( ) apparent vapor residence time based on N_2 flows at the specified temperature

Table 16 shows the carbon balances. For experiment 1, no organic liquid was collected and about 15.3 % of the biomass carbon was recovered in the aqueous phase product. Most of the biomass carbon ended up as regenerator off gas (70%) and about 10% as pyrolysis non-condensable gas. This can be attributed to the use of high fluidization flow in the mixing zone which established a short vapor residence time (< 1 s) which probably prevented complete devolatilization of the biomass and as a consequence more unconverted organic matter (char) was transferred to the regenerator as reflected in the off gas carbon. In contrast, as the vapor residence time (8.3 s) was high in the mixing zone for experiment 2, about a total of 25 % of the carbon was recovered as liquid product with 5.8% in the organic phase and 19.8 % in the aqueous phase. The carbon in the regenerator off gas consequentially decreased to 42%. In experiment 3, a total of 21.8 % of the biomass carbon was recovered in the liquid product with 7.2% in the organic phase and 14 % in the aqueous phase. It should be noted that even though the N_2 gas flow into the mixing zone for experiment 3 was relatively higher than that used in experiment 2, the total N_2 flow into the reactor for each experiment (2 & 3) was similar. At least,

the three experiments conducted with the red oak provided some indication that the vapor residence in the mixing zone and the riser would have to be optimized to enhance the liquid yield.

Table 16. Carbon distribution of the red oak CFP Products

Pyrolysis Products	Carbon Yields, %		
	Experiment 1	Experiment 2	Experiment 3
Organic liquid	-	5.8	7.2
Aqueous liquid	15.3	19.8	14.6
Total Liquid	-	25.6	21.8
Pyrolysis gas	9.8	10.9	9.4
Regenerator gas	70.2	42.4	38.7
Char (Ash pot)	-	0.1	0.1
"Tar-char"	-	5.3	10.8

The composition of the pyrolysis product gas is as shown in Table 17. For the 3 experiments with alumina, the volume composition of the pyrolysis gas product was identical and the carbon oxides; CO and CO_2 dominated (about 90%). The composition of hydrogen and light hydrocarbons including methane accounted about 10% of the pyrolysis gas from alumina.

Table 17.Pyrolysis Gas Composition, Vol% (N_2 free)

Pyrolysis Gas	Pyrolysis Gas Composition, Vol% (N2 free)		
	Experiment 1	Experiment 2	Experiment 3
H_2	2.4	2.2	2.0
CH_4	6.9	7.5	6.9
CO_2	39	39.7	38.9
CO	49.7	50.7	50.1
C_2+	1.8	<0.1	2.1

The CHON analysis showed that the bio-crude from red oak in experiment 2 had carbon and oxygen contents of 69.6% and 23.7 % respectively. On the other hand, the red oak biocrude from experiment 3 had relatively lower carbon content (63.4%) and higher oxygen content (29.2%) with respect to the biocrude from experiment 2. The results suggests that deoxygenation of the primary vapors in experiment 3 was not as effective as seen in experiment 2, and that could be because the contact time for primary pyrolysis vapors and the circulating catalyst was relatively shorter in experiment 3(due to high fluidization flow in mixing) than in experiment 2 (low fluidization flow in mixing zone).

Table 18. Organic elemental composition of the biocrudes

Organic Elements	Composition, wt% (dry)		
	Experiment 1	Experiment 2	Experiment 3
Carbon	-	69.6	63.4
Hydrogen	-	6.4	6.5
Nitrogen	-	0.3	0.9
Oxygen	-	23.7	29.2
Moisture	-	12.6	13.3

The bio-crude GC-MS chemical composition by area percent is shown in Figure 37. The analysis indicated that the biocrudes produced from red oak with the non-zeolite alumina based catalyst contained primarily methoxylated phenolics (primarily syringols) and carbonyl functionality compounds such as ketone (e.g. butanone) and aldehydes (e.g. furfural). The amount of acids, simples phenols, and mono-aromatics present in the biocrudes from experiment 2 and experiment 3 differed slightly. For instance, the biocrude from experiment 3 contained relatively higher amount of acidic groups and mono-aromatics. Also, the biocrude from experiment 2 had higher amount of polyaromatic hydrocarbons and simple phenols than the biocrude from experiment 3.

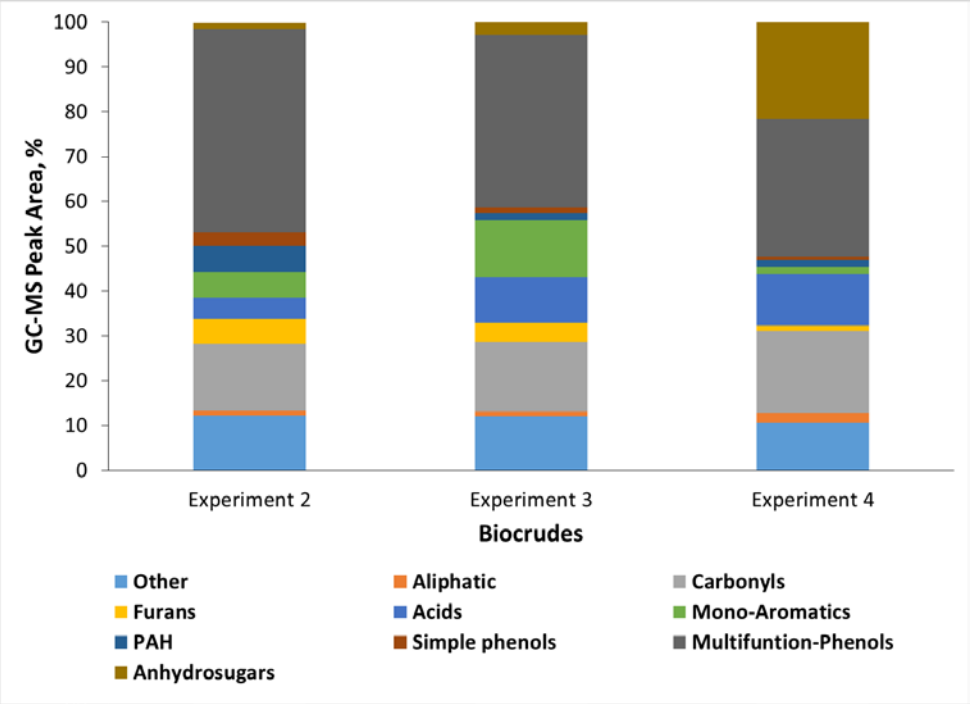

Figure 37: GC-MC Chemical composition of the biocrudes produced from experiments 2, 3, and 4

Bio-crude Characterization and Analysis

Chemical characterization of biocrude provides important information for downstream processing to biofuels and biochemicals. Up to date, complete analysis of bio-oil/biocrude is very challenging due to the presence of many polar and non-volatile species. For example, gas chromatography (GC) analysis is only limited to the detection of volatile species. Typically, for raw pyrolysis oils, it has been found that 38wt% and 14wt% of could be determined by gas (GC) and liquid chromatography (LC), respectively. These chromatographic techniques have been typically employed for the analysis of volatile and non-volatile components of pyrolysis oils, respectively. Thus, different number of techniques including HPLC and HPLC/electrospray MS, Fourier transform infrared (FTIR) spectroscopy, gel permeation spectroscopy (GPC), and nuclear magnetic resonance (NMR) are used together to fully characterize bio-oils/biocrudes.

In this project, existing and new analytical techniques were used to characterize the biocrude produced from the 1TPD pilot plant. Comprehensive two-dimensional GC (GC×GC) can be very efficient for the characterization of phenols and alcohols. Supercritical fluid chromatography (SFC) could also be used as a pre-fractionation step to improve the separation in GC×GC for a very complex mixture. In SFC, a super- or subcritical fluid (mostly CO_2 or a mixture with an organic solvent) is employed as the mobile phase allowing for a higher optimal velocity and shorter analysis times, which makes SFC a highly efficient chromatographic platform[11]. The separation can be described as normal-phase-like, i.e., nonpolar compounds are less retained than polar compounds. This can be highly advantageous for the analysis of oxygen-containing species, especially in combination with HRMS and negative electrospray ionization (ESI-) which is rather selective for hydroxylated and carboxylated compounds[12]. Furthermore, for thermally-labile and/or non-volatile compounds (e.g., with low vapor pressures caused by a high polarity), derivatization could be used to enhance analysis by GC. Fourier transform ion cyclotron resonance mass spectrometry (FT-ICR MS) is also a form of high resolution mass spectrometry that yields great insight to the characterization of complex mixtures. FT-ICR MS provides the unique combination of ultrahigh resolving power (the ability to resolve mass spectral signals differing by < 1 mDa) and accurate mass determination (determination of molecular masses to ~5 decimal places). Thus, the techniques used include GCXGC-FID, GCXGC-MS, SFC-ESI—MS, and FT-ICR MS.

Analytical Methods

Gas Chromatograhy by Gas Chromatography with Flame Ionization Detection (GC×GC-FID)

Biocrude samples were analyzed by GC×GC-FID using a Thermo GC×GC-FID instrument comprising of a programmed temperature vaporizing (PTV) injector, a dual-jet two-stage cryogenic (liq. CO_2) modulator and a flame ionization detector (FID). The column system comprised of two serially connected fused silica columns including a 30m*0.25mm*0.25um Rtx-1701 as 1D column and a 1.5m*0.15mm’0.15mm Rxi-5Sil MS as 2D column. The GC oven was programmed from 40° to 300° C @ 2.5° C/min, the He carrier gas flow was 1.5 mL/min. The modulation period was 8 sec, and the PTV was operated in split mode with a split ration of 1:100 and rapidly heated to 350° C for 2 min for sample transfer. The biocrude samples were dissolved in THF (1:1, v/v) and analyzed in duplicates in two different batches together with

solvent blanks, fraction blanks and QC (a dewatered non-fractionated raw pyrolysis oil dissolved in THF, 1:1) and a reference sample (light gas oil, dissolved in tetrachloromethane, 4:1). The analyses were in triplicates in three different batches, and together with control samples as above.

Gas Chromatograhy by Gas Chromatography with Mass Spectrometric Detection (GC×GC-MS)

The biocrude were also analyzed by GC×GC-MS using a LECO Pegasus 4D instrument comprising a PTV injector, a quad-jet two-stage cryogenic (liq. N2) modulator, a secondary oven and a time-of-flight mass spectrometer (ToF-MS). The column system was similar to that used for GC×GC-FID, just as the GC oven and PTV injector were operated in the same mode as described above. The secondary oven was operated with a 5° C offset to the main oven and the modulator with a 15° C offset to the secondary oven. The MS was operated at a scan rate of 100 Hz in a m/z range of 41 to 541, and with a source temperature of 225° C. The GC×GC-MS analyses were used for the identification of compound classes in the 2D color plots. Based on the GC×GC-MS identification of compound classes similar compound classes were identified in the GC×GC-FID color plots and used for setting up an integration template, that was used for integrating the area counts of each compounds class using a proprietary software including preprocessing (baseline subtraction and alignment) developed by Copenhagen University. Area counts were then normalized in two ways: 1) by normalizing to the sum of area counts for all compound classes giving the Area-%, and 2) by normalizing to the area count of the compound class of aliphatics. The latter because it was considered, that the aliphatics would remain relatively unaffected and thus give an unbiased normalization factor. Eventually, averages of the three batches were calculated.

Supercritical Fluid Chromatography with High Resolution Mass Spectrometric Detection (SFC-HRMS)

Biocrude Samples were analyzed in triplicates (A, B and C) with an Acquity UPC2 and G2-Si Synapt HRMS from Waters (Massachusetts, USA). 0.1 g of the samples was solved in 10 mL dichloromethane: methanol (50:50) and stored at -20°C in amber-glass vials until analysis (final concentration: 0.1 µg/mL).

Carbon dioxide and ethanol were used as A- and B-solvents, respectively. The gradient program followed: hold at 1% B for 0.75 min, increase 0.33% B/min for 10.5 min, 1.92% B/min for 13.25 min, hold at 30% B for 5.5 min, back to original conditions within 0.1 min and an isocratic hold for 4 min. The total run time was 35 min with a flow rate of 1.5 mL/min, and an injection volume of 1.5 µL. The separation was performed on a 2-picolylamine column (3.0×100 mm, 1.7 µm) plus VanGuard pre-column (2-picolylamine, 2.1×5.0 mm, 1.7 µm), both from Waters (Massachusetts, USA) at 40°C column temperature. The sample needle washing solvents were isopropanol and methanol-water (80:20) as weak and strong washing solvents, respectively. The backpressure was set to 2,176 psi (150 bar). The connection between SFC and MS was established via a splitter device (Waters, Massachusetts, USA) with methanol as a make-up solvent and flow rate of 0.3 mL/min. Ionization was performed via an electrospray in negative mode (ESI-). MS-parameters were: capillary voltage - 2.5 kV, source temperature - 120°C, scan rate - 0.5 sec/scan and mass range - 50 to 600 Da. A lockspray calibration was performed every 30 sec with leucine-enkephaline as the reference compound (mass: 554.2615 Da). MassLynx 4.0 was used for data acquisition and the data was converted into NetCDF files via Databridge

(Waters, Massachusetts, USA). Carbon dioxide (CO_2 N48) with a purity of ≥99.998% was purchased by AirLiquide, Paris, France. Ethanol, methanol, isopropanol and dichloromethane (all HPLC grade) were bought from Sigma-Aldrich, Missouri, USA. Water was obtained in-house with a type I ultrapure water purification system from ELGA-Veolia LabWater, High Wycomb, UK. Leucine-enkephaline was acquired from Waters, Massachusetts, USA.

Fouirier Transform-Ion Cyclotron Resonance Mass Spectrometry (FT-ICR MS)

Fourier transform ion cyclotron resonance mass spectrometry (FT-ICR MS) is a form of high resolution mass spectrometry that yields great insight to the characterization of complex mixtures. FT-ICR MS provides the unique combination of ultrahigh resolving power (the ability to resolve mass spectral signals differing by < 1 mDa) and accurate mass determination (determination of molecular masses to ~5 decimal places).

Mass spectrometry is a technique that measures the mass of an ion. For that reason, the ionization of compounds prior to analysis is crucial. There are many ionization technique and most of them target different types of chemicals. The work presented here focuses on data collected with negative-ion electrospray (- ESI), which targets acidic compounds such as carboxylic acids, phenols, and alcohols through deprotonation, and positive-ion atmospheric pressure photoionization (+ APPI), which targets a wide range of polar compounds such as phenols and non-polar compounds such as hydrocarbons through protonation and radical ion formation. Biocrudes are typically enriched in oxygen-rich compounds. As such, (-) ESI and (+) APPI are complementary ionization techniques for biocrudes and hydroprocessed biocrudes.

Regarding the analysis of FT-ICR data, mass spectral signals were calibrated and elemental formulas were assigned based on the accurate mass of each signal. Once elemental Formulas were assigned, two popular methods for data visualization were used: the heteroatom class distribution and the isoabundance contour plots of double bond equivalent (DBE) vs. number of carbon atoms (C #).

Results

GCXGC-FID/MS

Table 19 shows some physico-chemical properties including elemental composition (wt %) and moisture (wt %) of five loblolly pine biocrude oils that were characterized by the methods described above. The GCXGC-FID/MS data did show that the Feed D contained the highest amount of mono-aromatics and aliphatics. The Feed C had the highest amount of poly-aromatic compounds and abietic acid derivatives. Additionally, the results revealed that the Feed D had significant amount of aliphatic aldehydes and ketones. On the other hand, Feed B, Feed C, and Feed E were found to contain equally reasonable amount of benzofurans/benzaldehydes/acetophenons compared to Feed D. The amount of carboxylic acids, furanones, hydroxyfurans, and furfuryalcohols were found to be low in all the feeds. The results also showed that Feed E had the highest amount of catechols and alkylphenols. The Feed C had relatively higher amount of methoxyphenols than the other four feeds. It is also worth pointing out that anisoles (methoxybenzenes) were present in higher concentrations in Feed D than the other biocrudes. With respect to hydroxylated aromatics such as naphthalenols, biphenylenols, and phenathrenols; the feed D had the least amount in comparison to the other four feeds.

Table 19: Physico-chemical properties of the RTI biocrudes (wet basis)

Sample	Feed B	Feed B	Feed C	Feed D	Feed E
C (wt %)	62.9	64.5	72.8	73.9	62.9
H /wt %)	7.0	7.3	6.7	8.3	6.5
O (wt %)	28.0	25.5	14.9	17.0	28.8
Moisture (wt %)	9.9	9.4	8.9	8.0	10.4

The 16 compound classes were categorized into six groups that were considered best to represent the composition of the biocrudes. For a better overview of the data, area counts of the selected six pooled groups of compound classes were normalized to the area count of the compound class of aliphatics. The group of compounds are as follows:

Group A: Aliphatics (paraffins and naphthenes)
Group B: Aromatic compounds (abietic acid derivatives and mono-, di- and triaromatics);
Group C: the smaller aliphatic acids and aldehydes/ ketones (cellulosic origin)
Group D: the furan derivatives (cellulosic origin) (furans, furanons, furfurals)
Group E: various oxygenated aromatic compounds that did not seem to belong the phenolics (benzaldehyde/acetophenon, naphtalenols, biphenylols)
Group F: the phenolics from lignin origin (phenols, catechols, anisols, guaiacols, syringols)

Table 20: Area counts of groups of pooled compound classes normalized to the area count of aliphatics in RTI crude pyrolysis oils (non-fractionated) as determined by GC×GC-FID (average of duplicate analysis).

Sample\Group	Group B	Group C	Group D	Group E	Group F
Feed B	6.3	4.7	0.7	3.5	9.5
Feed B	6.8	4.9	0.6	3.4	9.5
Feed C	11.3	4.2	1.0	5.0	9.6
Feed D	2.6	2.1	0.1	0.4	2.3
Feed E	11.3	6.3	1.3	5.1	17.1

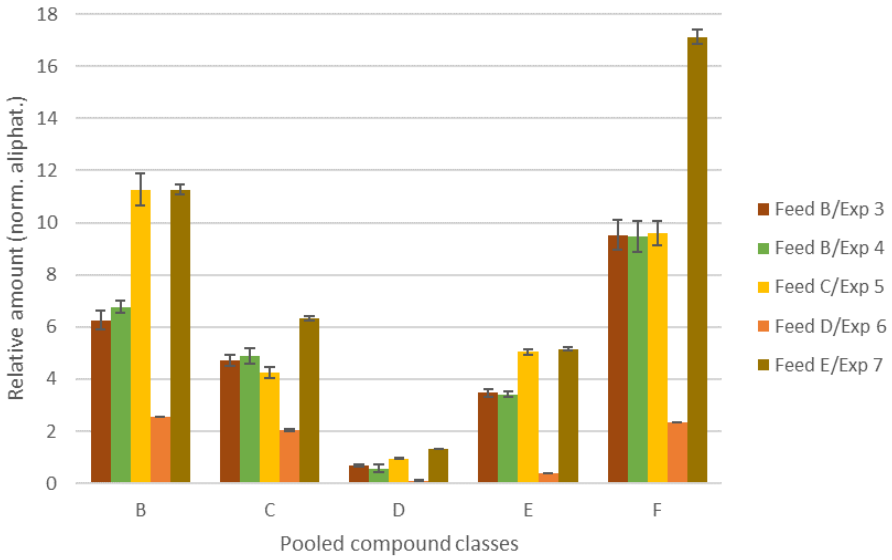

Figure 38: Relative amounts of different compound classes (normalized to aliphatics) as determined by GC×GC-FID (average of duplicate analysis). Data from Table 20.

Another four samples of biocrude from hardwood oak and loblolly pine were compared by GCxGC (Figure 39, Figure 40, Figure 41, and Figure 42). Table 19 shows their physicochemical properties. The simulated distillation curves for the four samples are presented in Figure 43 as well. From the analysis, it is seen, that the heavy fraction consists of large molecules and contain a high amount of oxygen, whereas the light fraction consists of smaller molecules with less oxygen. This is as expected. Of the heavy fractions the pine pyrolysis oil is lower in oxygen content then the hardwood and is expected to be easier to upgrade.

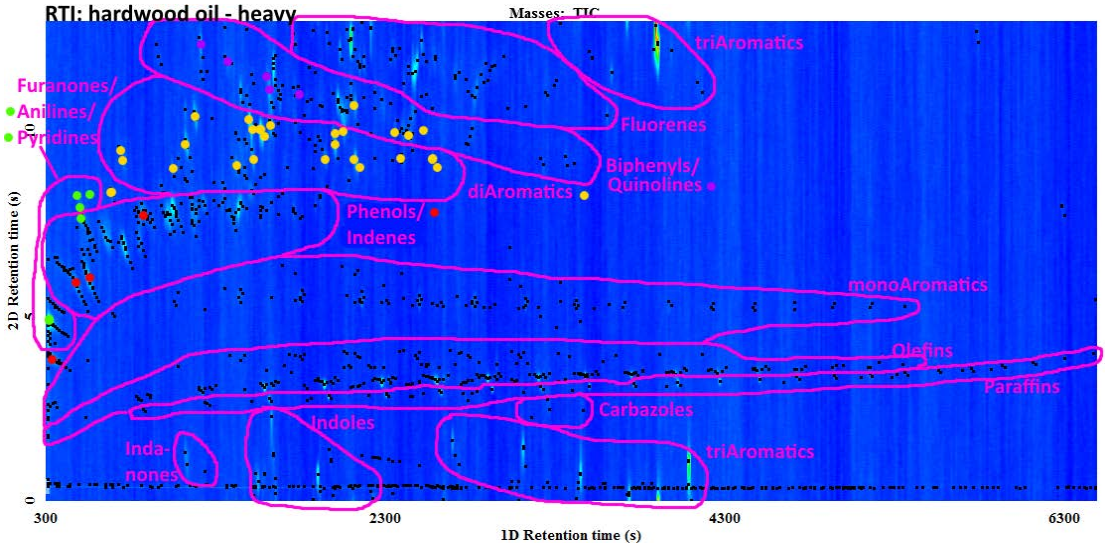

Figure 39: GCxGC analysis of the sample "Hardwood oil – Heavy"

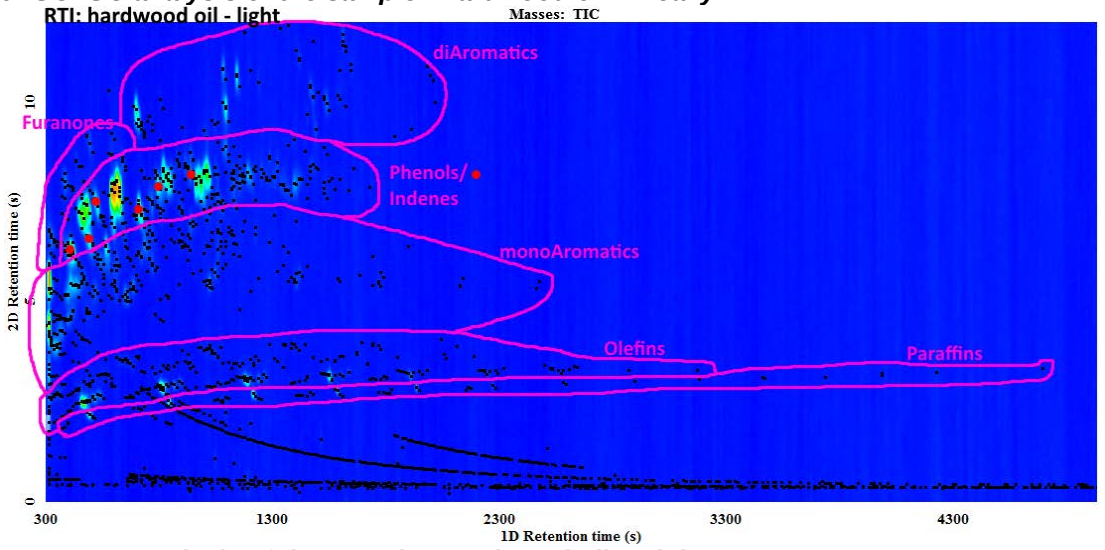

Figure 40: GCxGC analysis of the sample "Hardwood oil – Light"

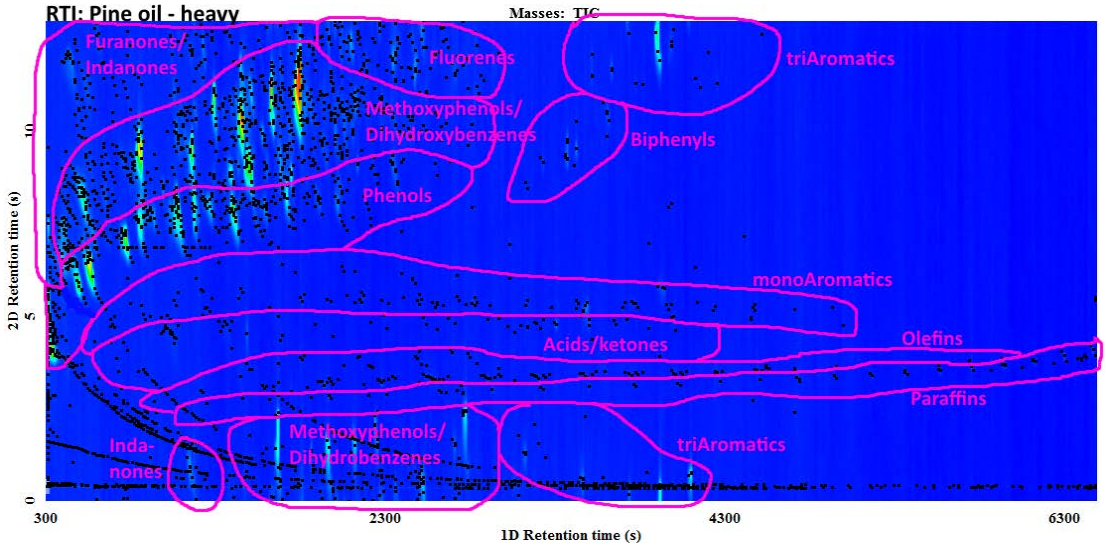

Figure 41: GCxGC analysis of the sample "Pine oil – Heavy"

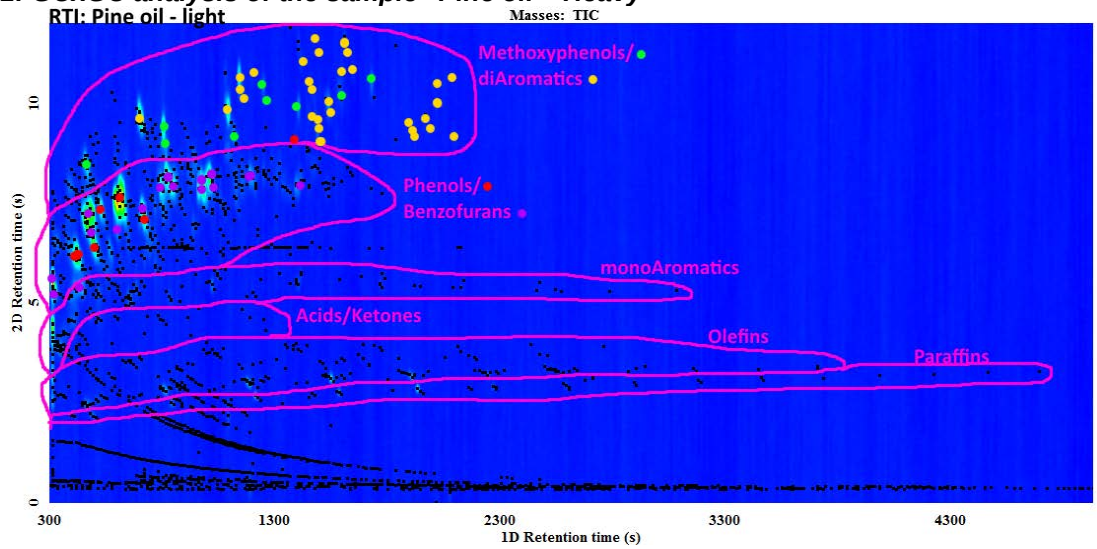

Figure 42: GCxGC analysis of the sample "Pine oil – Light"

Table 21. Analysis of samples received from RTI

Sample Name	Hardwood (Oak)		Loblolly Pine	
	Heavy Fraction	Light Fraction	Heavy Fraction	Light Fraction
S, wt%	0.02216	<0.000002	0.03698	0.04765
N, wt ppm	0.8	0.75	0.65	0.32
H, wt%	9.92	7.74	6.53	7.37
O, wt%	41	6	23	13
C, wt%	44.8	59.8	67	60.5
SG 60/60°F	1.0200	0.9503	1.1372	0.9900

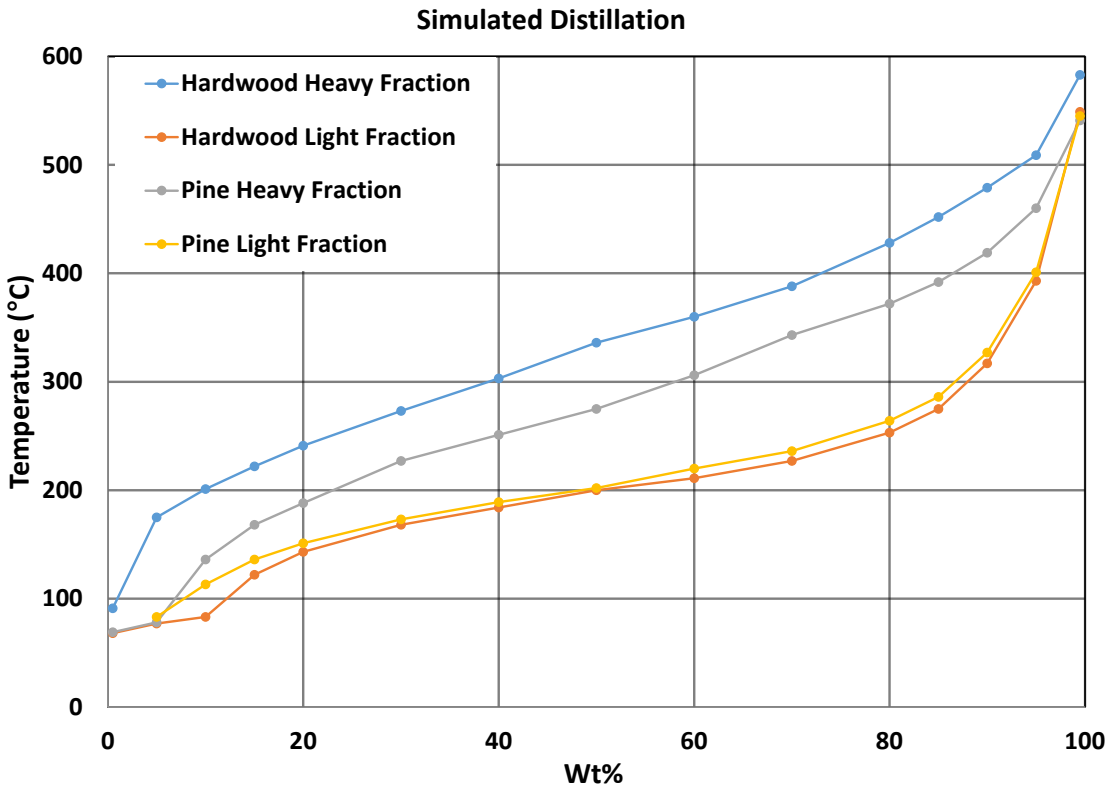

Figure 43: Simulated distillation of heavy and light bio-crude fractions

SFC-HRMS Analysis.

Initial tests of the samples revealed carry-over, unresolved areas in the end of the chromatograms (Figure 44) and compounds eluting in subsequent runs due to strong retention. Several measures were taken to minimize these observations and to improve the quality of the data. First, the washing solutions of the sample needle were adapted to isopropanol and methanol:water (80:20) as weak and strong washing solvents, respectively, to remove residual sample components from the injection system. Thereby, subsequent blanks after samples had cleaner chromatograms and indicated a reduction in carry-over. Second, flow rate (from 2 to 1.5 mL/min) and %B (20 to 30%) were adjusted in order to keep the system pressure below the instrument limits of 6,000 psi (413 bar) [15] and to extend the elution of more polar compounds. The run time was prolonged to 35 min likewise. Third, the sequence was setup batch-wise for replicates (i.e., first A, second B and third C) with one blank injection and a shorter blank clean-up run between each sample.

A standard mixture of 20 oxygenated polycyclic aromatic compounds (OPACs, 4 µg/mL) with carbonyl, hydroxyl and carboxyl functional groups was tested. Due to the chromatographic mechanisms in SFC with the given column and B-solvent, more polar compounds were expected to be retained stronger than less polar compounds. In a previous unpublished study, this was confirmed as carboxylated OPACs were more strongly retained than their hydroxylated derivatives, e.g. naphthol eluted earlier than naphthoic acid. Although this was tested solely on standards with mono- or bi-functional groups without alkylated chains, this trend was expected to hold true for the samples herein.

In Figure 44, one replicate of each of the five feeds were depicted in a two dimensional landscape (m/z vs. time [min]) with their intensities for each mass. The data was binned to the nominal masses in Matlab before plotting. The chromatograms were cut after 23 min and above 400 Da in order to focus the data analysis on the highest populated region. All chromatograms were normalized to a maximum intensity of 10×10^6 for comparative reasons. Broad signals in the end of the chromatograms (Region A, 100-180 Da, 11-20 min,) indicate a strong retention of more polar compounds and/or insufficient resolution of compounds with the same mass. Additionally, high-intensity signals between 250-320 Da and 5-10 min (Region B) illustrate an interesting region for further investigations and especially for the differentiation between the feeds.

Clear differences between the feeds can be identified from these regions. Feed B and E exhibit very similar features, whereas only intensities seem to differ. Feeds C and D show different patterns from the others with lower intensities for both regions in Feed D, and lower and higher intensities in Region A and B, respectively, for Feed C. These observations can be tentatively correlated with the lower oxygen content in Feed D and C (17.0 and 14.9 wt%, respectively). Despite the lowest comparable oxygen content, Feed C features the highest intensities in Region B.

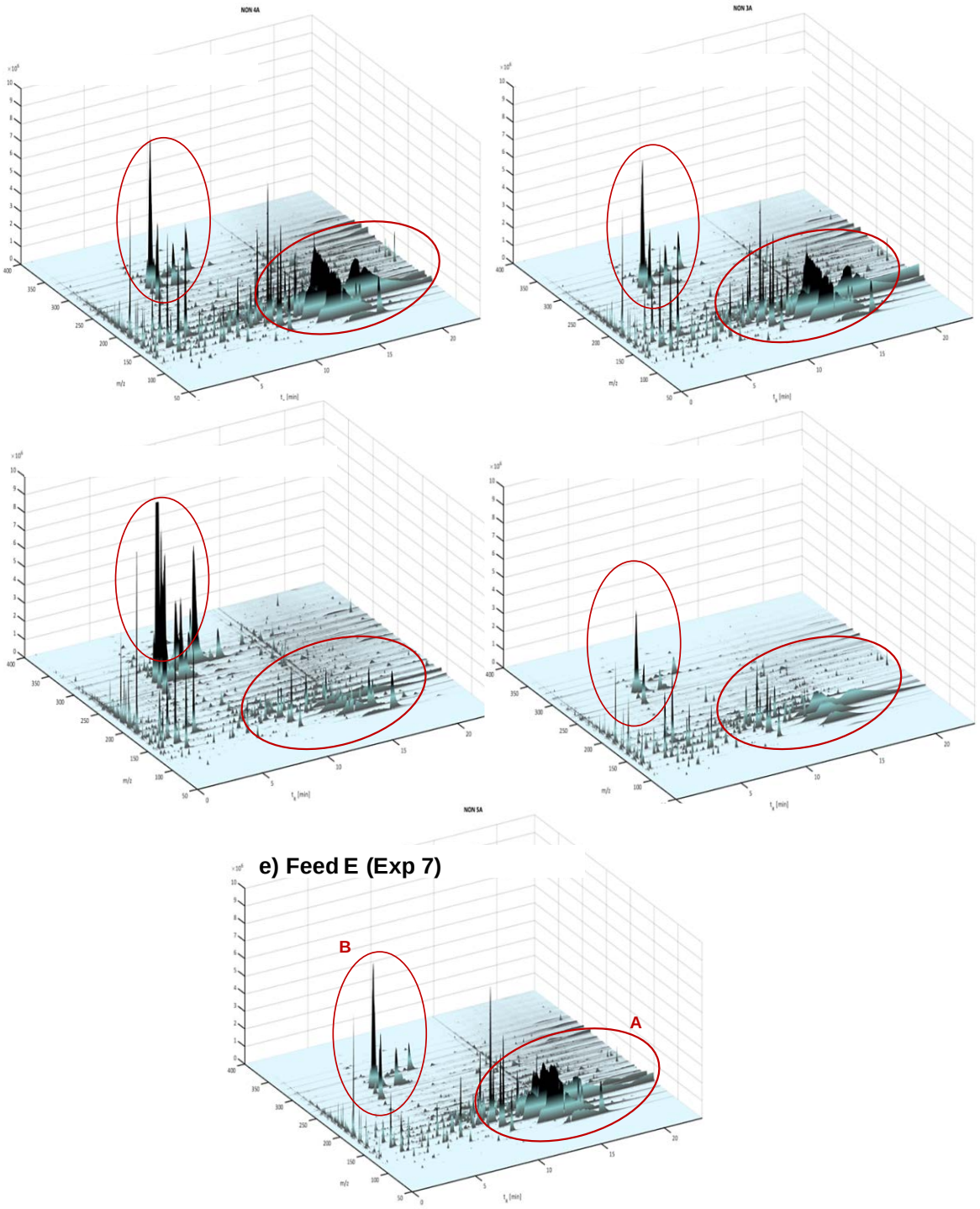

Figure 44: Two dimensional landscapes of the five feeds. Oxygen content: a) Feed D (Exp 6) (17.0 wt%), b) Feed C (Exp 5) (14.9 wt%), c) Feed B (Exp 4) (25.5 wt%), d) Feed B (Exp 3) (28.0 wt%), e) Feed E (Exp 5) (28.8 wt%). Regions A and B are regions of interest with the largest variation between the feeds.

FT-ICR/MS Analysis

Figure 45 shows a heteroatom class distribution for a (-) ESI-derived pyrolysis biocrude. This type of plot provides useful insight into the chemical composition of samples. Heteroatom class plots show the summed relative abundance for all observed ions with a specific number of heteroatoms. For example, a compound such as phenol would be considered an O_1 heteroatom compound whereas a compound such as coniferyl alcohol would be considered an O_3 heteroatom compound. Figure 45 shows that the pyrolysis biocrude sample is enriched in oxygen-containing compounds and that $O_4 – O_6$ heteroatom compounds are present in the greatest relative abundance.

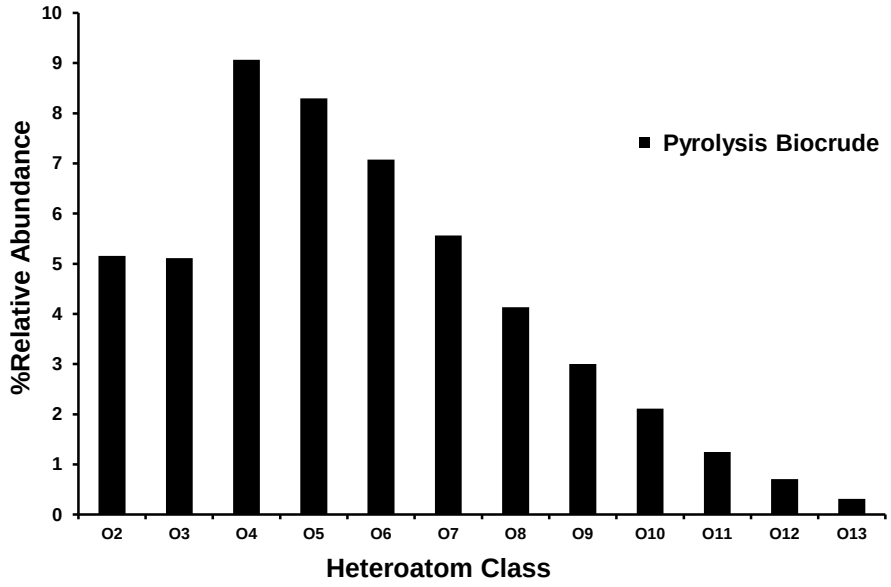

Figure 45: Heteroatom class distribution derived from (-) ESI FT-ICR MS analysis.

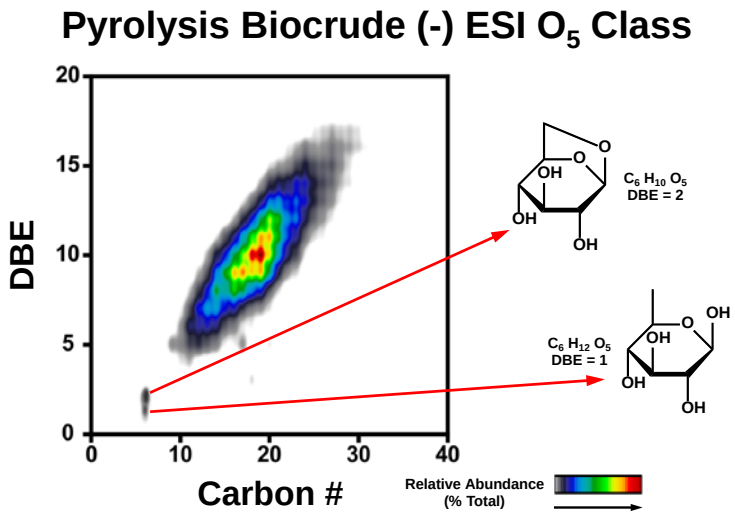

Figure 46: DBE vs C # plot derived from (-) ESI FT-ICR MS.

Figure 45 is an example of a DBE vs. C # plot. DBE or Double Bond Equivalent, is a measurement of hydrogen deficiency and is calculated using the following equation where C is

the number of carbon atoms, H is the number of hydrogen atoms, and N is the number of nitrogen atoms within a molecule:

$$DBE = C - \frac{H}{2} + \frac{N}{2} + 1$$

Plots of DBE vs. C # provide useful insight into the structural complexity and trends within a select heteroatom class. Figure 46 shows the DBE vs. C # plot for the O_5 class derived from the (-) ESI analysis of a pyrolysis biocrude. Two potential structures are shown for two observed ions, and these structures correspond to known pyrolysis products. However, it is important to understand that FT-ICR MS analysis provides only the elemental formula of an ion and does not directly provide insight into chemical structure unless MS/MS studies are conducted.

The biocrudes (B, D and E) were analyzed by FT-ICR MS The samples were dissolved in a mixture of toluene and methanol prior to (-) ESI analysis and ammonium hydroxide was added to aid in the deprotonation of acidic compounds. Figure 46 shows the (-) ESI-derived heteroatom class distribution for the pine biocrude samples. Oxygen classes range from O_2 – O_{13}, and very little difference is observed between the 4 samples. However, there is a slight shift in the oxygen distribution, and the weight average oxygen number for Feed D is less than those from the other three samples. Weight average oxygen numbers are shown in Figure 46 for all samples. Figure 47 shows the DBE vs. C # plots for O_3 – O_{10} heteroatom classes. Few differences are observed between the distributions of each sample. However, Feed D (light fraction) shows a slightly lower C # distribution and the DBE distribution appears to be broader for Feed D compared to the other three samples. One important thing to note for all samples is their carbon number distributions. Figure 47 shows that there is an increase in the maximum C # and DBE values with increasing oxygen content, and ions were observed up to ~50 carbon atoms and DBE values of ~25. Compounds with oxygen numbers greater than ~3 and C # greater than ~ 30-40 are often times not observed by GC or GC x GC analyses, which lends FT-ICR MS as a complimentary approach to GC x GC MS especially for the molecular analysis of highly aromatic and polar oxygen-containing compounds.

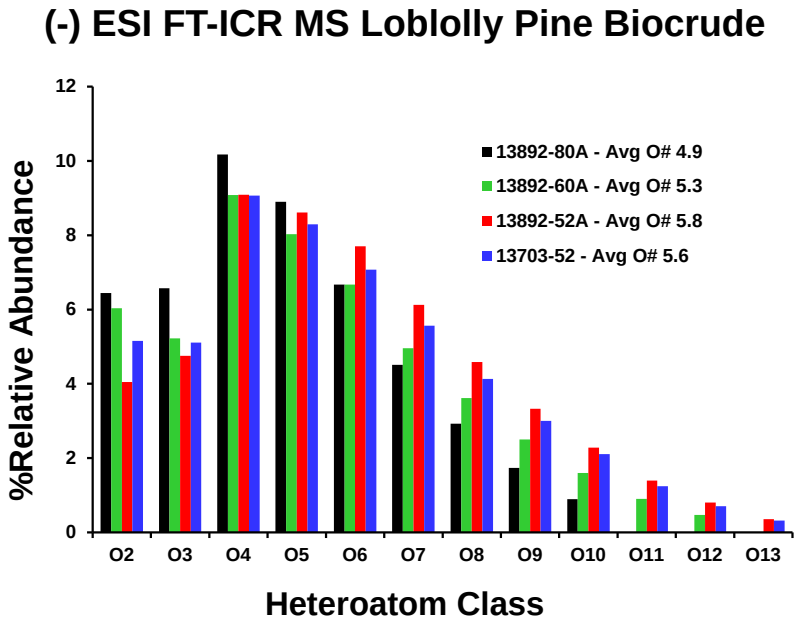

Figure 47: Heteroatom class distribution for loblolly pine biocrudes. Average oxygen numbers are shown in the graph legend.

Bio-crude Upgrading

Catalytic hydrotreating (HDT) of bio-oil offers a strategic opportunity to produce useful intermediates as refinery feedstocks or infrastructure-compatible finished fuels as blendstocks. Nevertheless, HDT of the raw bio-oil has proven to be challenging due to the complexity of the reactive oxygenated compounds; the thermal instability of the raw bio-oil cause issues such as reactor plugging and catalyst coking/deactivation. As a result, the raw bio-oil is typically subjected to a stabilization step prior to performing the required HDT.

In contrast to the traditional approach, RTI is developing an advanced biofuels technology that integrates catalytic biomass pyrolysis process and hydrotreating to produce hydrocarbon-based biofuels. It is hypothesized that the bio-crude oil from catalytic pyrolysis can be fairly hydrotreated without the stabilization step. The foreseeable advantage of this concept is the potential to minimize the overall hydrogen demand and also increase hydrocarbon product yield and quality.

To study and demonstrate this technology, RTI, in partnership with Haldor Topsøe, designed a pilot-scale hydroprocessing system to hydrotreat bio-crude oil from RTI's 1 ton per day catalytic pyrolysis unit. The hydrotreater consist of two (2) 350 mL fixed bed down-flow reactors which can be used to perform either 1- or 2- stage hydrotreating.

The main goal of this work was to understand how the quality of bio-crude in terms of its speciation affect bio-crude hydroprocessing. Several well characterized bio-crude oils were hydrotreated using HaldorTopsøe's HDT bio-catalyst to produce refinable feedstocks or finished products such as gasoline, diesel, and jet fuel range hydrocarbons. Optimal conditions (Feedstock quality, catalyst, temperature, H_2 pressure, H_2/Oil ratio, and LHSV) were investigated. Also, co-processing vacuum gas oil (VGO) and bio-crude oils was explored.

Initial Biocrude Upgrading (Haldor Topsoe)

Loblolly pine biocrude produced in RTI's CFP pilot plant was tested in a hydrotreating pilot plant at Haldor Topsoe. Two batches of bio-crudes (PO.X.RTI and PO.X.RTI.B2) were blended to maximize the amount of feed (PO.X.RTI.B3) for testing. GCxGC analysis of the two biocrude samples is shown in Figure 48. The two bio-crude samples had similar composition and that the primary oxygenates present are phenols, furans and furfurals. Other large contributors were ketones and alcoholic esters. The physicochemical properties of the individual and the blended biocrudes are shown in Table 22.

Table 22. Detailed analysis of the biocrude

Sample Name	Method	PO.X.RTI	PO.X.RTI.B2	PO.X.RTI.B3
S, wt ppm	ASTM D5453	576	55	278
N, wt ppm	ASTM D4629	1390	1390	1700
H, wt%	ASTM D7171	6.12	7.23	6.96
C, wt%	ASTM D5291	61.7	57.5	61.5
O, %wt	ASTM D5291	26	23	29
H_2O, wt%	ASTM D4928	11.3	11.1	9.3
H, wt% (dry basis, renormalized)		6	8	7
C, wt% (dry basis, renormalized)		75	75	70
O, %wt (dry basis, renormalized)		19	17	24
SG 60/60°F	ASTM D4052	1.16	1.16	1.16
Flash Point, °C	ASTM D93	130	135	133
Silicon, wt ppm	HTAS 1449[1]	25	9.5	7.9
Sodium, wt ppm	HTAS 1449[1]	16.3	38.3	16.5
Potassium, wt ppm	HTAS 1449[1]	8.3	5.9	3.2
Calcium, wt ppm	HTAS 1449[1]	23.5	17	9
Phosophorous, wt ppm	HTAS 1449[1]	8.5	1.1	1.4
Simulated Distilation	ASTM D7213			
0.5 wt% (IBP), °C		73	81	68
5 wt%, °C		125	145	75
30 wt%, °C		225	241	224
50 wt%, °C		268	288	275
70 wt%,°C		336	359	352
80 wt%, °C		368	390	385
95 wt%. °C		438	473	469
99.5 wt% (FBP), °C		482	555	557

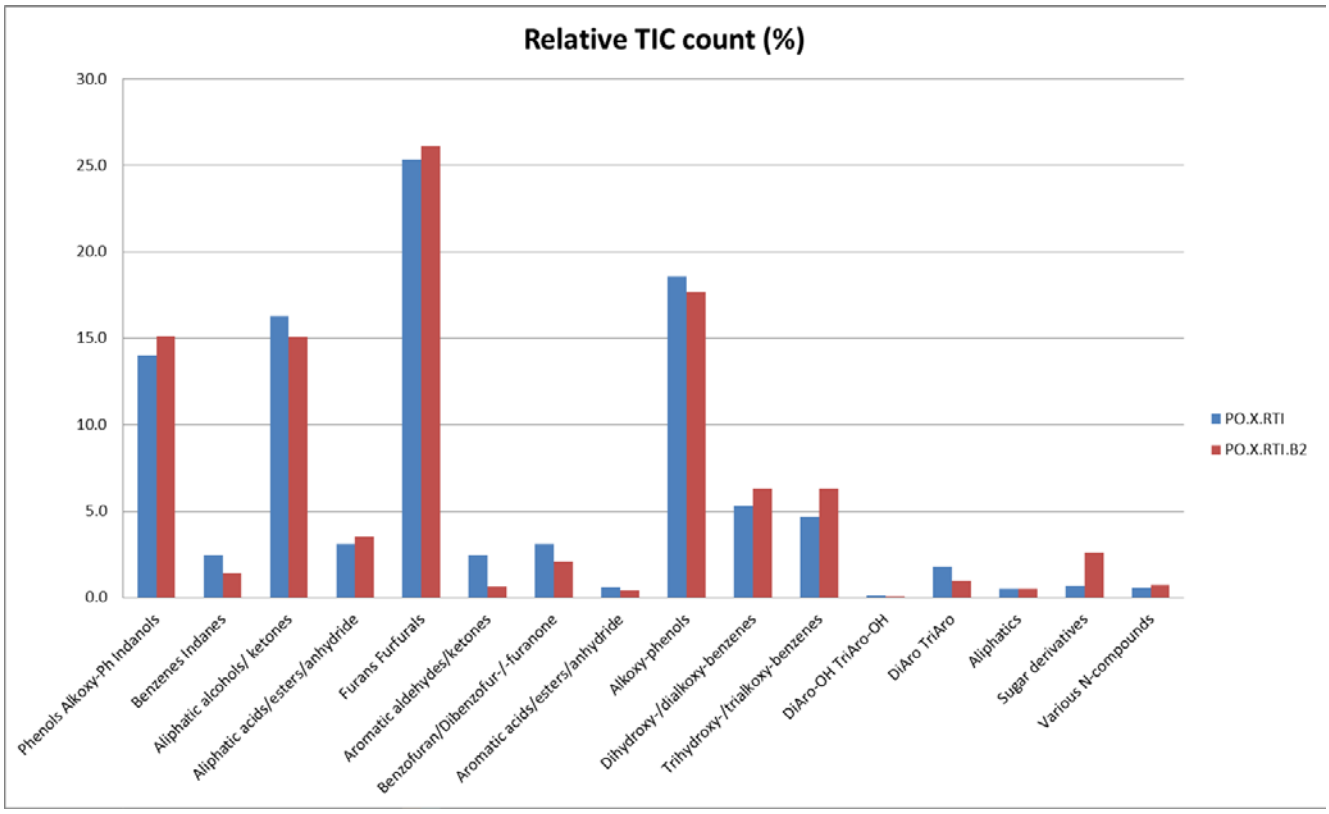

Figure 48: Relative concentration of different compounds in two sample of bio-crude

For the test, the loading of the catalyst was done using experience gained from previous pilot test. The hydrotreating unit contain two reactors and they were both loaded with the same catalyst as in previous test. However, it was decided to vary the dilution of the catalyst in the two reactors to better control the exotherm. The dilution was 60 % in the first reactor and 40% in the second reactor. Initially the heat was turned off in the top of the first reactor as shown in Figure 49.

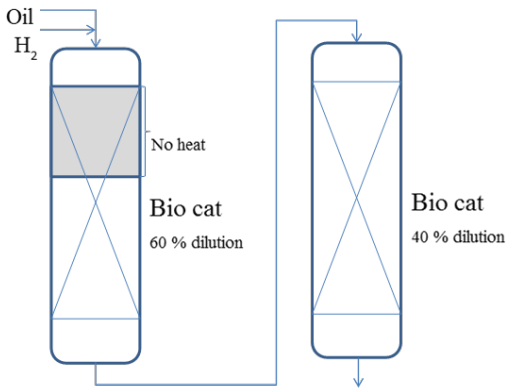

Figure 49.Illustration of the loading of the reactors

The following upgrading procedure was found to be optimal based on GCxGC. A stabilization step before the HDO step is necessary for the initial testing of the bio-crude. This is due to the relatively high oxygen content, approximately 20 %wt on a water free basis, and the compound classes identified through GCxGC analysis. For the stabilization step TK-341 was chosen as the appropriate catalyst, and the process conditions: LHSV =0.5 h-1, Temperature = 160 – 220°C, Hydrogen Partial Pressure = 100 Barg, H_2/oil ratio = 2000 Nl/l as presented in Table 23.

Table 23. Test Conditions

Temperature	350 °C	660 °F
Pressure	100 barg	1450 psig
LHSV	0.5 1/h	0.5 1/h
H_2/oil	2000 Nl/l	11870 SCF/BBL

The first strategy was to carry out the pretreatment, collect the stabilized product, and carry out the HDO. Unfortunately, the pretreated, stabilized product was more viscous than the starting bio-crude material and it did not flow through the system for hydrodeoxygenation.

The second strategy considered using the same loading of catalyst but a different temperature profile in the catalyst bed. The bottom 2/3 of the catalyst bed was operated at 350°C while the top of the bed was not heated so the temperature in the top 1/3 was much lower with a gradient to the higher temperature section. This simulated a pre-treatment stage followed by HDO in simple way. Two products were collected from this experimental arrangement at two different times. Each product contained an organic phase that was less dense than the aqueous/water pahse. When the reactors were removed, and unloaded, the catalyst was heavily coked. The initial results for the analysis of these products is shown in Table 24 and the simulated distillation of the products compared to the bio-crude feed are shown in Figure 53.

The hydrogen concentration in the products was 12 wt% compared to 7 wt% in the starting bio-crude material. This indicates clearly that the hydrotreating carried out was quite severe. This is also consistent with the specific gravity of the products compared to the bio-crude feed. While it is quite surprising that the distillation curves for the feed and the product are quite similar. However, a large amount of water was collected indicating a substantial level of HDO. Inspection of the simulated distillation curves indicates that the product mainly contains hydrocarbons in the diesel boiling range assuming almost complete HDO.

Table 24. Analysis results for pilot test FKT 1806

SAMPLE	METHOD	FEED	PRODUCT					
Run Hour			36	37	39	42	46	52
S, wt%	ASTM D5291	<0.02	0.07	0.03	0.02	0.02	0.01	0.01
N, wt ppm	ASTM D5291	2700	1466	1966	2176	2362	2293	2423
H, wt%	ASTM D7171	7.5	9.7	10.2	10.4	10.2	10.1	10.6
O, wt%	ASTM D5291	37	38	35	6	4	5	5
C, wt%	ASTM D5291	56.2	53.5	59.3	82.7	83	83.2	84.4
SG 60/60°F	ASTM D4052	1.1756	1.0113	0.9544	0.9418	0.9554	0.9504	0.9329
Aromatics								
Mono	ASTM D6591	See separate Table below						
Di								
Tri								
Simulated Distillation								
0.5 wt% (IBP), °C	ASTM D7213	84	51	65	87	86	87	66
5 wt%, °C		139	125	114	108	103	111	103
10 wt%, °C		177	155	142	138	136	145	132
15 wt%, °C		204	179	156	156	156	156	156
20 wt%, °C		217	201	175	171	175	179	170
30 wt%, °C		243	235	212	207	216	217	210
40 wt%, °C		265	275	242	236	249	247	242
50 wt%, °C		293	320	285	275	293	288	285
60 wt%, °C		325	361	322	312	328	322	319
70 wt%,°C		361	407	360	348	365	359	354
80 wt%, °C		395	457	419	400	426	413	408
85 wt%, °C		413	485	455	436	463	451	446
90 wt%, °C		435	518	497	480	506	497	492
95 wt%. °C		471	558	548	534	554	548	546
99.5 wt% (FBP), °C		551	609	608	604	608	607	608

Table 25. Aromatic content of samples from FKT 1806

SAMPLE	PRODUCT				
Run Hour	36	37	39	42	52
SPE Separation					
Total Aliphatics, Vol%	0.2	6.1	15	16	19
Total aromatics, Vol%	44	65	59	74.5	79
Recovery, Vol%	46	73	74	90	97
Aliphatic fraction					
Alkane, Vol%	41.9	24.9	16.6	19.7	9.7
1-ring napthens, Vol%	14.2	30.1	36.2	32.6	46
2-ring napthens, Vol%	14.3	20.4	21.9	20.2	19.6
3-ring napthens, Vol%	13.6	14.6	14.5	16.1	14.7
4-ring napthens, Vol%	6	5.5	6.2	5.8	4.7
5-ring napthens, Vol%	4.4	1	0.4	0	0
6-ring napthens, Vol%	1.5	0.1	0	0	0
Monoaromatics, Vol%	4	3.5	4.2	5.7	5.2
Aromatic fraction					
Monoaromatics, Vol%	48.6	58.3	58.3	52.7	56
Diaromatics, Vol%	23.6	19.6	20	23.3	21.8
Triaromatics, Vol%	7.1	4.5	6.7	8	5.5
Tetraaromatics, Vol%	1.5	2.1	0.8	1.7	1.6
Pentaaromatics, Vol%	0.8	1	0.2	0.6	0.4
Thiopheno Aromatics, Vol%	14.2	10.8	11.2	11.4	10.9
Unidentified Aromatics, Vol%	4.1	3.6	2.8	2.4	3.9

The samples from run hours 42, 46 and 52 were analyzed by GCxGC-MS. The contour plots (TIC, total ion chromatograms) of the three samples, FKT 1806 42 AP1 (2015126179), FKT 1806 46 AP1 (2015126201) and FKT 1806 52 AP1 (2015126223), are shown in Figure 50 to Figure 52, respectively. The X-axis represents 1D retention times (sec) and the Y-axis 2D retention times (sec). A visual evaluation of the three contour plots indicates that the samples are very similar in chemical composition showing the same 2D structural characteristics and compound classes with apparently similar concentrations. Due to the apparent similarity between the three samples the identified compound classes have been marked in only one of the samples (Figure 50).

Referring to Figure 50, a brief qualitative description of the compound classes is given here. Starting from top (longest 2D retention times, about 8 sec) of the contour plot a band of primarily normal paraffins (from about nC8 to about nC25) is observed. Normal paraffins n-C15 to n-C18 are in present significantly higher concentrations than other paraffins, and, in contrast to petroleum samples, hardly any iso-paraffins are detected. Below the paraffins, two naphthenic bands are present. The upper band is mono-Naphthenes (about 7 sec) and the lower band is the

di-Naphthenes (about 6 sec). These two bands do not seem to extend as far in carbon number as the paraffins. At 2D retention times of 4.5-5 sec, a band of monoAromatics (primarily linear alkylbenzenes) is observed, and below this compound class is a band of Naptheno-monoAromatics (Indanes/Tetralines).

While the compound classes described above are relatively well separated regarding 2D retention times, the additional compound classes at lower 2D retention times are less well separated, and they all elute within 2D retention times of 2.5 to 3 sec. However, these compound classes seem to be more separated by 1D retention times, but significant co-elution still occurs. An intense band of Phenols/Methoxybenzenes is present between 1D retention times of 1000 sec to 2500 sec. A group of diAromatics (Naphthalenes) tend to co-elute with the Phenols at 2000 sec 1D retention time and Biphenyls also co-elute with the Phenols (cf. Figure 1) at about 2500 sec 1D retention time, although they seem to have slightly shorter 2D retention times. At even longer 1D retention times and with slightly different 2D retention times, two other classes of aromatics; triaromatics (Fluorenes and Phenanthrenes) and tetraAromatics (Pyrenes) are observed (Figure 50). A group of intense peaks at the far end of the contour plot and intersecting the Naphtheno-monoAro-matics, Phenols and tri-/tetraAromatics is observed. These peaks have not been fully identified, but they are believed to be “biomarkers” of the original bio-crude material.

In summary, the hydrotreated pyrolysis oils are dominated by saturated aliphatic compounds (paraffins and naphthenes) together with oxygenated compounds (phenols and methoxy-benzenes). MonoAromatics (alkylbenzenes and indanes/tetralins) are present at lower concentrations, while higher aromatics (di-, tri- and tetra-) are present at significantly lower concentrations.

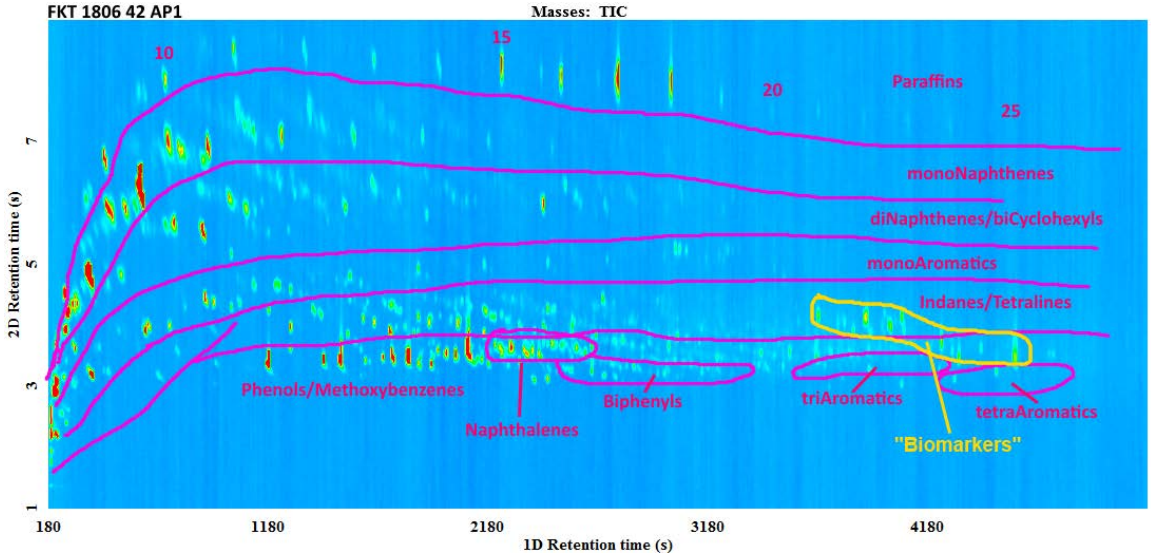

Figure 50: GC×GC-MS contour plot (TIC) of the FKT 1806 42 AP1 sample of hydrotreated pyrolysis oil showing the identified compound classes. Color code: red (highest intensity) to faint blue/green (lowest intensity).

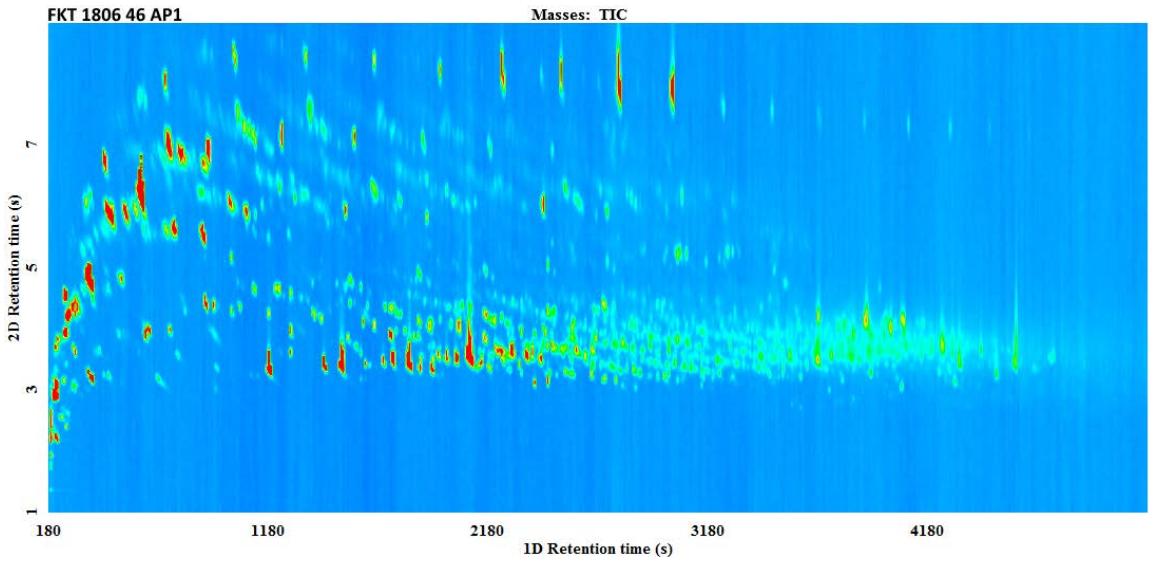

Figure 51: GC×GC-MS contour plot (TIC) of the FKT 1806 46 AP1 sample of hydrotreated pyrolysis oil. Cf. Figure 50 for identification of compound classes. Color code: red (highest intensity) to faint blue/green (lowest intensity).

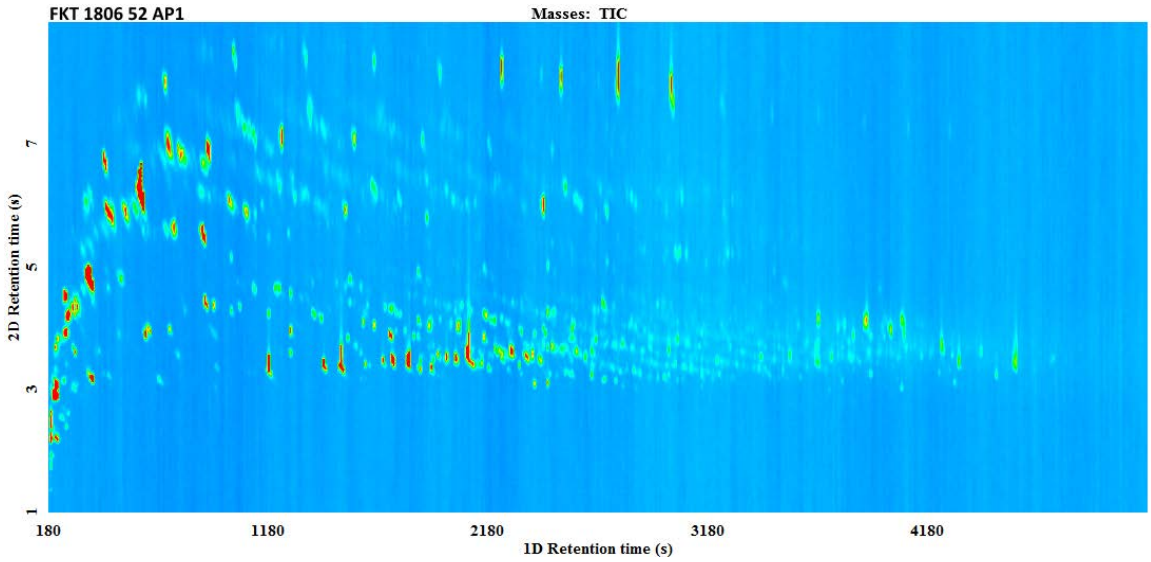

Figure 52: GC×GC-MS contour plot (TIC) of the FKT 1806 52 AP1 sample of hydrotreated pyrolysis oil. Cf. Figure 50 for identification of compound classes. Color code: red (highest intensity) to faint blue/green (lowest intensity).

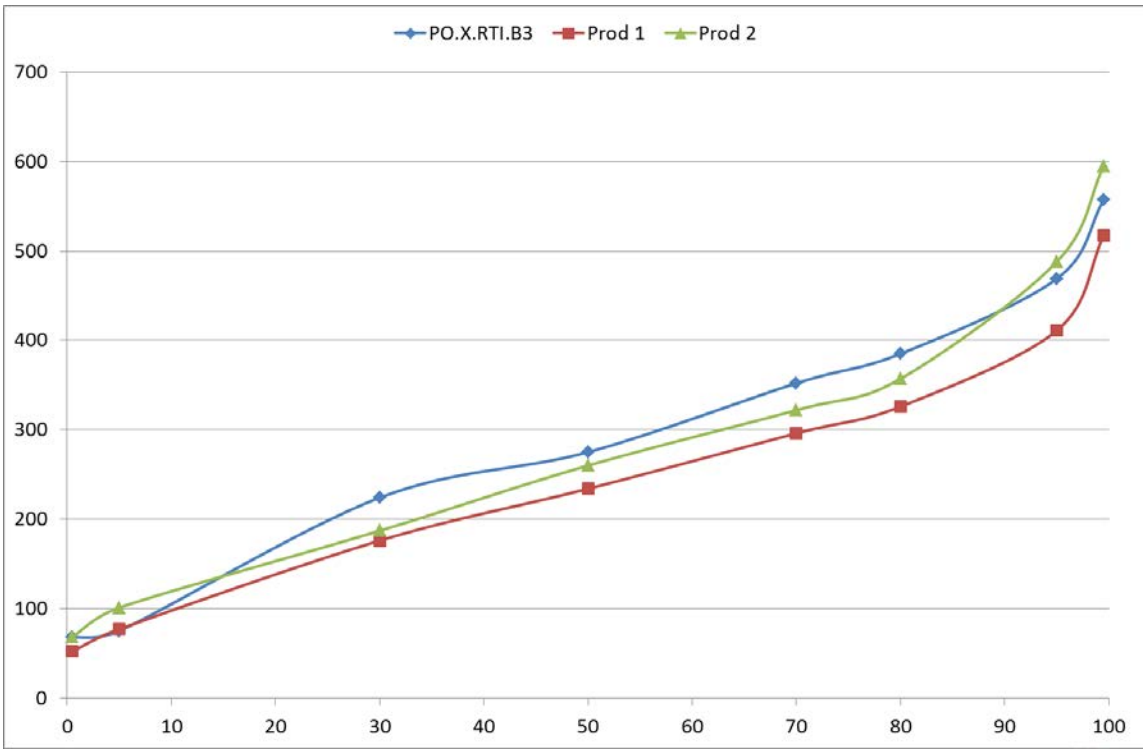

Figure 53: Simulated distillation of the bio-crude feed and the products from the HDO testing

Biocrude Upgrading (RTI)

Hydroprocessing Unit Design

The Hydroprocessing Unit consists of 5 unit operations: 1) oil feed system equipped with pumps and flow control; 2) gas feed system; 3) reactor system; 4) gas/liquid separator system; and 5) gas and liquid sampling system. The reactors, vessels, fittings (Swagelok), and tubing are all made of 316 SS/316L SS and their pressure ratings are much higher than the operating conditions. The design constraints and allowable operating conditions (for temperature and pressure) for the major equipment are provided in Table 26. A process flow diagram (PFD) is presented in Figure 54.

The Hydrotreater is equipped with instrumentation and control systems for full automation. It is designed with many safety features to ensure safe operation. For example, the unit is housed in a fume hood-style transparent enclosure with a common exhaust system that is equipped with a differential pressure gauge to ensure negative pressure. Also, the entire system seats in a secondary containment/catch tray. A key safety feature of the Unit is a comprehensive interlocking matrix for system shutdown to prevent overheating and over pressurizing of the unit. Additionally, high alarm alerts for CO, H_2, and H_2S are interlocked with every piece of instrumentation and control system for a complete shutdown. The system also has an alarm for inadequate ventilation monitored by a differential pressure gauge.

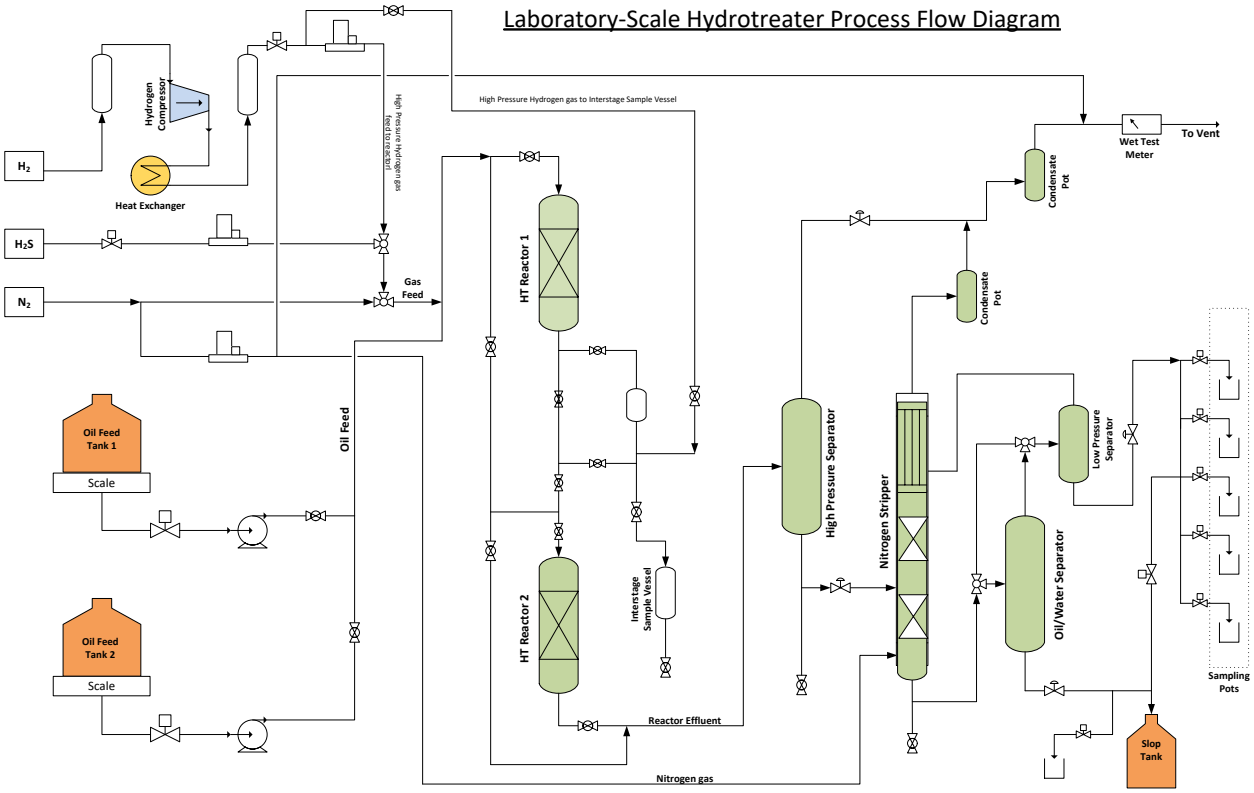

Figure 54: Process Flow Diagram of Pilot-scale Hydroprocessing Unit

During operation, a positive displacement pump will be used to charge preheated feed into the Reactors at pressures between 1000-2500 psig. The holding tanks for the feed will be maintained at a maximum temperature of 120 ^{o}C and pressure of 15 psig. Hydrogen gas will be mixed with the feed and it will be introduced into the reactor at a maximum operating pressure of 2500 psig with the aid of a diaphragm compressor. The required suction pressure for the hydrogen gas is 315 pisg and the temperature is 30 ^{o}C. The reactor section consist of two fixed bed reactors which are designed to hold pressures up to 3000 psig. They are externally heated with an ATS split tube electric furnaces and the design temperature is 450 ^{o}C. For all other heated sections of the Hydrotreater (piping/tubes/vessels), a fiberglass cloth or a silicone rubber heating tape is used to achieve all required temperatures. An interstage sample vessel maintained at the same temperature and pressure as the Reactor 1 will be used to sample out reaction product stream from the first reactor prior to entering the Reactor 2. The hydrotreating reactions will be promoted by metal oxide catalyst (e.g., NiMO and CoMo). After the feed has been hydrotreated, the reactor effluent is sent to a High Pressure Separator which will operate at a maximum pressure of 2500 psig. The recovered products from the bottom of the high pressure flash separation unit is sent to a Nitrogen Stripper. The product then exit the Stripper and flows subsequently into an Oil/Water Separator and Low Pressure Separator. The products are finally recovered from the Low Pressure Separator and Condensate Pots. Most of the water and the other reactor effluents not captured in the Condensate pots and the Low Pressure Separator will be sent to a Slops Tank. The gases (H_2, H_2S, N_2, CO, CO_2, CH_4, and C_2-C_6 light hydrocarbons) will be sent to the common venting system.

Table 26. Design and Operating Conditions for Major Equipment

Equipment	Design Conditions	Maximum operating conditions
Hydrogen Compressor	Discharge P=3000 psig Suction P=740 psig	DP=2515 psig SP=315 psig
Oil Feed Pumps	Flow=500 mL/h Suction P=10 Discharge P=3000	Flow=30-300 mL/h Suction P=10 Discharge P=1000-2550
Oil Feed Tanks	Temp.=150°C Press.=120 psig	Temp.=120°C Press.=15 psig
Reactors (1 and 2)	Temp.=450°C Press.=3000 psig	Temp.=430°C Press.=2500 psig
Interstage Sample Vessel	Temp.=450°C Press.=3000 psig	Temp.=430°C Press.=2500 psig
High Pressure Separator	Temp.=150°C Press.=3000 psig	Temp.=90°C Press.=2500 psig
Nitrogen Stripper	Temp.=150°C Press.=150 psig	Temp.=90°C Press.=90 psig
Oil/Water Separator	Temp.=150°C Press.=150 psig	Temp.=90°C Press.=90 psig
Low Pressure Separator	Temp.=100°C Press.=150 psig	Temp.= 25°C Press.=80 psig
Condensate Pot (1 and 2)	Temp.=100°C Press.=150 psig	Temp.= 25°C Press.=80 psig
Slops Tank	Temp.=150°C Press.=120 psig	Temp.= 120°C Press.=5 psig

Process Hazards Analysis

A process hazards analysis (PHA) for the hydrotreater unit was performed April 24-25, 2015 at RTI. The meeting was facilitated by Craig Browning, Senior Process Safety Consultant from EN Engineering. Also in attendance at the meeting were RTI's project team, Gary Howe (ETD Facilities Manager), and representatives from RTI's Environmental Safety and Health group. The hydrotreater design was separated into four nodes: Node 1 – Liquid Feed Section, Node 2 – Gas Feed Section, Node 3 – Reactor Section, and Node 4 – Product Recovery Section. Each node was indicated on the P&IDs. The team then evaluated each vessel, reactor, valve, and equipment item in terms of specific parameters: level, temperature, flow, pressure, containment, etc. The consequence and qualitative frequency of each item was then assigned a risk rating, with A being the most severe and D being the least. The risk ratings identified were all either C or D. Two recommendations were made as a result of the process hazard analysis to reduce the risk. In Node 1, secondary containment for the 2 bio-crude feed tanks was recommended to reduce or eliminate the potential of bio-crude being released to the sanitary sewer. The design was subsequently modified to include catch trays for the feed tanks. In Node 2, the team noted that if the hydrogen compressor discharge is deadheaded, the design temperature and pressure could be

exceeded. The design was subsequently modified to include both a high temperature and high pressure interlock to shut down the compressor. A complete copy of the PHA report is available upon request.

The hydrotreater design was finalized after the PHA recommendations were incorporated and procurement and fabrication were started. Detailed engineering activities this quarter included completing the P&IDs, Equipment Specifications, Line List, and Bill of Materials for construction. Control valve sizing was completed and data sheets were provided by Unitel. The vessel drawings were also completed and the 3D Model and Layout were finalized. The 3D layout is show in Figure 55.

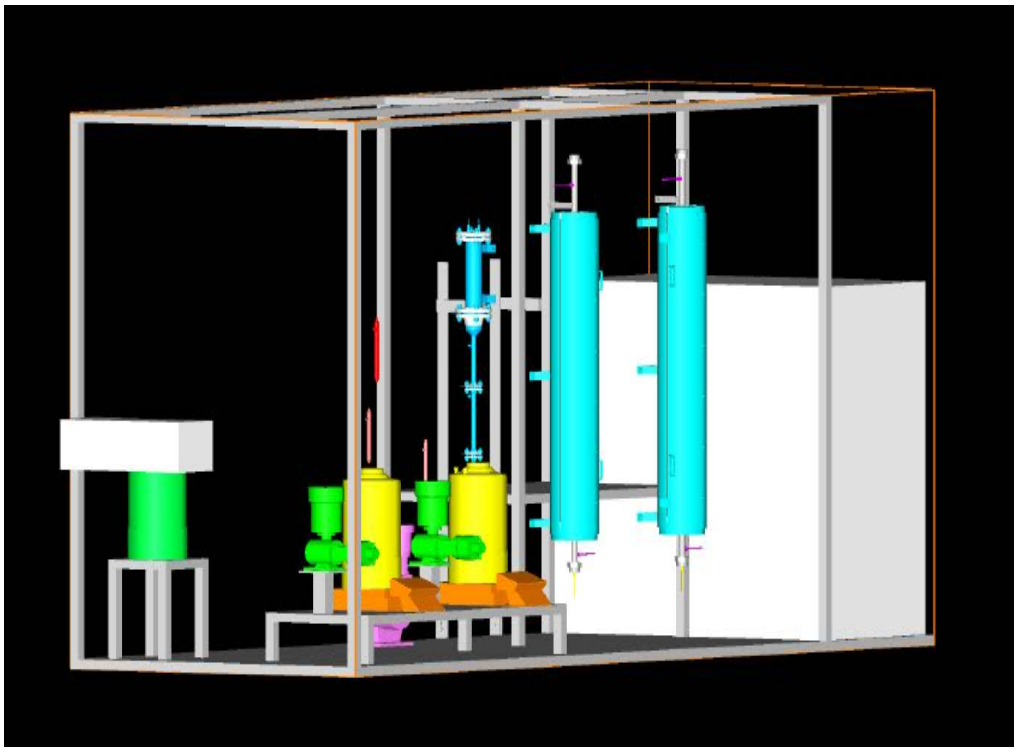

Figure 55: 3D Layout of RTI Hydrotreater Unit

Hydroprocessing Unit Installation and Commissioning

The hydroprocessing unit fabrication was completed and the factory acceptance test was performed at Petrack Industries on November 12-13, 2014 in Joliet, IL. The control system was tested and all pneumatic actuated valves and instrumentation checked out. The unit was crated and shipped to RTI. It arrived at RTI on November 22, 2014 and was installed in Lab 160 in the Johnson Science and Engineering Building.

All utilities were connected, including; process nitrogen, process hydrogen, chilled water, instrument air, and electrical power. The unit is contained in a plexiglass enclosure that was connected to the laboratory ventilation system.

Haldor Topsoe provided a hydrocracking catalyst and diluent for the initial charge of the reactors. They also sent 55 gal of vacuum gas oil (VGO) to RTI for commissioning the hydrotreating unit. Catalyst loading procedures, catalyst activation (sulfidation) instructions, and initial operating conditions for VGO upgrading were also provided by Haldor Topsoe.

Hydroprocessing Baseline Tests

The hydroprocessing unit was successfully commissioned with vacuum gas oil (VGO) following a comprehensive shakedown which was performed to ensure that all the various equipment, instruments, and control systems were working in accordance to the design specifications. The commissioning campaign consisted of three baseline experiment at different conditions (temperature, oil flow, space velocity, and H_2 flow). Nonetheless, the 3 experiments were designed to have similar hydrotreating effect on the VGO. The campaign was performed for more than 300 hours and about 30 gallons of VGO was hydrotreated. The VGO, test conditions, the reference hydrotreating NiMo catalysts, catalyst diluent, and catalyst loading/presulfiding protocols were furnished by Haldor Topsoe. Two down-flow reactors loaded with 60% catalysts and 40% diluent by volume were used. Sulfidation of the catalysts was done in-situ with 10% H_2S in H_2 at 116 psig. All the experiments were conducted at a pressure of 2030 psig and an H_2/Oil of 765 N l/l. The hydroprocessing unit was continuously run without any major issues. A minimum of 2 steady-state material balances were performed on each baseline test. Three liquid products were sampled at different run hours per baseline test. The VGO feed and the liquid products were analyzed for CHNS and the off-gas composition was monitored. The results show good mass closures and the elemental analysis indicate complete hydrodesulfurization of the VGO sample. It was evident from the baseline experiments that the hydroprocessing unit performed as designed and is ready to be used for the bio-crude upgrading.

Baseline Experiments

Sulfidation of the catalyst was done with 10% H_2S in H_2 at 116 psig for a total of about 23 hours. The total flow of the gas mixture corresponded to 550 Nl/h per liter of catalyst, thus the flow rate used was 180 Nl/h. Figure 2 below shows a typical sulfidation temperature ramp. Upon completion of the sulfidation step, the Reactors were cooled to 250 °C prior to switching gas feeds. The gas feed was then changed from 10% H_2S to hydrogen gas and the system was set to the first test condition with the required oil flow. Prior to that, the VGO feedstock had been preheated/homogenized and filled into the two 10-gallon feed tanks. The tanks were maintained at 60 °C under nitrogen pressure of 30 psig. The required feed rate was controlled by the pump's stroke frequency and length. The total average feed rate for both pumps at a speed of 13.5 Hz and stroke length of 15 mm was about 228.6 g/h; which equals 247 ml/h. Table 27 details the three reaction conditions utilized in the commissioning campaign. The operating pressure, H2/oil ratio, LHSV, and the reference temperature were kept constant for tests over the "active" catalysts. To ensure that the LHSV and H2/oil ratio were the same across the three tests, the oil flow and the hydrogen flow were both doubled when the two reactors were tested together in series as the baseline-3 test. Also, both reactors were kept hot (set at the reference reaction temperature) for baseline-3. In baseline-1, reactor-1 was heated and reactor-2 was set at 40 °C, and the reverse was done in baseline-2. All heat traced piping and vessels were maintained between 50-80 °C. The low pressure section of the hydroprocessing unit was maintained at 80-90 psig.

During operation, preheated VGO feed stream mixed with compressed hydrogen gas enter the top of the first reactor and flow through the glass beads and down the catalysts bed; the effluent subsequently flow into the second reactor. After the feed has been hydrotreated, the reactor effluent enter into a high pressure separator (HPS) maintained at 2030 psig. The liquid products from the bottom of the HPS unit then flow into a nitrogen stripper. The product that exit

the Stripper flow into an Oil/Water Separator and a low pressure separator. The liquid products are finally recovered from the low pressure separator and condensate pots into a slops tank. The off-gas from the HPS and the nitrogen stripper go through condensate pots before it exits to a wet-test meter to monitor the gas flow. A stream of the off-gas are continuously analyzed by an online micro-GC. Figure 56 shows an example of the experiment timeline for condition 1. A minimum of two steady-state mass balances were performed for each baseline condition. Per protocol, the experiments were allowed to run for at least 48 h prior to measuring a mass balance. Also, the steady-state material balance was based on data acquired over a period of at least 5 h. The total mass of feed charged was determined gravimetrically by the change in weight of the feed-tank from the start to the end of the mass balance period. The HDT product oil was also determined gravimetrically by weighing the sampling bottles before and after each mass balance. The density of the feed was used to determine the volumetric flow rate. Mass flow meters and a wet test meter were used to measure the input and output gas volumetric flow. Additionally, elemental (carbon and hydrogen) balances were determined based on the chemical composition of the input VGO feed, gas input feed, product oil output, and product gas output streams. The mass balance was verified by indirectly determining the total input flow of VGO feed and the total flow of the output product gas output from the elemental balance and comparing the calculated values to the measured values. An oil correction value (oil corr) is defined as the ratio of the calculated total flow of oil input feed to measured total flow of oil input and was used to validate the material balance. For example, a mass balance was considered good if the oil corr deviated from 1 by ±1%; the mass balance was acceptable if the oil corr deviated from 1 by ±2%; and if the mass balance deviated from 1 by ±3 %, the mass balance was not good, but might be acceptable.

Table 27. Baseline Experiment Process Conditions

Condition	Baseline-1	Baseline-2	Baseline-3
Pressure (bar)	140	140	140
Average R1 Temperature (°C)	Tref	-	Tref
Average R2 Temperature (°C)	-	Tref	Tref
Oil Flow (ml/h)	249.7	249.7	499.4
H_2 Flow (NLPH)	191.28	191.28	382.56
LHSV (h^{-1})	1.15	1.15	1.15
H_2/oil ratio (Nl/l)	765	765	765
TOS, (h)	125	86	101

Tref = Reference Temperature; R1: Reactor 1; R2: Reactor 2

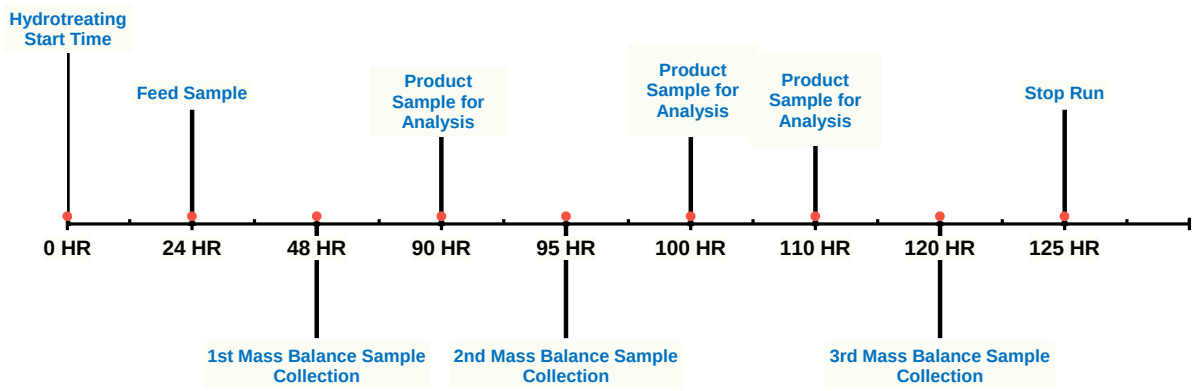

Figure 56: Experimental timeline for baseline test condition 1.

Baseline Performance Validation

Table 28 shows a summary of the results from the VGO baseline experiments. The material balances performed for each condition were good; they varied between 98% and 101%. Also, the oil corr values were between 0.986 and 1.037, which corresponds to a deviation of –1.4% and 3.7% from 1. Hence, the material balances in general were considered to be fairly good. Furthermore, the sulfur and nitrogen contents of product oils sampled for baseline test-1 (at 90 h, 100 h, and 110 h TOS), baseline test-2 (at 60 h, 70 h, and 80 h TOS), and baseline test-3 (at 60 h, 70 h, and 80 h TOS) show that hydrodesulfurization (HDS) and hydrodenitrogenation (HDN) of the VGO were achieved to a large extent, and the concentration of sulfur and nitrogen were significantly reduced. For example, in the baseline-1 test, the sulfur content was reduced from 1.9 wt% to an average of about 0.1 wt%, and the nitrogen content was decreased from 1405 ppm to an average of 170 ppm. Similar hydrotreating effects were also observed in tests 2 and 3. Also, the increase in hydrocarbon (H/C) ratios indicates the occurrence of hydrogenation. In summary, the degree of HDS was between 93.8% and 95.3%, and that of HDN ranged from 84.1% to 89.7%. The targeted degree of HDS and HDN were 98% and 96%, respectively. The amount of sulfur and nitrogen measured in the HDT products was somewhat higher than the expected targets, suggesting that the actual HDT temperature was probably slightly lower in the reactor than what was measured. Importantly, the elemental composition of the HDT liquid products was fairly stable and consistent for all the three experiments performed using reactor-1, reactor-2, and both reactors. Overall, the baseline studies provided the necessary validation of the hydrotreater performance prior to biocrude upgrading.

Table 28. Elemental composition of VGO feeds and hydrotreated products

Sample	Specific Gravity	H/C Ratio	Elemental Composition		Mass Balance	Oil Corr (Elemental)
			Nitrogen, wt ppm	Sulfur, wt %		
Baseline 1						
VGO Feed	0.919	1.70	1405.46	1.8850		
90 Hr. Run	0.8912	1.78	180.63	0.1067	99.6	1.016
100 Hr. Run	0.8914	1.79	183.25	0.1075	100.1	1.017
110 Hr. Run	0.8909	1.78	144.91	0.0968	101.2	1.037
Baseline 2						
VGO Feed	0.9206	1.70	1375.6	1.8830		
60 Hr. Run	0.8908	1.79	161.02	0.0889	99.1	1.031
70 Hr. Run	0.8924	1.78	192.52	0.1091	100.2	1.014
80 Hr. Run	0.8911	1.78	163.04	0.0904		
Baseline 3						
VGO Feed	0.9202	1.70	1384.67	1.8900		
60 Hr. Run	0.8917	1.79	196	0.1104	99.4	1.012
70 Hr. Run	0.8920	1.79	220	0.1172	98.8	1.002
80 Hr. Run	0.8909	1.79	157	0.0932		

Bio-crude Hydroprocessing

Bio-crude upgrading was started after a successful commissioning of the laboratory-scale hydroprocessing unit which consists of two (2) 350 mL fixed bed down-flow reactors.

Hydrotreating of softwood biocrude feedstock

Three experiments were initially conducted with the goal of identifying suitable process conditions to hydrotreat the loblolly pine bio-crude produced in the 1TPD pilot plant. The bio-crude feed contained 26.5 wt% oxygen at a moisture level of 10.1 wt%. All the upgrading experiments were performed with bio-cat (TK-341) supplied by Haldor Topsoe. The catalyst was sulfide in the reactors with 10% H_2S in H_2 at 118 psig prior to the runs. The experimental conditions explored are provided in Table 29. The bio-crude feeding system worked well without major issues. Each experiment was run continuously for more than 80 hours except for Exp. 2; which lasted for a very short time (16 hours) due to an early plug that built up in the reactor. In total, over 200 hours of operation was achieved during these 3 experiments.

Steady-state material balances were performed and the yields and hydrogen consumption were determined. Liquid products were sampled at different run hours and characterized for

CHNO, specific gravity, and viscosity. Some of the liquid products were also characterized by distillation (ASTM 1160) and carbon number distribution.

Table 29. Experimental Conditions

Condition	Experiment 1	Experiment 2	Experiment 3
H_2 partial pressure (psig)	1450	1450	2000
Temperature (^oC)	350	350	300
LHSV (h^{-1})	0.5	0.5	0.25
H_2/oil ratio (Nl/l)	2000	2000	3000
Catalyst Loading, Vol %	R1=40, R2=60	60	40
Catalysts	TK-341	TK-341	TK-341
TOS, (h)	89	16	103

The condition for the first experiment was based on Haldor Topsoe's earlier findings on hydrotreating the bio-crude oil that was shipped to them. Experiment 1 was started using both reactors in series. The first reactor was loaded with 40 vol% bio-cat and 60 vol% SiC and the second reactor loaded with 60 vol% bio-cat and 40 vol% SiC. After 31 hours of run time, the first reactor was bypassed and only the second reactor used because of a pressure build up in the first reactor. The experiment continued using only reactor 2 at the same space velocity that was used in the dual-reactor configuration. In the subsequent runs (i.e., 2 and 3), the experiments were exclusively performed in a single-stage. For experiment 2, the reactor was loaded with 60 vol% catalyst and 40 vol% SiC and in experiment 3, the reactor was loaded with 40 vol% bio-cat and 60 vol% SiC. In experiment 2, a large exotherm was observed as the bio-crude hydrotreating started. The duration of experiment 2 was quite short (16 hr) suggesting that the higher catalyst concentration resulted in a more active bed that accelerated polymerization reactions that led to the formation of a plug.

Based on the outcome of experiment 2, less catalyst (40 vol%) was used in experiment 3 and the H_2/oil ratio was increased to 3000 Nl/l. The hydrogen partial pressure was also increased to 2000 psig and the temperature and LHSV were reduced to 300 °C and 0.25 h^{-1} respectively. At these conditions, experiment 3 was run continuously without any pressure drop across the reactor as shown in Figure 57, the hydrotreating study was performed for 103 h as planned.

A summary of the results from the bio-crude hydrotreating experiments are shown in Table 30. Per protocol, the experiments were allowed to run for at least 24 hours before performing a mass balance. The steady state mass balances ranged between 91 and 98% and the carbon balances ranged from 83% to 96%. The missing carbon can be attributed to carbon on the catalyst and gaseous species/light vapors which were not identified in the gas analysis. The average mass yield of the hydrotreated liquid product was 73.1 wt.% and its respective carbon yield was 83.4%. On average, the yield of the aqueous fraction and the product gas were 16.9 wt.% and 6.1 wt.% respectively. The compositional analysis showed that light hydrocarbons constituted a larger fraction of the product gas than carbon oxides. A typical distribution for the product gas yield is as follows (for TOS 26-34): CH_4 (1.68 wt%), CO_2 (1.89 wt%), and C_2^+(3.23wt%). Carbon monoxide was below the detection limits of the GC. The hydrogen consumption ranged between 600-700 Nm^3/m^3. In other words, 0.06-0.07 g of hydrogen was consumed by 1g of dry bio-crude (~3600 scf/bbl). It is worth noting in Table 30 that the hydrogen consumption decreased with time on stream; which could be an indication of activity loss due to catalyst deactivation or fouling.

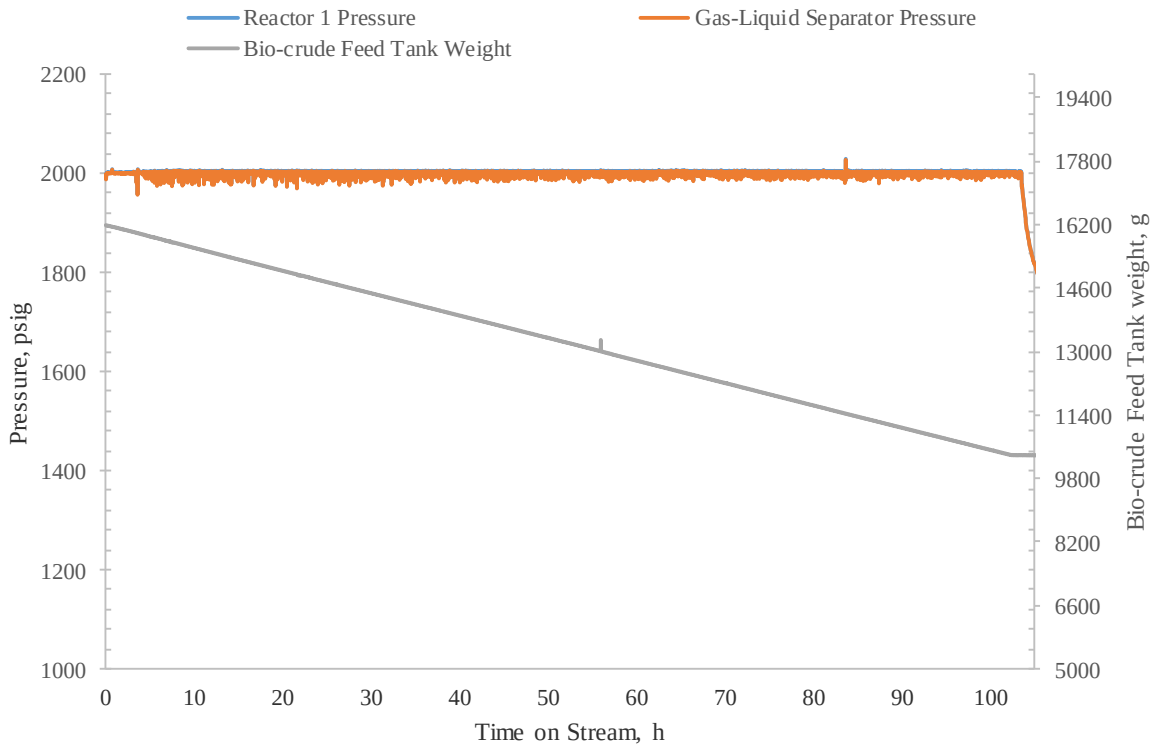

Figure 57: Plot showing reactor pressure and the change in weight of the biocrude feeding tank during experiment 3

Table 30. Hydrotreating results for Experiment 3

TOS, h	26-34	34-50	50-57	57-73	73-97
Mass yield of product oil, wt.%	77.3	68.94	72.56	73.91	72.69
Carbon yield of product oil, %	90.16	79.1631	82.45	83.4	81.76
Mass yield of aqueous fraction, wt.%	16.06	16.55	18.58	16.54	16.69
Product Gas yield, wt.%	6.84	6.84	5.66	5.65	5.52
H_2 consumed, g of H_2/g of dry bio-oil	0.0699	0.0687	0.0653	0.0654	0.0638
H_2 consumed, Nm^3/m^3	701.1	679.5	636.1	631.8	608.5
Mass Balance, %	96.96	98.29	95.35	95.05	94.56
Carbon Balance, %	96.66	85.75	87.89	88.65	86.85

The physicochemical properties of the hydrotreated products were monitored and a change in oil quality with time on stream was observed; it was even obvious in appearance as the color of the product changed over time. Figure 58 is a photograph of the first set of products collected in Experiment 1. As can be seen, the color of the product oils changed from golden to black. Monitoring of the density and the viscosity of the product oils was the standard protocol used in evaluating the quality of the product and performance of the experiments with time. As illustrated in Figure 59, the density changed from 0.876 to 0.988 g/cm^3 and the viscosity increased from 3.31 to 41.28 cSt for products collected between TOS window of 12-102 hours during experiment 3. The increase in both density and viscosity corresponded to an increase in the oxygen content of the oils from 0.63 wt% to 8.12wt% as detailed in Table 31. The increase in oxygen content with time is indeed indicative of catalyst deactivation. The results suggest that

the degree of deoxygenation was high in the first 24 hours of the experiment since the oxygen contents were below 2.5 wt%.

Figure 58: Photograph of the first batch of hydrotreated product collected in the first 30 hour run of experiment 1.

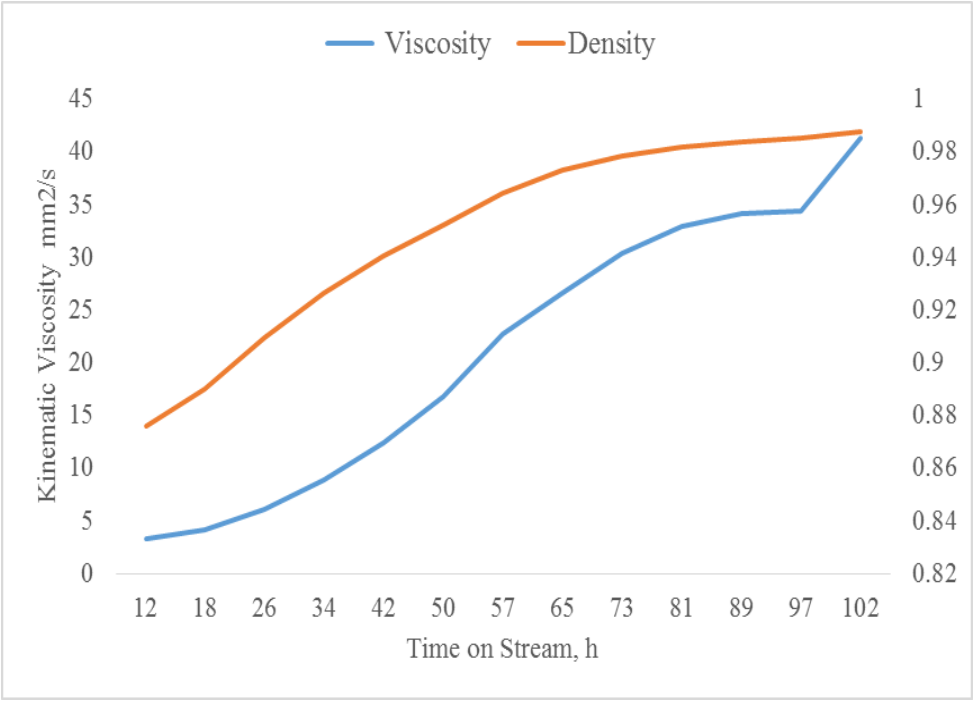

Figure 59: Density and Kinematic viscosity of product oils collected in experiment 3

Table 31. Elemental composition, Density, and Viscosity of Hydrotreated Product for Experiment 3

Time on Stream, h	C, wt%	H, wt%	N, wt%	O, wt%	Density, g/cm^3	Viscosity, cSt
12	86.52	12.28	0.56	0.63	0.876	3.31
18	86.09	11.79	0.49	1.63	0.890	4.17
26	85.31	11.71	0.58	2.40	0.910	6.11
34	84.28	11.25	0.54	3.93	0.926	8.90
42	83.58	10.93	0.55	4.93	0.940	12.43
50	83.28	10.82	0.63	5.28	0.952	16.78
57	82.57	10.53	0.60	6.29	0.964	22.67
65	82.55	10.35	0.51	6.59	0.973	26.63
73	81.71	10.09	0.48	7.73	0.978	30.42
81	81.90	10.09	0.54	7.46	0.982	32.92
89	81.79	10.01	0.53	7.67	0.984	34.13
97	81.49	10.00	0.55	7.96	0.985	34.40
102	81.39	9.85	0.64	8.12	0.988	41.28

The chemical composition of the oils was analyzed by FTIR and GC/MS. The FTIR spectra in Figure 60 characterizes the time on stream composition of the product oils from Experiment 1 and the plot in Figure 61 shows the change in the chemical classes of compounds identified by GC/MS for product oils collected in Experiment 3. The FTIR results did show that C-H stretches indicative of saturated hydrocarbons decreased with time while unsaturated C-H stretches, aromatic ring stretches, and OH stretches increased with time on stream. This implies that the product oils became more enriched with aromatic hydrocarbons and phenolics probably due to decrease in hydrodeoxygenation (HDO) and hydrogenation activity. Specifically, the GCMS result indicates that the naphthenic fraction decreased with time and compounds belonging to classes such as Monophenols and aromatics (Mono-, Di-, and Tri-) increased. There was also a gradual increase in other oxygenated species such as alcohols, ketones, aldehydes, acids, and multifunctional phenols.

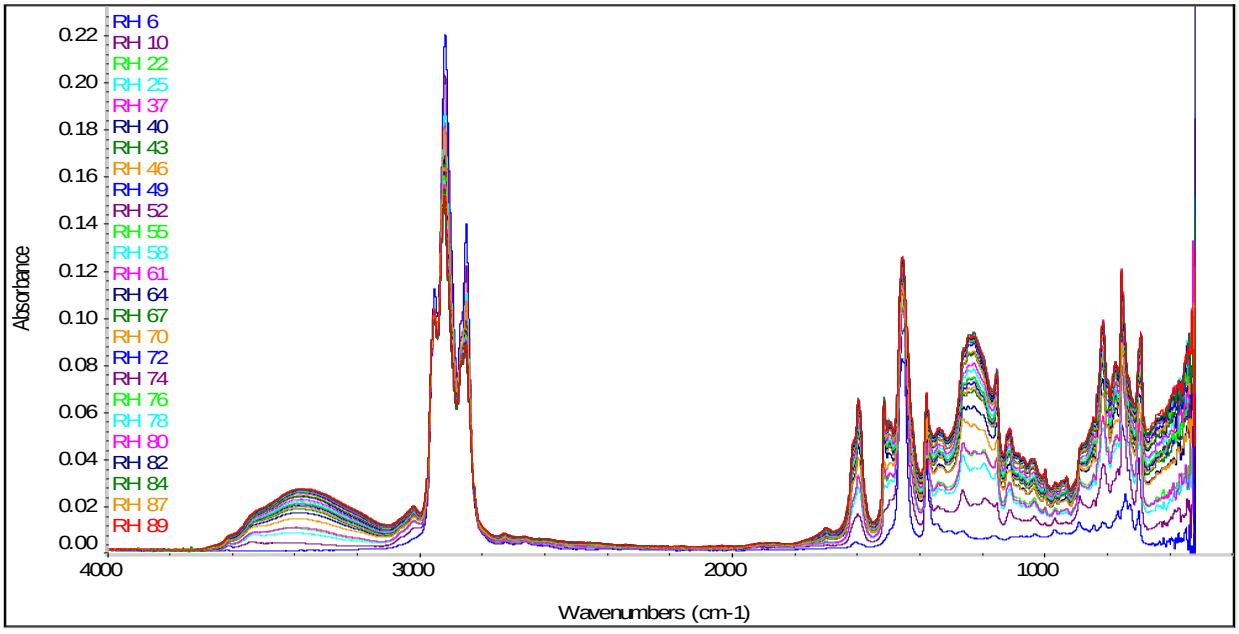

Figure 60: FTIR spectra showing TOS composition of product oils collected in experiment 1.

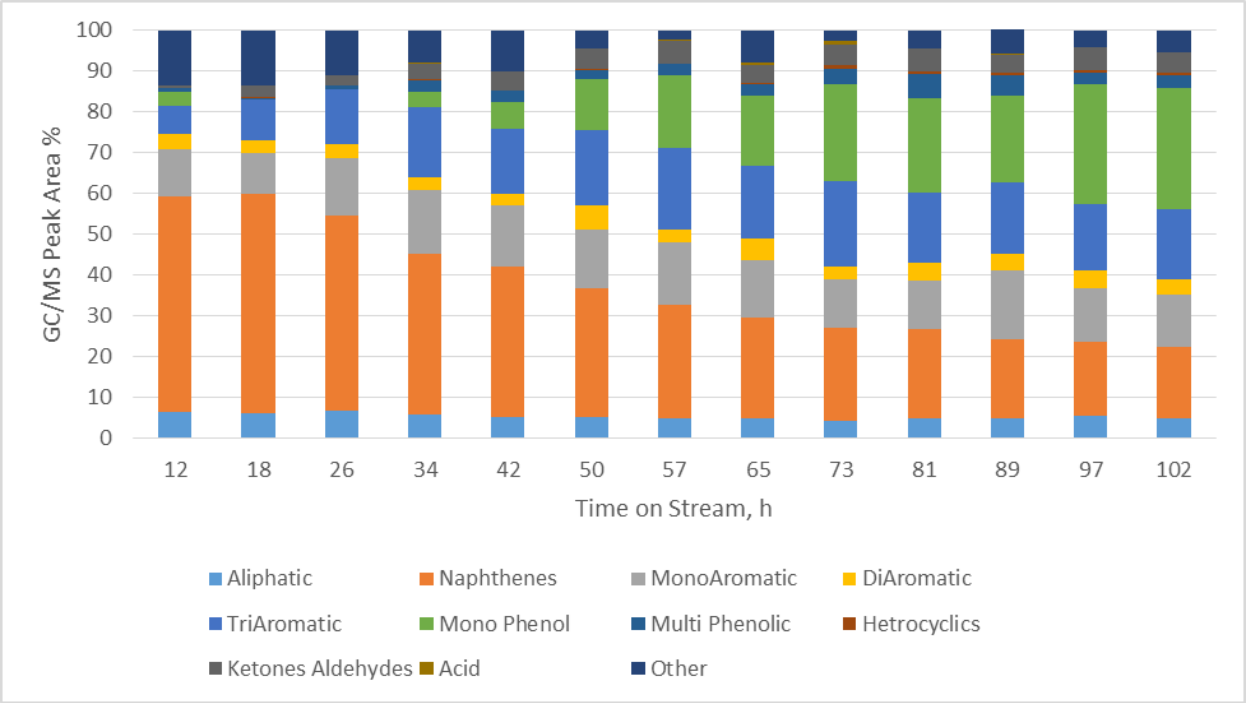

Figure 61: GC/MS peak areas showing the change in major classes of compounds with time for product oils collected in Experiment 3.

The product oils were also found to have carbon number distribution up to C25 (Figure 62). The analysis showed that the distribution of the carbon numbers varied with time. Compounds with carbon number of C10 and below and C15-C20 were higher in oils that were sampled within the first 20 hours of the run. In contrast, compounds with carbon numbers between C11-C15 and C21-C25 were found to be higher in product oils that were sampled beyond the 50 hour run time. Distillation results for some of the product oils collected in experiment 1 and 2 are presented in Table 32 and Figure 63.

In general, product oils with less than 1% oxygen content were found to contain higher fractions of naphtha/gasoline, kerosene/jet fuel, and diesel/heating. On the contrary, product oils with oxygen contents above 4wt% had higher fraction of gas oil. Overall, the results showed that the product oils collected from the hydrotreating of the bio-crude had fair distribution of the 4 major cut-points.

Table 32. Distillation results of selected product oils from the hydrotreating of pine bio-crude oil

Fractions (TBP range)	TOS=10-22	TOS=12-18*	TOS=37-40	TOS=49-52	TOS=52-55	TOS=55-58
Naphtha/Gasoline IBP-165°C	30.1%	28.2%	22.9%	24.8%	23.3%	22.3%
Kerosene/Jet Fuel 165-250°C	34.8%	20.0%	26.2%	25.2	26.6%	25.5%
Diesel/Heating 250-340°C	23.6%	27.6%	17.2%	17.8%	13.6%	15.9%
Gas oils 340-410°C	6.5%	19.4%	24.7%	19.3%	30.9%	31.4%
Oxygen, wt%	0.73	0.63	4.32	4.94	4.74	5.16

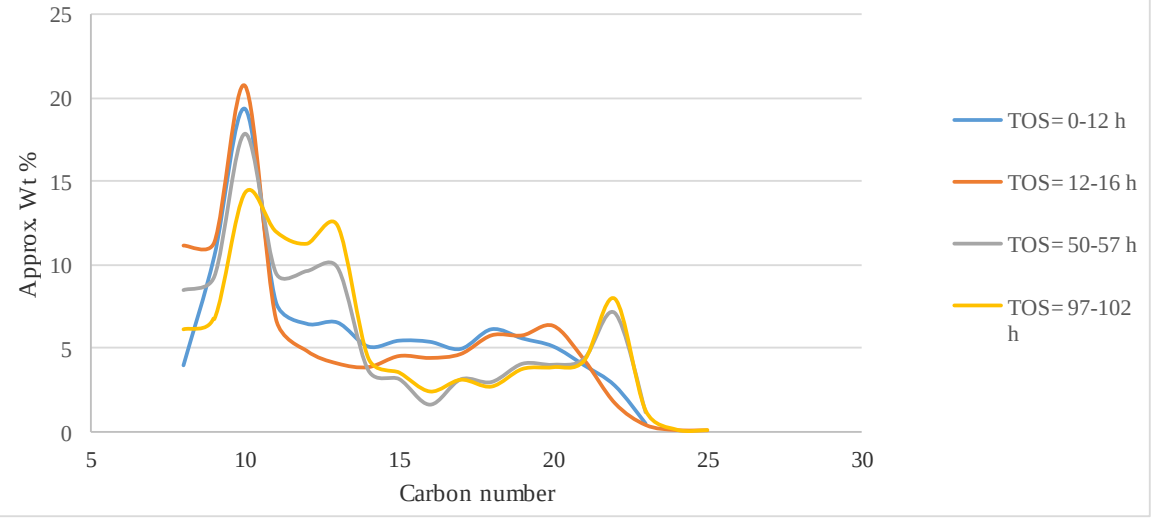

Figure 62: Carbon number distribution of product oils collected in experiment 3.

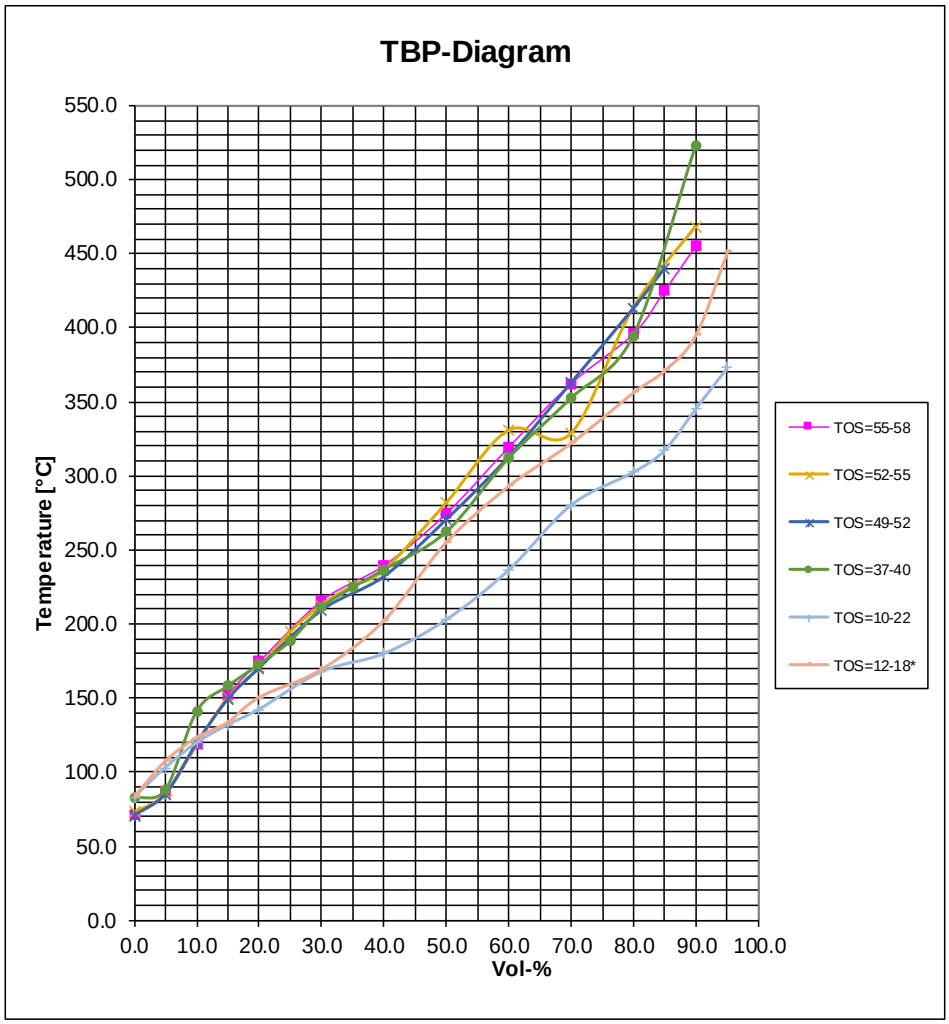

Figure 63: Distillation results of selected product oils from the hydrotreating of pine bio-crude oil.

Further hydrotreating experiments were performed to achieve about 900 cumulative hours on stream of bio-crude hydroprocessing. Table 33 summarizes all the experimental conditions.. The upgrading experiments were performed with a sulfided bio-cat (TK-341) supplied by Haldor Topsoe and four different kinds of loblolly pine bio-crude feeds produced from the 1TPD unit.

Table 33. Experimental Conditions

Condition	Exp. 1	Exp. 2	Exp. 3	Exp. 4	Exp. 5	Exp. 6
Bio-crude Feed	Feed A	Feed A	Feed B	Feed B	Feed C	Feed D
H_2 partial pressure (psig)	1450	1450	2000	2000	2000	2000
Average Temperature (°C)	R1=290, R2=350	350	300	290	R1=290, R2=350	300
LHSV (h^{-1})	0.5	0.5	0.25	0.25	0.25	0.25
H_2/oil ratio (Nl/l)	2000	2000	3000	3300	3300	3300
Catalyst dilution, Vol %	R1=60, R2=40	40	60	60	R1=60, R2=60	60
TOS, (h)	89	16	103	365	222	118

The elemental composition and GC-MS chemical composition of the bio-crudes are shown in Table 34. Sulfidation of the catalysts was done in-situ with 10% H_2S in H_2 at 118 psig prior to the runs. Steady-state material balances were performed and the yields and hydrogen consumption were determined. Per protocol, the experiments were allowed to run for at least 24 hours prior to performing a mass balances. HDT liquid products were sampled at different run hours and characterized for CHNO, specific gravity, and viscosity. Some of the liquid products were also characterized by distillation (ASTM 1160) and carbon number distribution.

Table 34. Elemental and chemical composition of the bio-crude feeds

Elemental, wt.%, dry basis	Feed A	Feed B	Feed C	Feed D
C	72.7	73.1	69.7	76.6
H	7.1	7.1	7.2	7.9
N	0.6	0.3	0.3	0.5
O	19.6	19.5	22.8	15.0
GC-MS Chemical composition (Peak Area %)				
Aliphatic	1.90	2.33	0.84	3.53
Carbonyls, mono	2.21	0.00	0.00	0.96
Carbonyls, multi	5.16	4.87	6.07	9.05
Furans	6.04	2.15	1.07	4.11
Acids	7.24	1.51	9.93	0.00
Mono-aromatic	3.91	8.78	1.13	28.50
PAH	10.77	15.87	20.44	14.34
Phenol, mono	11.42	3.41	0.56	3.00
Phenol, multi	38.84	49.45	42.05	33.47
Sugar	1.18	0.00	0.44	0.00
Unknown	11.35	11.63	17.45	3.03

The hydrotreating condition used in experiment 3 was re-tested in experiment 4 to ascertain how many run hours could be achieved since experiment 3 was stopped after 103 hours without any operational issues. Experiment 4 was run successfully for 365 hours without any pressure

drop across the reactor. Nonetheless, the hydrotreating was stopped because it appeared that the catalyst had deactivated. This was evident in the density and viscosity of the products. The reactor was then washed with isopropanol and the catalysts was re-sulfided with H_2S in an attempt to recover catalytic activity. Continuation of the experiment subsequently showed that solvent washing and re-sulfidation did not improve the activity of the catalyst. Surprisingly, removal of catalysts from the reactor was very difficult even though there was no pressure drop across the reactor. Experiment 5 was then conducted with the goal of achieving similar run hours in experiment 4 but addressing the issue with the quality of the liquid products. With that in mind, two reactors loaded with a 40% dilution of the bio-cat was used at similar conditions. The bio-crude feed C which had oxygen content slightly higher than feed B was used. The outcome of experiment 5 was quite different from experiment 4. For experiment 5, a pressure drop of about 6-8 psi across reactor 1 was observed within the first 24 hours of the run. Also, reactor 2 started building pressure (6-10 psi) after 36 hours. This unexpected observation, especially with reactor 2 suggested that the product from reactor 1 was not well upgraded. As a result, the temperature of reactor 1 was increased. The adjustment actually alleviated the pressure buildup in reactor 2. Moreover, compositional analysis of the effluents from reactor 1 revealed that the oil produced at the relatively low severity was less upgraded than the liquid produced at the high severity. Both reactors were run for 138 hours before the pressure drop across reactor 1 increased significantly and the run had to be stopped. The experiment was then continued on reactor 2 for additional 84 hours before it was shutdown. The upgrading of bio-crude feed D in experiment 6 at similar conditions used in experiment 4 was by far the most successful run in terms of operation and quality of the HDT product. This observation was attributed to the composition and oxygen content of the bio-crude feed (15wt% oxygen). However, the hydrotreating couldn't continue after 118 hours due to the lack of bio-crude feed.

Figure 64 shows a summary of the HDT liquid product yields from all the first six (6) experiments. The steady state mass balances ranged between 91 and 98% and the carbon balances varied from 83% to 98%. The carbon yields ranged between 55% and 95%. The yield of the hydrotreated liquid varied between 45wt% and 85wt% depending of the hydrotreating condition and the characteristic of the bio-crude feed. The lowest carbon yields were obtained from experiment 5 and the highest carbon yields were achieved in experiment 4. High yield of aqueous fraction (30-40 wt %) was observed in the experiment 5. Typical yield of the aqueous fractions were between 7-20 wt.% . In general, the yields of the liquid products increased with time on stream due to a decrease in deoxygenation activity; thus, those high HDT product yields within each experiment had relatively higher oxygen contents. The data suggests that high severity (lower space velocity and higher operating temperature/pressure) tend to decrease the HDT product yields. Compositional analysis of the product gas showed that light hydrocarbons constituted a larger fraction than carbon oxides. In fact, carbon monoxide was hardly detected in the product gas. Figure 65 shows a plot of hydrogen consumption against oxygen content and H/C ratio of the HDT product. The hydrogen consumption ranged between 4-11g H_2/100g of dry bio-crude feed. The chart indicates that hydrogen consumption significantly increased as oxygen content decreased below 2wt% oxygen and as the H/C ratio increased above 1.7. The consumption values from experiment 2 suggest that hydrogen consumption can be minimized by decreasing the HDT severity (lower pressure and higher space velocity). Also, oxygen content and aromaticity of bio-crude seem to have significant effect on hydrogen consumption.

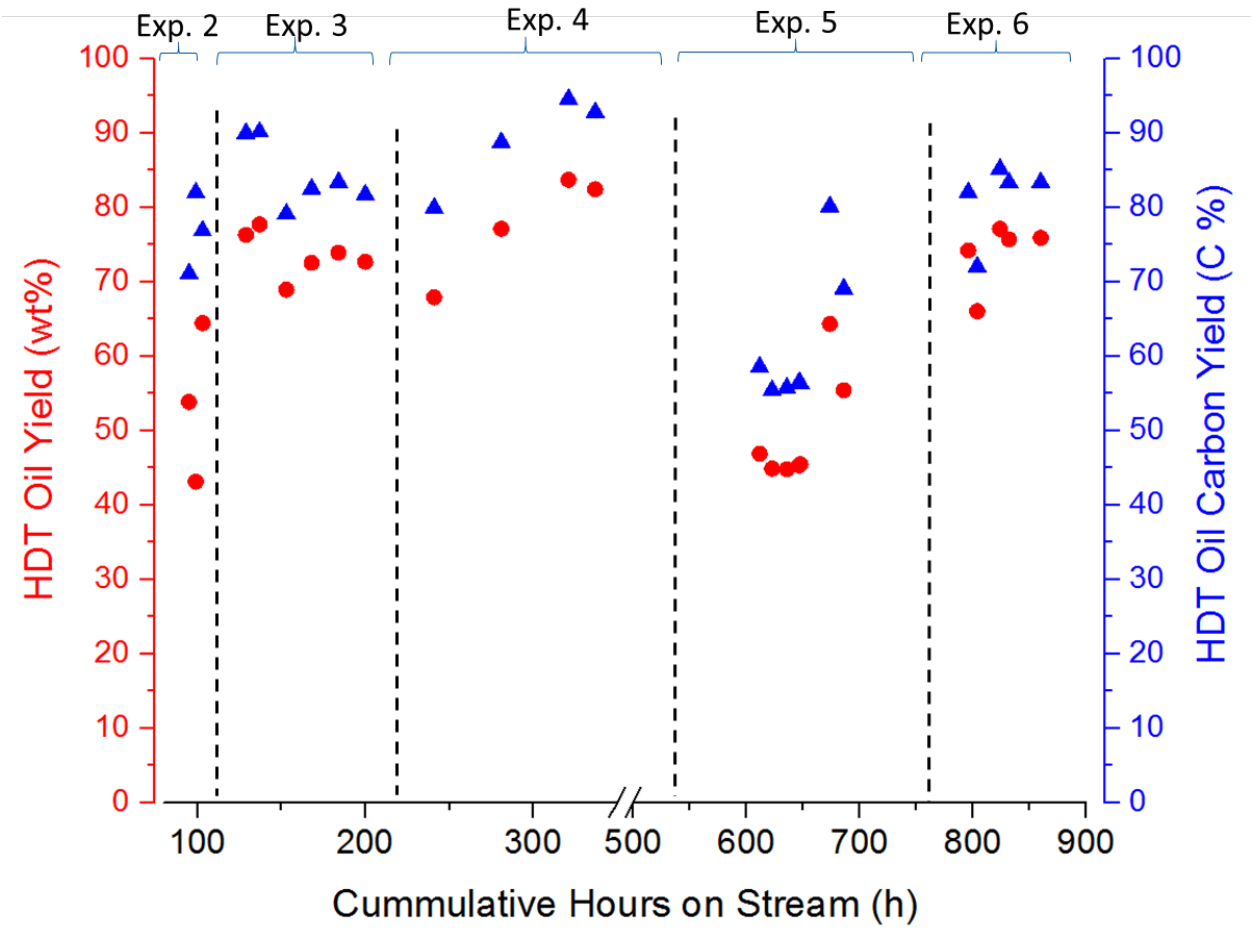

Figure 64: Results showing yields of HDT liquid product from the hydroprocessing of loblolly pine bio-crude

.

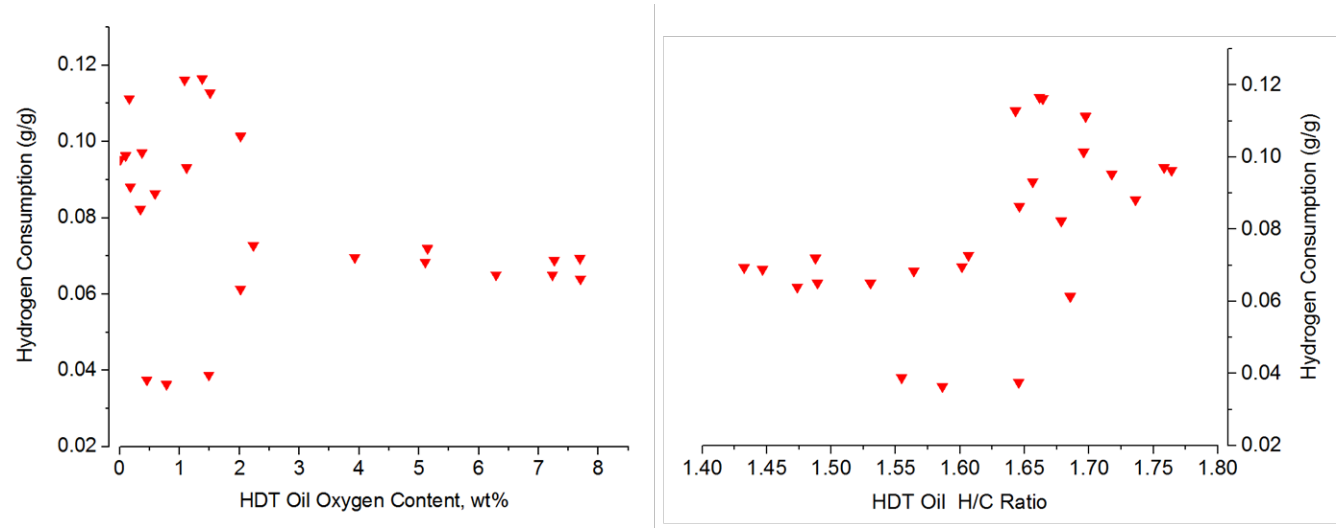

Figure 65: A plot of hydrogen consumption and oxygen content of the HDT product

Figure 66 shows the change in the density, viscosity, and the oxygen content of the HDT liquid products with time on stream within each experimental brackets. The change in these physicochemical properties was used in evaluating the quality of the product and performance of the experiments with time. In general, the results show that the catalyst bed starts to deactivate after about 25 hours of run time. It can be seen from experiments 1-4 that the quality of the product oils decreased with time on stream due to a decrease in HDO activity, probably as a result of catalyst deactivation. In contrast, it can be seen from experiment 5 and 6 that the changes in the density and the oxygen contents of the liquid products weren't strong as compared to the other experiments. Clearly, the use of a 2-stage approach in experiment 5 helped in improving the overall stability of the catalyst bed. Likewise, the use of the less oxygenated bio-crude feed D in experiment 6 proved to have less deactivating effect on the catalysts bed.

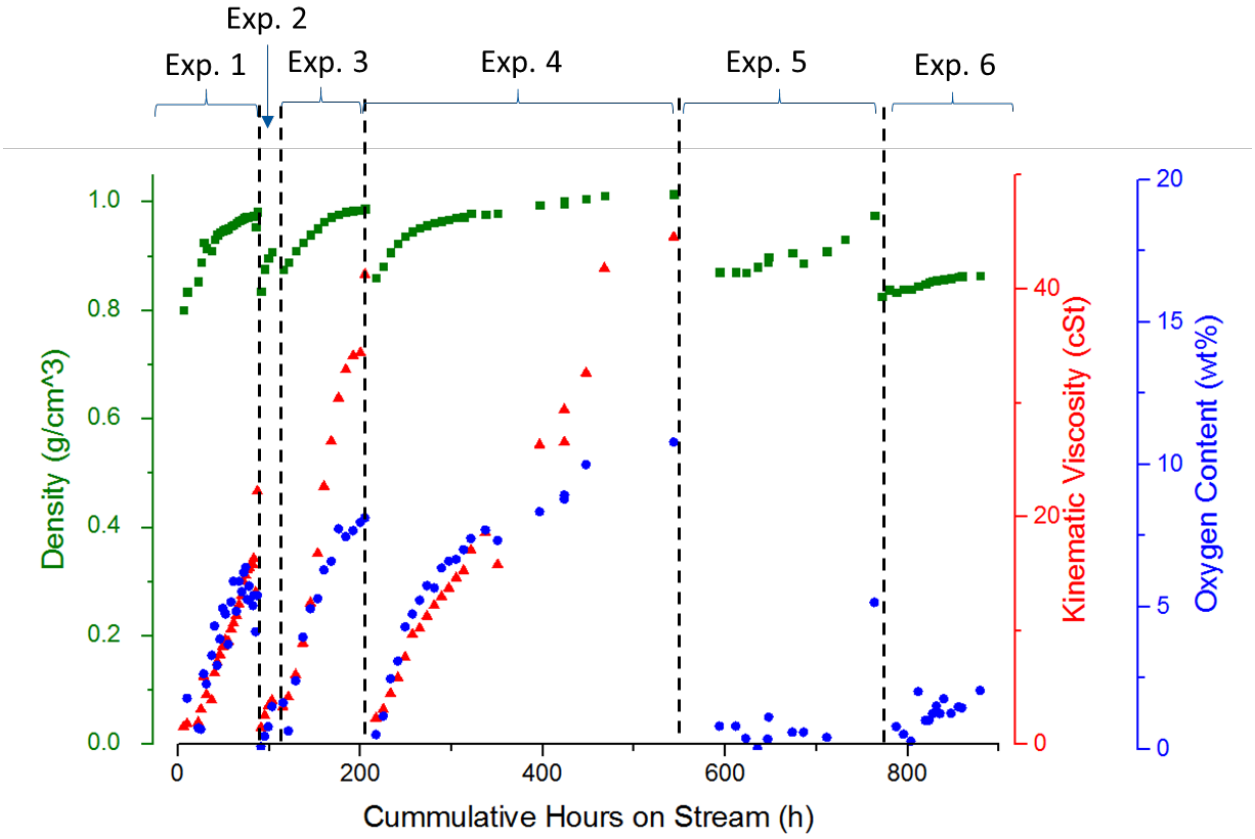

Figure 66: Plot showing a change in density, viscosity, and oxygen content of the HDT oils with time on stream within each experimental bracket

Furthermore, as shown in Figure 67, the GC-MS chemical composition of the HDT products from the upgrading on bio-crude feed D did not change significantly with time on stream as compared to the products obtained from the upgrading of bio-crude feed B. These results indicated that as the catalyst bed deactivates and the HDO activity decreases, the concentration of naphthenic hydrocarbons also decreases whilst the concentration of aromatic hydrocarbons (mono-, di-, and tri-) and phenols increases. Additionally, the concentration of other oxygenated species such as alcohols, ketones, aldehydes, and acids gradually increases as the catalyst bed deactivates. It can be inferred from the chemical composition of the products that

catalyst deactivation doesn't significantly affect demethoxylation of the multi-functional phenolics.

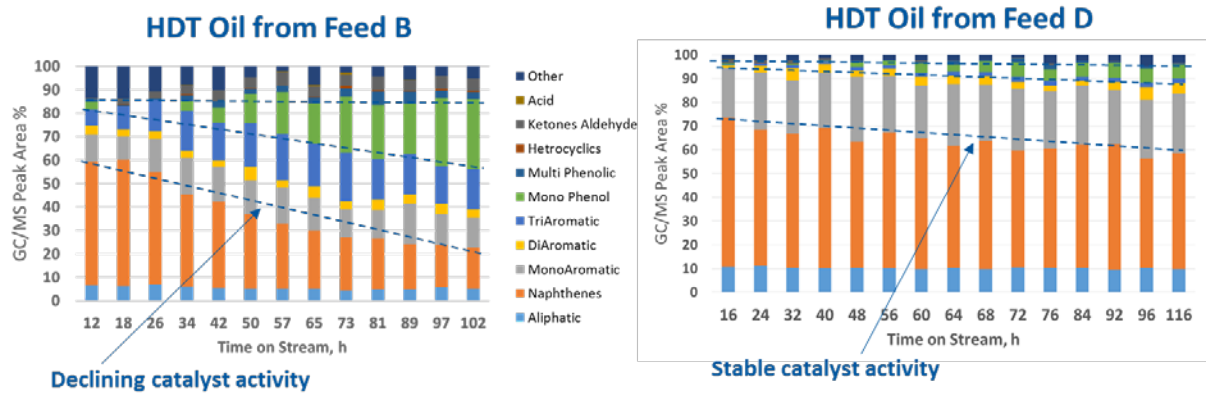

Figure 67: GC-MS compositional analysis of HDT products with time on stream showing the effect of bio-crude feedstock on the stability of the catalyst bed.

Hydrotreating different biocrude feedstocks over a single charge of catalyst

Four different biocrude samples were hydrotreated continuously over a single charge of HDT catalyst for a total of 213 hours. Table 29 shows the experimental condition that was used. The upgrading experiments were performed with a sulfided bio-cat (TK-341) supplied by Haldor Topsoe. Sulfidation of the catalysts was done in-situ with 10% H_2S in H_2 at 118 psig. The catalyst was regenerated twice during operation. The regeneration process consisted of washing the catalyst bed with a tri-solvent (toluene, acetone, and methanol) and then re-sulfiding the catalyst after the wash. HDT liquid products were sampled at different run hours and characterized (CHNO, specific gravity, and by GC-MS). Material balances were also performed for each biocrude feedstock evaluated.

Table 35. Experimental Conditions

Bio-crude Feed	Feed-F	Feed-G	Feed-H	Feed-I
H_2 partial pressure (psig)	2000	2000	2000	2000
Average Temperature (°C)	300	300	300	300
LHSV (h^{-1})	0.3	0.3	0.3	0.3
H_2/oil ratio (Nl/l)	3300	33000	3300	33000
Catalyst dilution, Vol %	60	60	60	60
TOS, (h)	45	24	28.5	116

Table 36. Organic elemental composition of biocrude feedstocks

		Elemental Composition, dry wt%			
Biocrude	Moisture, wt%	C	H	N	O
Feed ***F***	0.63	84.15	8.96	0.99	5.91
Feed ***G***	1.13	84.05	10.06	0.28	5.62
Feed ***H***	27.93	55.34	6.29	0.22	38.14
Feed ***I***	5.80	70.54	6.98	0.13	22.35

Table 36 shows the elemental composition of each feedstock evaluated. The feed-F and feed-G had the lower oxygen contents; 5.91wt% and 5.62 wt% respectively. The oxygen contents of feed-I (22.25 wt %) and feed-G (26.46 wt %) were higher. The feed-F was produced from catalytic pyrolysis of hardwood; the feed-G on the other hand was a once-through product from HDT of loblolly pine biocrude; and feeds H and I were both biocrudes produced from catalytic pyrolysis of loblolly pine.

Even though feeds F and G have comparable oxygen contents, their chemical compositions determined by GC-MS were quite different as shown in Figure 68. Feed-F was rich in di- and mono- aromatic hydrocarbons. The mono-aromatic hydrocarbons were mainly alkylated benzenes and the di-aromatics were alkylated indenes to a large extent and napthalenes to a lesser extent. The oxygenates present in feed-F were primarily benzofurans, cyclopenten-1-ones, and simple phenols. Since feed-G had already undergone a single stage hydrotreating, the oxygenates present were primarily simple phenols and the hydrocarbons were mainly paraffins and napththenes. Also, the aromatic hydrocarbons in feed-G were predominantly tri-aromatics. For feeds H and I, oxygenates such as methoxyphenols, anhydrosugars, furans, acids, ketones, aldehydes, and other unknown species were the main chemicals present. Distinctively, the last two feeds lacked both aliphatic and aromatic hydrocarbons. Between the high oxygenated feedstocks, feed-I had high amount of multifunctional phenolics and PAH than the feed-H which was high in carbonyl compounds and anhydrosugars.

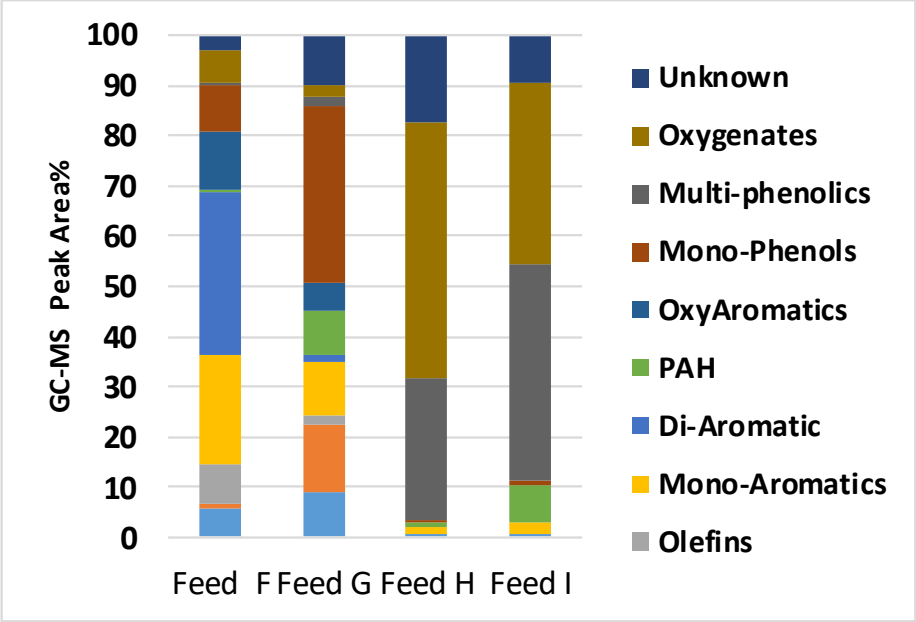

Figure 68: GC-MS chemical composition of various bio-crude feeds

The results of the HDT studies summarized in Table 37 show how the input chemical composition of the various feeds studied affected the HDT product distribution and hydrogen consumption. Specifically, Figure 69 shows a correlation between the oxygen content of the biocrude feed and the HDT liquid product yield. The hydrotreating of the feeds (F & G) with less than 6 wt% oxygen content resulted in very high HDT liquid product. For feed-F, the liquid product yield was 95.62 wt% and about 98.6% of the feed carbon was retained in the liquid

product. In the case of feed-G, 98 wt% was converted into the liquid product and almost all the feed carbon was retained. Clearly, minimal amount of both feeds was loss to the gas and aqueous phases. Also, the material balances seem to suggest that any loss due to carbon buildup on the catalyst or fouling may be negligible for the time window that the mass balance was conducted. The data show that about 0.062 g and 0.052g of hydrogen was consumed per 1g each of feeds E and F respectively.

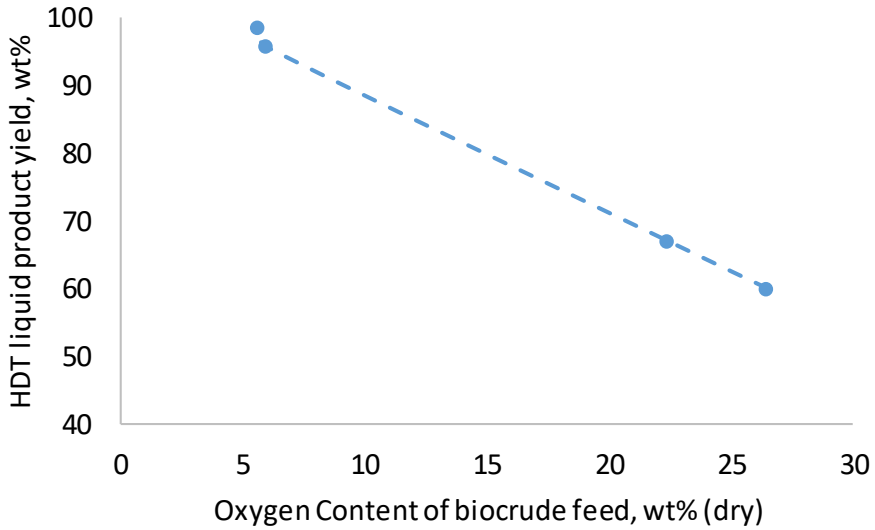

Figure 69: Effect of oxygen content of biocrude on the HDT liquid product yield

Table 37. Hydrotreating Results

Feedstock	Feed F	Feed G	Feed H	Feed I	Feed I	Feed I
TOS, h	10-25	51-68	73-91	96-120	121-144	145-168
Mass yield of product oil, wt.%	95.64	98.52	59.97	64.73	66.88	69.45
Carbon yield of product oil, %	98.55	100.70	79.39	78.77	80.77	83.68
Mass yield of aqueous fraction, wt.%	3.11	2.09	14.41	24.29	23.78	23.60
Carbon yield of aqueous fraction, %	0.033	<0.01	0.44	0.21	0.22	0.21
Product Gas yield, wt.%	3.02	2.21	11.29	7.30	7.02	6.83
Carbon yield of product gas, %	2.96	2.17	11.94	7.08	6.78	6.57
H_2 consumed, g of H_2/g of dry bio-oil	0.062	0.052	0.1275	0.095	0.097	0.096
Mass Balance, %	101.76	102.82	85.67	96.91	98.24	95.15
Carbon Balance, %	101.56	102.88	91.79	86.07	87.77	90.41

The HDT of feeds H and I resulted in relatively lower liquid product yields. The liquid product yield for feed-H was determined to be about 60wt% and that for feed-I varied from 64.7wt% to 69.45wt% with time on stream. The amount of aqueous phase fraction formed from these two feeds was significantly high. About 14.1 wt% of feed-H was converted to aqueous phase and 23.6wt%-24.4 wt% of feed-I as well. Moreover, the gas yields were far higher than those from feeds F and G. The amount of gas phase product formed from feed-H was 11.3wt% and that for feed-I ranged between 6.8wt% and 7.30 wt%. The hydrogen consumption for feed-H was the highest; it was determined to be 0.128 g of hydrogen per 1g of dry feed. The hydrogen

consumption for feed-I averaged at 0.096 g of hydrogen per 1g of dry feed. The relatively high amount of hydrogen consumed in the HDT of feed-H is not surprising since it had high oxygen content. The carbon balance which show that about 10% or more of feeds H and I were unaccounted could suggest carbon loss due to carbon deposition or fouling.

Figure 70 shows the change in the physicochemical properties with time on stream for all the liquid products collected from the HDT of the four different feeds. The changes in the density and the oxygen content indicate the quality of the HDT product and performance of the experiments with time. As shown in Figure 70, the density changed from 0.841 to 0.941 g/cm^3 for HDT liquid products collected between TOS window of 9-75 hours. The increase in density corresponded to an increase in the oxygen content of the oils which increased from 0.54 wt% to 3.41wt%. The increase in oxygen content with time is indeed indicative of catalyst deactivation. Therefore, prior to processing feeds H and I, the catalyst bed was regenerated and as can be seen the immediate HDT oils collected afterwards had lower density and oxygen content. Again, it can been seen that the density and oxygen content gradually increased with time and at TOS of 190 h, the density of the HDT product had reached 0.920 g/cm^3 with a corresponding oxygen content of 4.01 wt%. As a result, the catalyst bed was regenerated for the second time and consequentially a decrease in density and oxygen content was observed. Shortly afterwards, the experiment was terminated because the pump wasn't feeding very well. It is worth noting that even though the feeds used in the first half of the experiment had oxygen contents lower than 6wt%, deactivation of the catalyst bed was observed in less than 100 hours of run time.

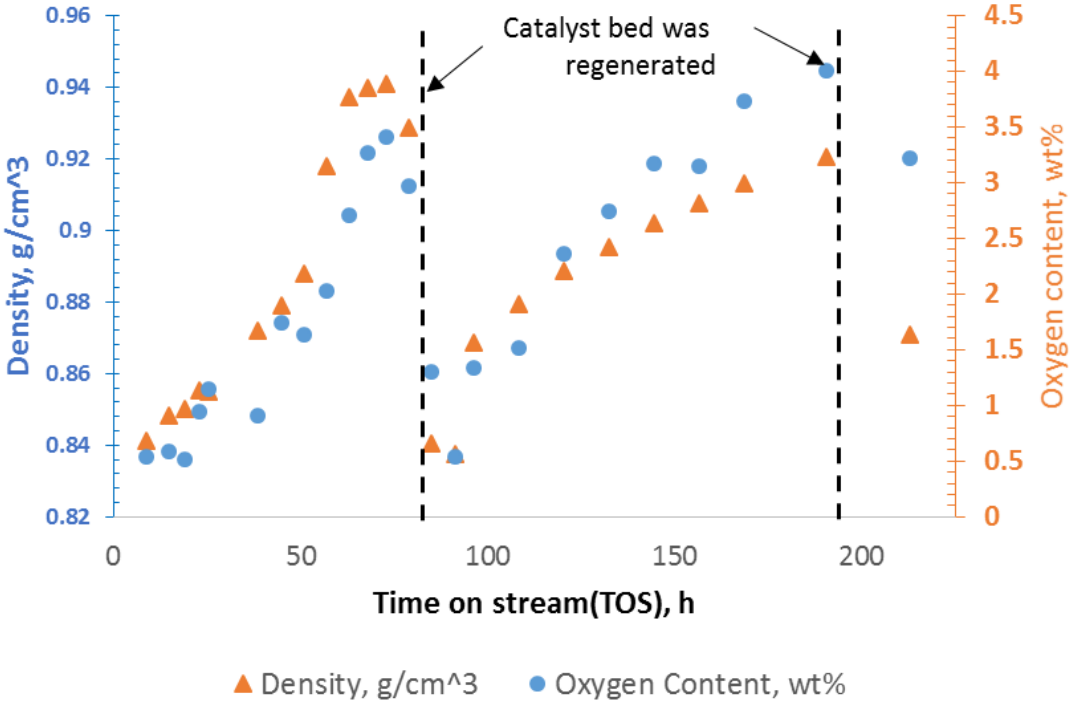

Figure 70: A Plot showing a change in density and oxygen content of the HDT oils with time on stream

The chemical composition of the liquid products collected from the HDT of feed-F is presented in Figure 71. It can be seen that the chemical constituents of HDT products collected were mainly paraffins, napthenes, and mono-aromatics. The chemical analysis indicates that

most of the hydrogen consumed during HDT of feed-F was used to a large extent for hydrogenation of indenes and monoaromatics. The increase in, oxyaromatics and simple phenols with time in the HDT products suggests that the hydrodeoxygenation of these oxygenates may require relatively higher catalyst activity than the saturation of the aromatic rings and olefins.

The products collected from the HDT of feed-G were found to be higher in naphthenic hydrocarbons, simple phenols, and PAH than the products collected from feed-F (Figure 72). Based on the results, it seems that hydrogenation and hydrodeoxygenation of simple phenols and other oxyaromatics leads to the formation of naphthenes and monoaromatics more than paraffins. The presence of PAH in the products also suggest that they might be difficult to saturate at the conditions used or may require higher catalyst activity.

Similarly, the products collected from the feeds H and I were richer in naphthenic hydrocarbons (Figure 73). The amounts of paraffins and monoaromatics were lower compared to the products from feeds F and G. This means that phenolics and other oxygenates were primarily converted to cyclic hydrocarbons. The lack of high amount of monoaromatic hydrocarbons in the products as the catalyst deactivated may suggest that the route to the formation of cyclic hydrocarbons is largely by hydrogenation (HYD route) instead of a direct deoxygenation route. In general, as the catalyst bed deactivated, the amount of simple phenols and other oxyaromatics increased.

Overall, the HDT of the four feeds provide additional information on how the chemical speciation of biocrude and the bulk oxygen content affect the hydrotreating upgrading step in terms of performance and the quality of the products.

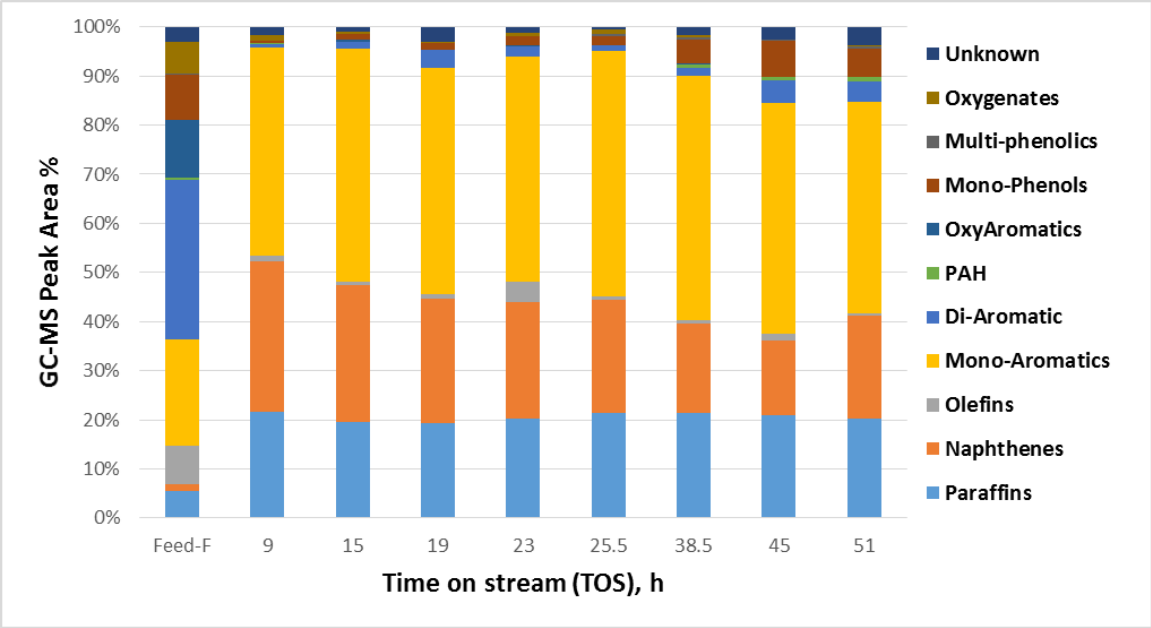

Figure 71:GC-MS compositional analysis of liquid products collected from HDT of feed-F

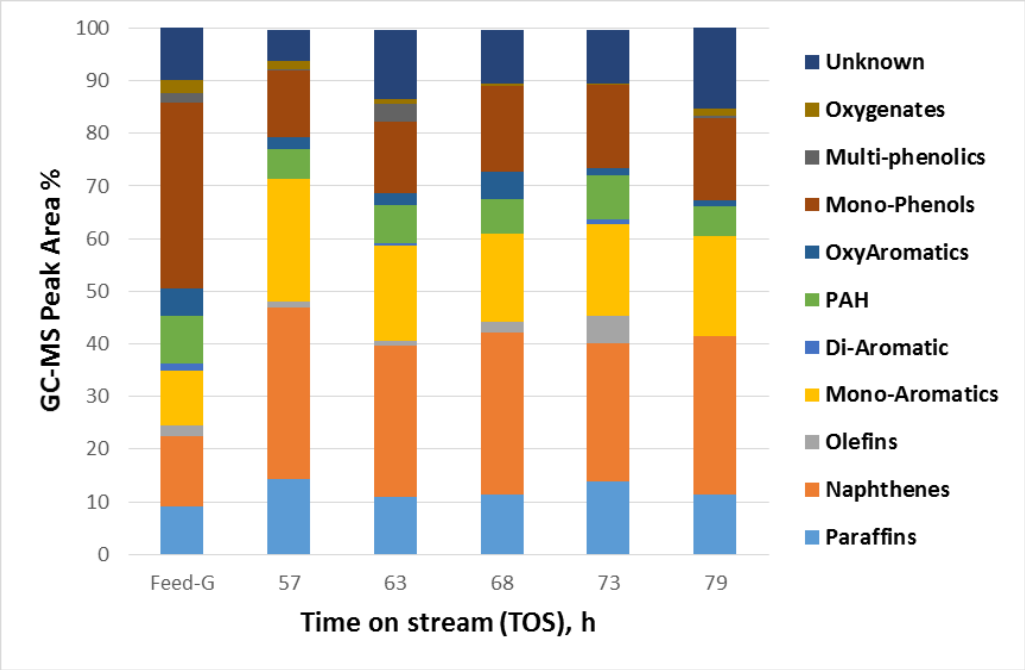

Figure 72.GC-MS compositional analysis of liquid products collected from HDT of feed-G

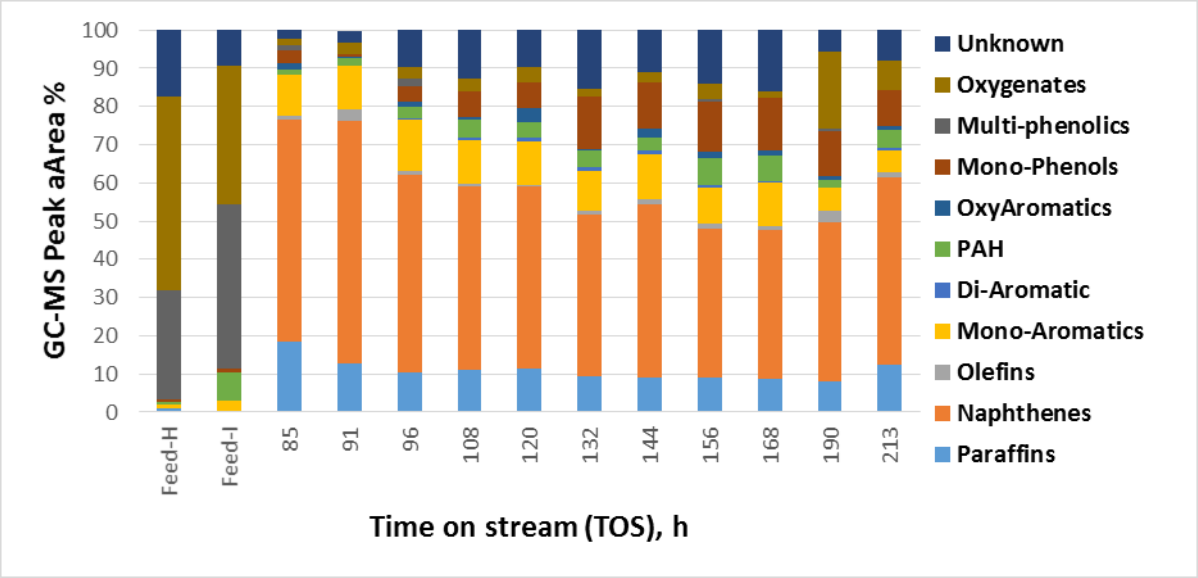

Figure 73: GC-MS compositional analysis of liquid products collected from HDT of feeds H and I.

Hydrotreating of hardwood biocrude feedstock

The milestone for hydrotreating biocrude from hardwood (red oak) for 500 hours was completed. The upgrading experiment was performed with a sulfide hydrotreating catalyst - bio-cat (TK-341) supplied by Haldor Topsoe. Sulfidation of the catalysts was done in-situ with 10% H_2S in H_2 at 118 psig prior to the run. The

Table 38. Experimental Conditions	
Condition	Exp. 6
H_2 partial pressure (psig)	2000
Average Temperature (°C)	300
LHSV (h^{-1})	0.33
H_2/oil ratio (Nl/l)	3300
Catalyst dilution, Vol %	60
TOS, (h)	>200

experimental conditions used are summarized in Table 38.

The red oak biocrude used for the hydrotreating study had carbon and oxygen contents of 68.7 wt% and 24.5 wt% respectively on dry basis. GC-MS analysis showed that the biocrude contained predominantly phenolic compounds. Unlike the pine biocrudes, the phenolic compounds in the red oak had a high concentration of syringols (e.g. Phenol, 2,6-dimethoxy-4-(2-propenyl)-) in addition to guaiacols(e.g. Phenol, 2-methoxy-4-methyl-) as expected. Aromatic hydrocarbons accounted fo about 12 % of of the total ion chromatogram. The biocrude also had a reasonable amount of carbonyl oxygenates like furfural, 5-methyl -2-Furancarboxaldehyde, and 2(5H)-Furanone. Anhydrosugars such as levoglucosan constituted about 4% of the total ion chromatogram.

Overall, hydrotreating red oak biocrude for 500 hours was achieved without any operational issues. Due to catalyst deactivation, the experiment was stopped intermittently to regenerate the catalyst. The regeneration process consisted of washing the catalyst bed with a tri-solvent (toluene, acetone, and methanol) and then re-sulfiding the catalyst after the wash. The catalyst bed was finally replaced after a significantly pressure drop (60psig) across the reactor around TOS of 398 hours was observed. The experiment was completed over the second charge of catalyst.

Table 39 shows a summary of the HDT liquid product yields from the experiments. The steady state HDT liquid yield varied between 67 wt% and 82 wt%. The carbon recovered in the HDT liquid was from 79% to 97%. The amount of aqueous liquid product was between 11.6wt% and 28 wt%; however, the carbon recovered in the aqueous liquid product was negligible (0.1% to 1.7%). The product gas yield was between 4.3 wt% and 9 wt%. Compositional analysis of the product gas showed that light hydrocarbons constituted a larger fraction than carbon oxides. The hydrogen consumption analysis with respect to the feed and the HDT products indicated that about 3.4-5.1g of hydrogen was consumed per 100g of dry bio-crude feed.

Figure 74 below is a plot showing the change in HDO activity and density of the HDT product liquids with time on stream for the hydrotreating experiment over the initial charge of catalyst. The HDO activity as used herein refers to the degree of deoxygenation of the biocrude. As can be seen from the plot, the HDO activity decreased from 94% to 70% within the TOS window of 7-250 hours, and then it leveled off through TOS of 398 h. The slight increase in HDO activity at TOS 168h and 316h is actually when the catalyst bed was washed with the tri-solvent (toluene, acetone, and methanol) to regenerate the catalyst. Nevertheless, from the plot, it appears that the solvent wash helped the hydrotreating experiment to run longer but did not significantly recover the catalyst activity. This is also true for the density of the HDT oils; the density changed from 0.826 to 0.941 g/cm3 for products collected between TOS window of 7-168 hours. After the solvent wash, the density decreased from 0.941 to 0.905 g/cm3, but it then increased again gradually to 0.905 g/cm at the end of the experiment. Notably, the wash at TOS 316 did not cause a decrease in the density of the HDT product liquids collected afterwards. Figure 75 shows the GC-MS chemical composition of some of the HDT products. Clearly, the composition was made up of naphthenes to a large extent, paraffins, and mono-aromatic hydrocarbons for the initial products collected. However, olefins, oxygenated aromatics, and simple phenols in particular, were produced as the HDO activity decreased. As a result, the concentration of naphthenic hydrocarbons.

Table 39.Summary of the biocrude HDT results

Time on stream (TOS), hrs	**28-64**	**74-98**	**98-136**	**147-168**	**214-238**	**239-246**	**247-269**	**248-268**	**269-296**	**297-312**
Mass yield of product oil, wt%	69.4	69	72.1	72.8	67.6	81.4	77.4	74.1	74.7	67.7
Mass yield of aqueous fraction, wt%	21.8	19.1	20.5	19.5	25.4	17.5	11.6	23.6	28.2	22.6
Mass yield of product gas, wt%	8.4	7.8	7.4	7	4.7	4.2	4.3	4.3	5.2	4.3
Mass balance, %	99.5	95.9	100.1	99.3	97.7	103.1	93.3	102	108.1	94.6
Carbon yield of product oil, %	86.3	85	87.6	87.8	80.6	96.4	91.9	87.7	87.9	79.7
Carbon yield of aqueous fraction, %	0.1	0.1	0.1	0.1	1.5	0.1	1.7	0.1	1.6	1.4
Carbon yield of product gas, %	8.6	7.8	7.3	6.8	3.9	3.5	3.5	3.5	4.1	3.4
Carbon balance, %	95	92.8	95.1	94.8	86	99.9	97	91.3	93.6	84.4
H_2 consumed, g of H_2/g of dry bio-oil	0.051	0.044	0.046	0.043	0.038	0.044	0.053	0.043	0.049	0.034

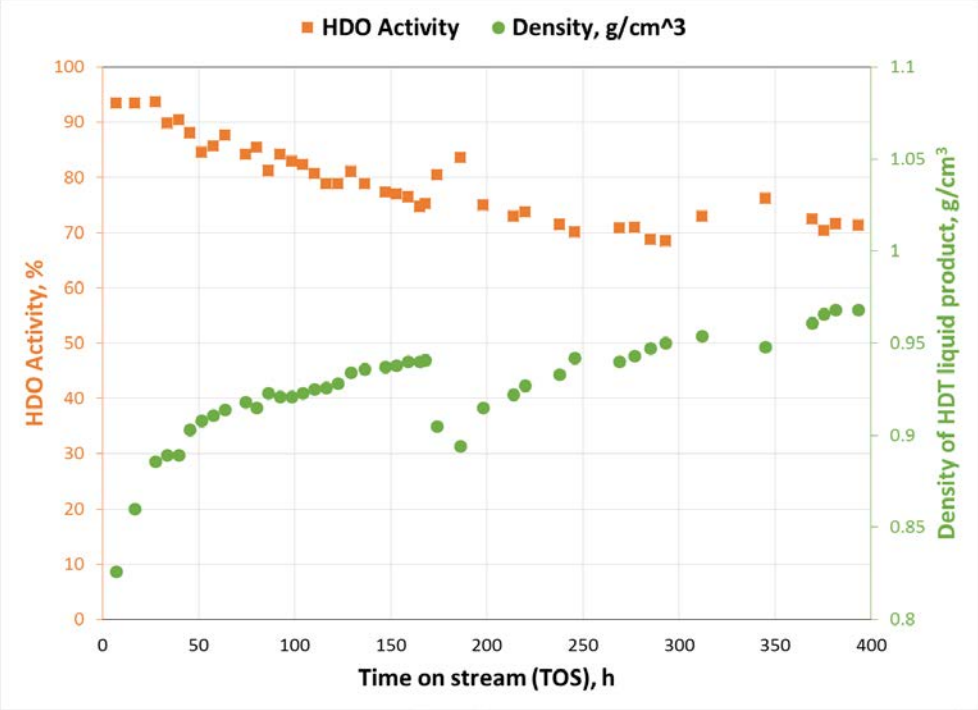

Figure 74: HDO Activity and change in density of HDT oils with time on stream

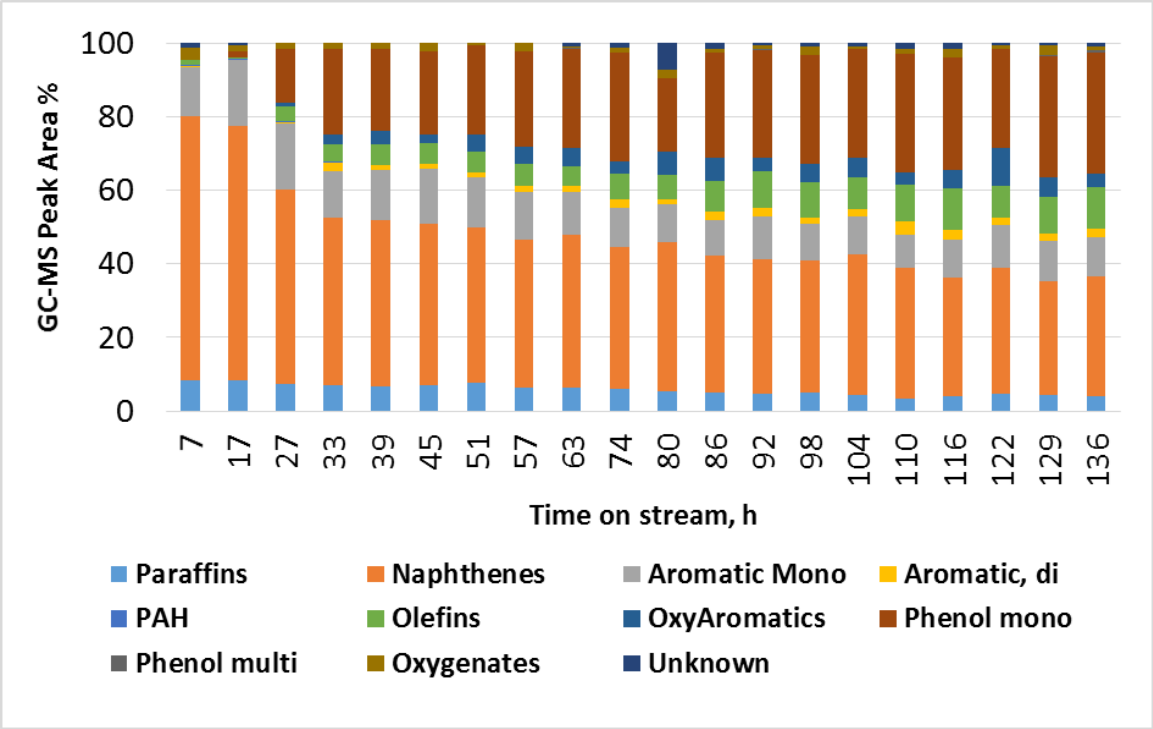

Figure 75. GC-MS analysis of HDT product liquids collected between TOS of 7h and TOS of 136h

Bio-crude and Refinery Intermediates Co-Processing Studies

In order to find an optimal insertion point for the bio-crude in a refinery, a blending test with various fossil feedstocks was carried out. Five different feedstocks were identified based on their different properties. The identified feedstocks were; Straight run naphtha, FCC naphtha, Straight run gas oil, Light cycle oil and Aromatic extract (Table 40). The reasoning behind selecting the different fossil feeds was that they are different interesting blendstocks from a process point of view and have different amounts of aromatics. The aromatic extract was mainly chosen due to the high amount of aromatics, not so much in order to make a good fuel. Properties of the different feedstocks used for the blends and pictures of the blends can be seen in Table 40 and Figure 76.

Table 40. Properties of the RTI bio-crude along with the fossil feedstocks used for blending

Oil type	RTI Biocrude	Straight Run Naphtha	FCC Naphthta	Straight Run Gas Oil	Light Cycle Oil	Aromatic Extract
SG 60/60°F	1.16	0.73	0.74	0.86	0.93	1.02
Aromatics						
1 Ring, wt %		12.47	15.89	15.76	24.13	11.95
2 Ring, wt %		<0.1	<0.1	10.5	39.01	10.23
3+ Ring, wt %		<0.05	0.1	2.46	7.03	43.38
Simulated Distillation						
0.5 wt% (IBP), °C	68	-	-	131	59	330
5 wt%, °C	75	-	-	220	143	365
15 wt%, °C	148	56	63	263	202	390
30 wt%, °C	224	74	86	285	241	414
50 wt%, °C	275	99	111	311	269	440
70 wt%,°C	352	117	136	341	297	466
90 wt%, °C	430	145	162	380	336	506
95 wt%. °C	469	159	169	397	352	524
99.5 wt% (FBP), °C	557	179	183	424	390	575

Figure 76: Pictures of the blends.

The blending ratios are in volume % and the blending was done at room temperature. Unfortunately, the blending was not very successful. The aromatic extract looked like it was promising, but it separated when it sat for a while. It is difficult to see from the picture, as both the aromatic extract and the pyrolysis oil is a black liquid, but when held up to the light, a bottom phase with a tinge of green can be observed. After the initial blending, all of the blends were heated to around 60 °C to see if this would increase the solubility of the pyrolysis oil in the fossil feedstocks. This was not the case.

Pilot test co-feeding of pyrolysis oil and hydrotreated diesel

The blending test carried out using pyrolysis oil and fossil oils had shown that it's not possible to get a homogeneous solution with several fossil refinery streams. But, because of the problems experienced during the previous pilot tests (getting the pyrolysis oil through the unit and coking and pressure drops in the reactor), it was decided to try co-feeding of the pyrolysis oil with a hydrotreated diesel feed. A hydrotreated diesel was chosen to minimize the hydrogen consumption connected to HDS and HDN in the reactor, making the feed easier to hydroprocess. The properties of the two feeds used for co-feeding can be seen in Table 41. Also, it was decided to try a grading of the activity of the catalysts down the reactor. See illustration in Figure 77.

Table 41. Properties of the two feedstocks used for co-feeding in FKT 1849

Sample Name	Method	PO.X.RTI.B5 (Bio-crude)	3.LG.X.SK.B4 Tr 33 (HT Diesel)
S, wt%	ASTM D4294	0.0031	0.0080
N, wt ppm	ASTM D4629	476	28
H, wt%	ASTM D7171	5.86	-
O, wt%	ASTM D5291	26.8	-
C, wt%	ASTM D5291	63.8	-
SG 60/60°F	ASTM D4052	-	0.8399
Simulated Distillation			
0.5 wt% (IBP), °C	ASTM D7213	89	90
5 wt%, °C		161	195
30 wt%, °C		260	274
50 wt%, °C		315	303
70 wt%,°C		377	333
85 wt%, °C		425	366
90 wt%, °C		448	380
95 wt%. °C		490	398
99.5 wt% (FBP), °C		570	428

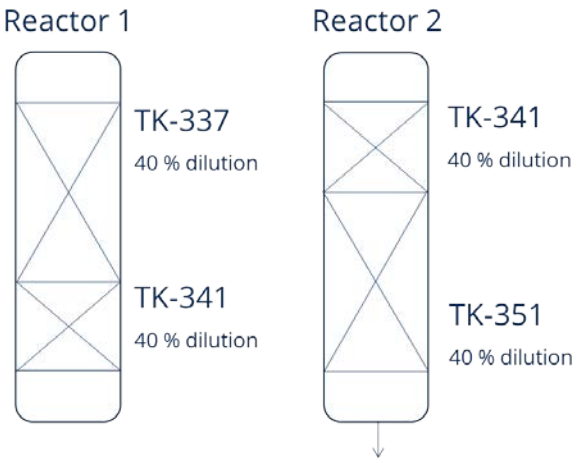

Figure 77: Illustration of the test setup for FKT 1849.

The test was started up at the following conditions:

	Test conditions	
Oil flow, PO.X.RTI.B5	50 ml/h	
Oil flow, 3.LG.X.SK.B4	500 ml/h	
Temperature	330 °C	625 °F
Pressure	120 barg	1750 psig
LHSV (based on pyrolysis oil)	0.2 1/h	0.2 1/h
H_2/oil (based on pyrolysis oil)	3000 Nl/l	17800 SCF/BBL

The co-feeding was simulated by simultaneously pumping both the pyrolysis oil and the hydrotreated diesel into the unit. In this way, the feeds were assumed to mix in the pipes. The flows of the two pumps were set to give a blended feed consisting of around 10 vol% pyrolysis oil in the hydrotreated diesel. Unfortunately, the test shut down due to pressure build-up after approx. 4 hours. The test was started up again, but was closed down after another 2 hours. Coke was found both in the piping before the reactor and in the first reactor, which explains the pressure build-up. Also, it was not believed that the two feeds formed a homogeneous blend simply by the mechanical mixing in the pipes and that the pyrolysis oil, therefore, build up in the pipes. Co-feeding of the pyrolysis oil without an initial hydrotreating step that can facilitate the mixing does not seem feasible.

Another test was run with the same type of loading as in FKT 1849, but with no co-feeding, only pyrolysis oil. In the previous test, only reactor 1 was heavily coked while reactor 2 seemed fine. Therefore it was decided to reload reactor 1 while keeping the loading from FKT 1849 in reactor 2. To reduce the coking in the reactor, the temperature was also decreased to 290 °C.

This test ran for approx. 10 hours, but with a number of shutdowns. Two samples, that looked very promising, were taken. These two samples consisted of two phases, a bottom water phase and a top organic phase, which suggested that significant HDO had been performed. The samples were taken hereafter consisted of solidified, but not completely hardened, pyrolysis oil with a little water. This is believed to be the cause of the plug in the reactor and HPS and the reason the unit had to be shut down.

Table 42. Analysis results of the two product samples taken during FKT 1863.

SAMPLE	METHOD	FEED	PRODUCT	
Run Hour			7	10
S, wt ppm	ASTM D4294	31.2	-	-
N, wt ppm	ASTM D4629	476	-	-
H, wt%	ASTM D7171	5.86	13.48	13.30
O, μg O/mL	O-AED	-	500	<100
C, wt%	ASTM D5291	63,8	-	-
SG 60/60°F	ASTM D4052	-	0.8417	0.8562
CCI	ASTM D4737		59.5	48.4
Aromatics				
Mono	ASTM D6591	-	23.7	17.0
Di		-	3.2	1.69
Tri		-	1.28	3.3
Simulated Distillation				
0.5 wt% (IBP), °C	ASTM D7213	89	81	83
5 wt%, °C		161	207	153
10 wt%, °C		200	235	178
15 wt%, °C		218	252	210
20 wt%, °C		238	261	232
30 wt%, °C		260	273	262
40 wt%, °C		292	288	279
50 wt%, °C		315	302	296
60 wt%, °C		354	316	315
70 wt%,°C		377	332	333
80 wt%, °C		407	354	359
85 wt%, °C		425	366	376
90 wt%, °C		448	380	398
95 wt%. °C		490	399	441
99.5 wt% (FBP), °C		570	431	589
Calculated D86				
0.5 vol%, °C	ASTM D7213	160	189	154
5 vol%, °C		206	240	187
10 vol%, °C		224	255	213
20 vol%, °C		247	268	242
30 vol%, °C		271	280	264
50 vol%, °C		313	297	292
70 vol%, °C		363	322	323
80 vol%, °C		388	336	344
90 vol%, °C		426	357	380
95 vol%, °C		461	374	415
99.5 vol%,°C		482	384	451

Detailed analysis was performed on the organic phase of the first two samples and the results can be seen in Table 42. The simulated distillation curves for the feed along with the product samples are shown in Figure 78. As expected the product obtained from the test is very

good. Around 85-90 wt% of the samples is in the diesel boiling range and SG and CCI are very close to fulfilling the EN 590 standards.

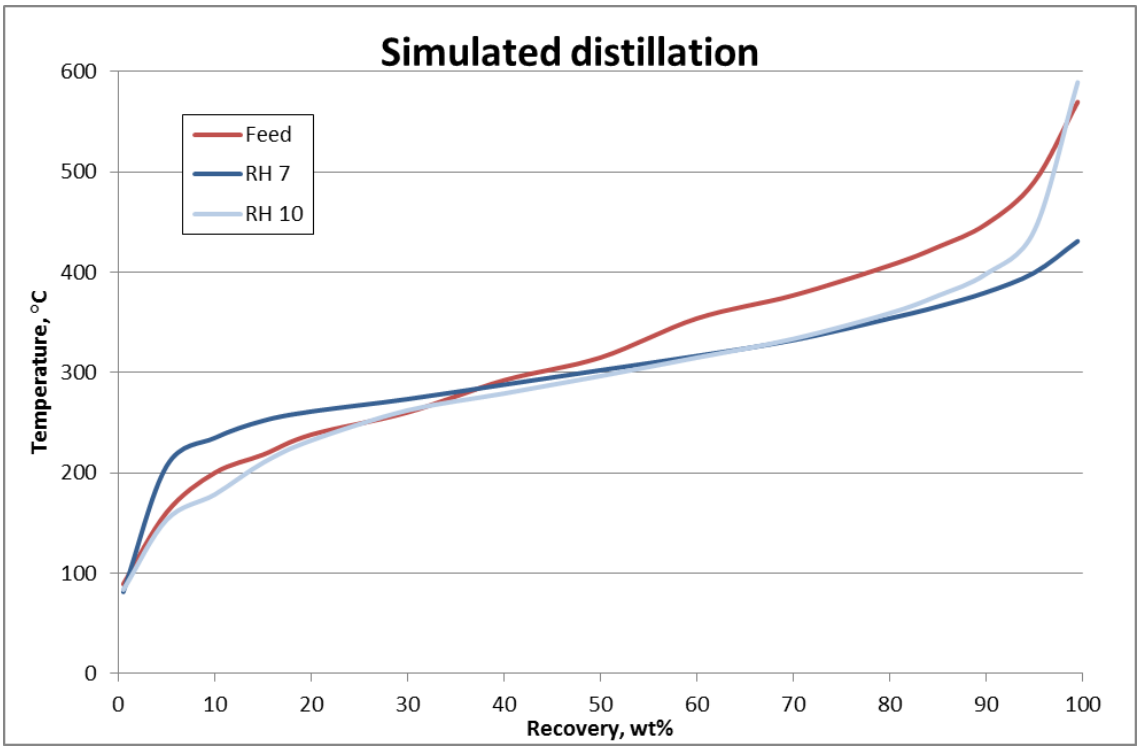

Figure 78: Simulated distillation curves for the pyrolysis feed and the two product samples taken during FKT 1863.

Co-processing of partially hydrotreated bio-crude from catalytic fast pyrolysis for production of renewable diesel

The purpose of the test was to investigate the opportunity of integrating bio-crudes form RTI into an existing refinery and investigate the impact on the refinery operation. Bio crudes produced in RTI's 1TPD unit were immiscible with any standard refinery feedstock. The high polarity may be due to the high concentration of oxygen-containing compounds. The bio crudes typically contain 20-25 %wt oxygen. Therefore, in order to make the bio crudes miscible with fossil feed-stock, a first hydrotreating step was carried out, at RTI, on the bio crude to obtain partially hydrotreated bio crudes with oxygen concentrations in the range between 2 - 9 %wt. The partially hydrotreated bio-crudes were readily miscible with a fossil feedstock such as a straight run gas oil. Thus the impact of the bio crude on product yields, product properties, hydrogen consumption and HDS/HDN activity was investigated. Since the bio crude contains many ring structured molecules and high concentrations of nitrogen it was decided to compare co-processing of pretreated bio-crudes and straight run gas oil with co-processing of light cycle oil (LCO) and straight run gas oil. LCO is a product from a fluid catalytic cracking unit which boils in the diesel range. The goal is to produce an ultra-low sulfur diesel (ULSD) in the pilot experiments.

The pilot plant test was carried out in an isothermal test unit using fresh once-through hydrogen. The feed used in the pilot plant test was partially hydrotreated biocrude mixed with straight run gas oil. The detailed feedstock properties, before blending, can be found in Table 43 and the properties of the blended feedstock can be found Table 44.

The two different LCO's used for blending were chosen in order to have similar nitrogen content as the different CPO's. LC1 was chosen to match the nitrogen content of CPO1 while LC2 was chosen in order to match the nitrogen content of CPO's 2 and 3. The reason why the nitrogen content of the tested feedstock should be similar is that nitrogen is a powerful inhibitor for HDS when using NiMo hydrotreating catalyst. Thus, in order to make a fair assessment of the impact on HDS activity when hydrotreating CPO and LCO the feed stock should have similar nitrogen content.

The catalyst loading used in the pilot plant test was 20% TK-341 and 80% NiMo hydrotreating catalyst. The catalyst TK-341 is developed for fixed bed HDO service while the NiMo hydrotreating catalyst is an active HDS and HDN catalyst. The HDO catalysts are typically loaded in a stacked bed where the activity of the catalyst increases towards the bottom of the bed. This is done to distribute the exotherm in the reactor. The catalyst was diluted with 40% carborundum. The test conditions used during the pilot plant test were:

- PH_2 = 70 barg
- H_2/oil = 625 NL/L
- T (R1) = 330 - 345°C
- LHSV= 0.4 h^{-1}

Table 43. Properties of the pure feeds used for the pilot plant test

Property	Method	LG	LC1	LC2	CPO1	CPO2	CPO3
C, wt %[1]	ASTM D 5291	85.35	88.14	89.72	84.9	82.3	82.1
H, wt %	ASTM D 7171	13.41	10.63	9.60	11.60	10.26	9.76
O, wt %	ASTM D 5291	-	-	-	2.23	6.33	8.44
S, wt %	ASTM D 7212	1.23	1.18	0.563	0.003	-	0.007
N, wt ppm	ASTM D 4629	87.9	536	1156	607	950	1431
SG	ASTM D 4052	0.8379	0.9194	0.9543	0.9104	0.9683	0.9985
Carbon Residue	ASTM D 4530	-	-	-	0.793	0.492	3.191
Aromatics[2]	ASTM D 6591						
1 ring, wt %		15.48	22.07	17.94	-	-	-
2 ring, wt %		9.07	27.38	42.77	-	-	-
3+ ring, wt %		1.13	8.76	11.59	-	-	-
Simulated Distillation	ASTM D 7213						
0.5 wt% (IBP), °C		115	117	130	67	71	69
5 wt %, °C		178	173	203	79	118	94
10 wt %, °C		204	199	221	102	154	152
50 wt %, °C		288	272	272	257	288	304
90 wt %, °C		367	357	338	466	482	497
95 wt %, °C		384	371	353	527	534	545
99.5 wt % (FBP), °C		415	398	398	605	596	605

[1]Measured by difference for the fossil based feedstock

[2]Not measured for the pre-treated catalytic fast pyrolysis oil since oxygenates always are recognized as 3+ ring aromatics

Table 44. Properties of the blended feeds used for the pilot plant test

Property	Method	30/70 LC1/LG	30/70 LC2/LG	30/70 CPO1/LG	30/70 CPO2/LG	30/70 CPO3/LG
H, wt %	ASTM D 7171	12.46	12.14	12.80	12.58	12.31
O, wt %	ASTM D 5291	-	-	1.26	1.84	2.47
S, wt %	ASTM D 7212	1.19	1.00	0.828	0.903	0.717
N, wt ppm	ASTM D 4629	213	433	258	327	377
SG	ASTM D 4052	0.863	0.873	0.861	0.867	0.882
Simulated Distillation	ASTM D 7213					
0.5 wt% (IBP), °C		116	116	79	86	91
5 wt %, °C		178	185	142	156	162
10 wt %, °C		203	210	172	187	190
50 wt %, °C		283	282	284	288	290
90 wt %, °C		363	357	383	381	388
95 wt %, °C		380	376	422	411	432
99.5 wt % (FBP), °C		413	413	557	567	581

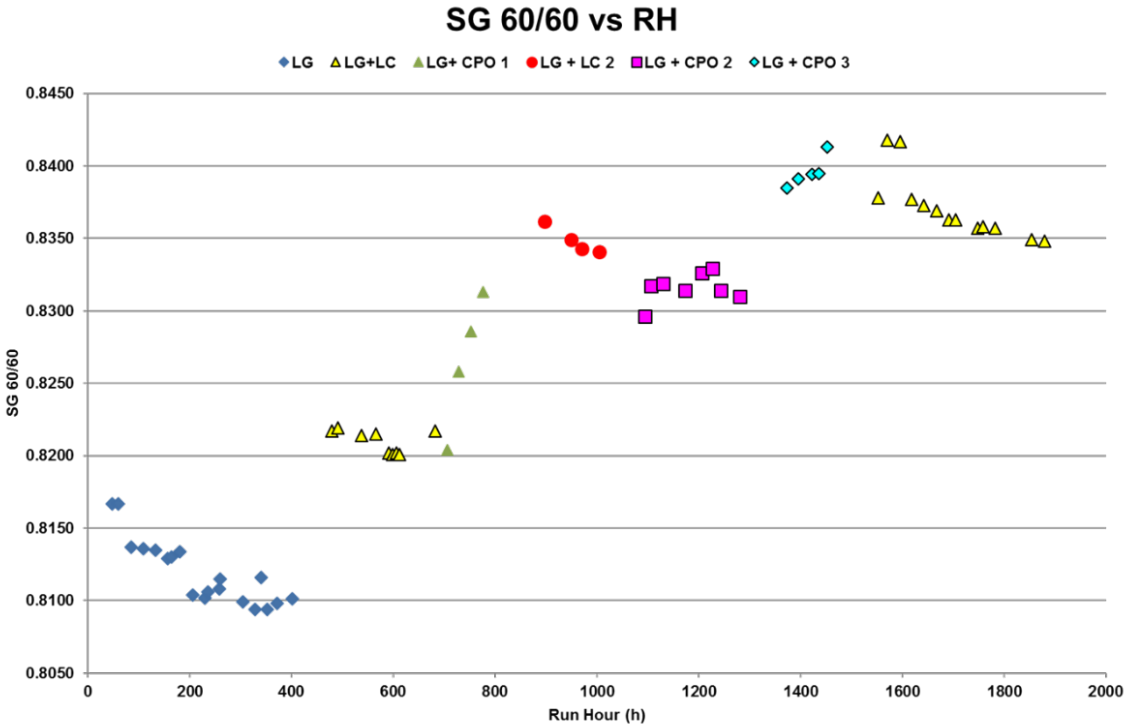

Figure 79: Specific gravity of the organic fraction of the total liquid product as a function of run hours

The pilot test ran for 1880 hours, processing five different feedstock. During the test no problems were encountered with regards to increase in pressure drop over the reactor. This indicates that pressure drop would not be a major concern if the process was implemented industrially. In Figure 79 the specific gravity (SG) of the organic fraction of the liquid product is plotted as a function of run hour. Comparing the SG measured the first and the second time when running 30/70 LC1/LG (yellow triangles). it is clear that some deactivation of the catalyst has

taken place. SG of the liquid product is a good way to measure the hydrogenation activity of the catalysts since a highly hydrogenated product will have a low SG. Comparison of the hydrogen measured in the two products, 14.18 %wt and 13.61 %wt respectively, show the same trend. Based on experience with hydrotreating fossil feedstock using the same pilot unit under similar operating conditions the deactivation seen in this test is on par with what is expected.

Based on the plot in Figure 79 it's clear that line out was not reached when processing 30/70 CPO1/LG (green triangles), but for the other feeds and conditions lineout appears to have been reached. In Table 45 test conditions including hydrogen consumption and yield structure of the product along with properties of the total liquid product (TLP) after hydrotreating are presented. Detailed results for the blend 30/70 LCO3/LG (red circles) have been omitted since the liquid flow during that condition was not stable and mass balance measured was poor. It should be highlighted that for all feeds except 30/70 CPO3/LG a condition where the sulfur concentration in the product was below 20 wt ppm was carried out. The reason why 30/70 CPO3/LG did not have low sulfur in the product was that the reactor temperature was set low to get a significant concentration of oxygenates in the product. This was done to investigate the most refractory oxygen compounds. The remaining oxygen compounds are mainly phenolics and dibenzofurans.

Examination of the results presented in Table 45 show that when changing from 30/70 LC1/LG to 30/70 CPO1/LG the sulfur concentration in the product is similar, while for 30/70 CPO2/LG the temperature has to be increased by 15°C to 345°C in order to get a similar sulfur concentration in the product. There are probably two explanations for this. The first is that line out was not reached when running 30/70 CPO1/LG, thus at lineout the sulfur concentration would be slightly higher, the second is that 30/70 CPO2/LG contains more nitrogen which is inhibiting HDS. But the results clearly show that HDS activity is not heavily affected by introducing the pretreated CPO compared to LCO.

Hydrogen consumption, gas- and naphtha yields are comparable when hydrotreating the LCO and pre-treated CPO's blended with LG, while the diesel yield is significantly lower, approximately 6 percentage points, when hydrotreating a pre-treated CPO blended with LG. The main part of diesel lost is to water and to the 390°C+ fraction of the organic liquid product. In Figure 80 the yield structure of the organic gas and liquid products are presented.

When hydrotreating a pretreated CPO blended with a straight run diesel and comparing to a feed stock with the same amount of LCO blended with the same straight run diesel the following conclusions can be drawn from the conducted pilot tests:

- No additional pressure drop is caused by the pretreated CPO
- The HDS activity is not negatively affected when compared to a feed stock with a similar nitrogen concentration
- The yield of diesel produced is approximately 6 percentage points lower, partly due to the oxygen in the feedstock and partly due to a light and a heavy part in the CPO which does not fall into the diesel range
- The hydrogen consumption is lower for the pretreated CPO compared to the LCO

Two clear challenges for the proposed process is that the CPO has to be pre-treated in order to be miscible with a fossil feedstock and the yields of liquids in the fuel boiling range are low compared to hydrotreater where a typical LCO is treated blended with a straight run gas oil. Furthermore, due to the oxygenates in the feedstock and the CO_2 produced the material selection in the refinery may have to be revisited.

Table 45. Test conditions including hydrogen consumption and yield structure of the product along with properties of the TLP after hydrotreating.

Feed		LG	30/70 LC1/LG	30/70 CPO1/LG	30/70 CPO2/LG	30/70 CPO2/LG	30/70 CPO3/LG
Temperature	°C	325	330	330	334	345	330
LHSV	h^{-1}	0.5	0.4	0.4	0.4	0.4	0.4
H_2/oil	NL/L	625	625	625	625	625	625
Hydrogen Pressure	barg	70	70	70	70	70	70
SG, ASTM D4052		0.810	0.820	0.829	0.833	0.831	0.840
H, ATSM D7171	% wt	14.47	14.18	13.96	13.76	13.73	13.49
S, ASTM D5453	wt ppm	13	16	18	35	18	130
N, ASTM D4629	wt ppm	1	1	1	4	2	12
Oxygen	wt ppm	-	-	-	5	2	200
H_2 consumption	NL/L	106	186	125	123	124	128
Yield C1 - C4	wt % feed	0.49	0.66	0.54	0.40	0.44	0.94
Yield C5 - 150°C	wt % feed	4.46	6.16	8.32	7.03	7.34	5.18
Yield 157 - 390°C	wt % feed	92.30	91.75	85.20	85.50	85.82	84.74
Yield 390°C+		2.57	2.08	5.17	5.44	4.74	6.81
Yield water	wt % feed	-	-	1.4	2.1	2.1	2.8
Yield CO	wt % feed	-	-	0	0	0	0
Yield CO_2	wt % feed	-	-	0.03	0.02	0.01	0.03

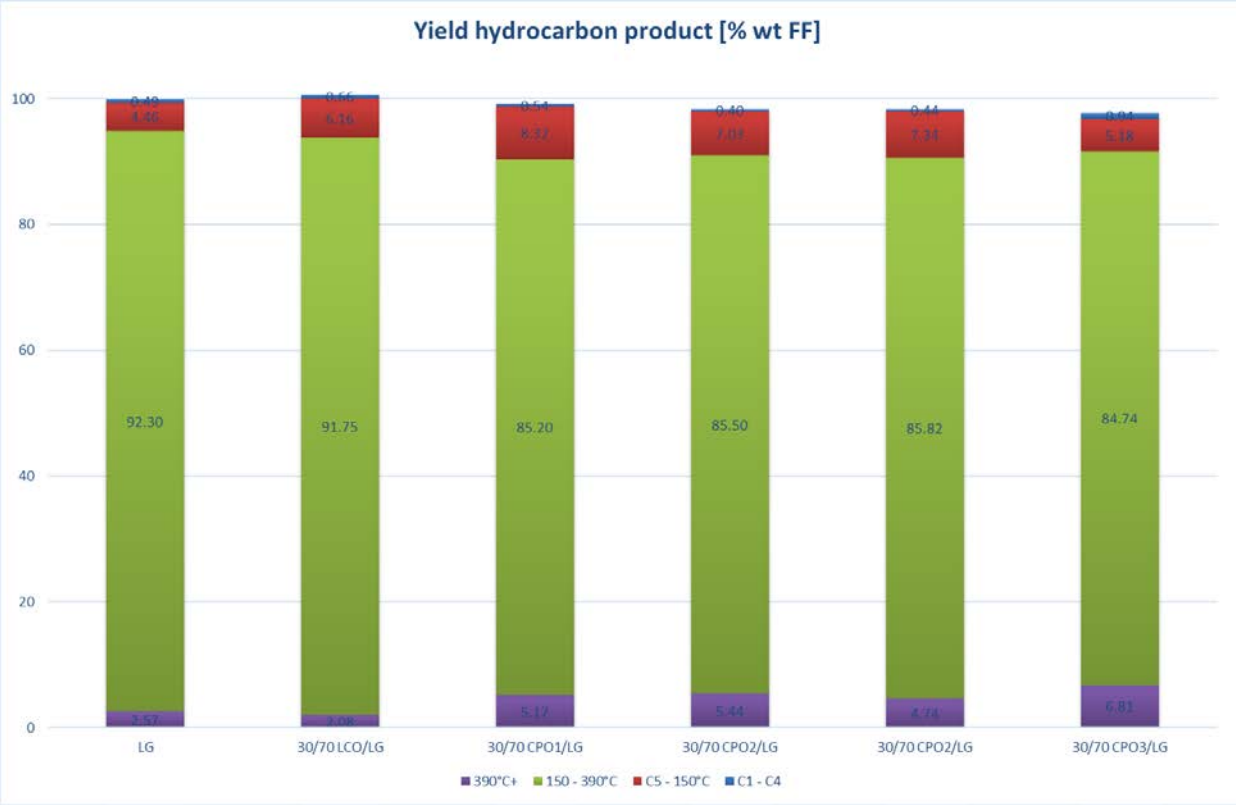

Figure 80: Yield structure of the organic fraction of the product in the pilot test

Techno-economic Analysis

In 2011, a technical and economic analysis was performed for this process designed for 2000 dry tons per day of biomass. This preliminary process model was developed based on a scale up of the experimental results in which white oak was used as the feedstock. The previously developed process model and economic analysis were updated with scaled up results from the pilot-scale 1 tonne/day (1TPD) catalytic biomass pyrolysis system at RTI. The updated process model is based on the results from the 1 TPD unit operating with Loblolly Pine as the feedstock. The previously developed process model was based on using white oak as the feed stock. This model was updated with the feed stock characteristics of Loblolly pine and product yields calculated from the pilot plant data. The ultimate analysis of White Oak and Loblolly pine are given in Table 46.

The process model consists of seven integrated sections: feed preparation (wood yard and wood drying and storage), catalytic biomass pyrolysis (reactor and regenerator), quench system, hydrogen production (production, purification, and compression), hydrotreating, and balance of plant. Detailed process flow diagrams were developed for each of these sections to determine material and energy balances, as well as a comprehensive equipment list to estimate capital costs.

Table 46. Feedstock Elemental Analyses

	White Oak	Loblolly Pine
	Wt%, dry basis	Wt%, dry basis
Carbon	49.82	46
Hydrogen	5.86	6
Oxygen	43.81	47
Nitrogen	0.10	0.5
Sulfur	0.01	0.027
Ash	0.39	0.6

The feed preparation section was designed to process both logs and chips. All biomass materials are size reduced to 0.5-in top size. The moisture content of as received biomass (both logs and chips) was assumed to be 50wt%. Biomass is dried to a moisture content of 10wt% and the moisture leaves the dryer as steam at 50 psia and is used for steam reforming, water gas shift and regeneration of rich solvent in an amine plant. The dried biomass is stored in a dry chip day bin sized for 2 days capacity.

A circulating fluidized bed reactor is used for catalytic pyrolysis of biomass. Biomass chips are mixed with hot, regenerated catalyst in the mixing zone that is fluidized with recycled pyrolysis product at 65 psia. Hot catalyst enters the mixing zone at 700°C and heats biomass up to 470°C and also supplies the heat required for pyrolysis reaction. For every ton of biomass fed, 10 tons of catalyst are circulated to supply enough heat and catalytic activity. The product yields used in the model were determined from the component yields from the 1 TPD pilot plant data. The material balances of the gas, liquid and solids productions and the composition of the product streams were used as input into the process model. Based on the product yield determined from scaling up the pilot plant results, 70 gallons of crude bio-oil was produced for every 1 dry-ton of biomass entering the pyrolysis unit. A summary of product yields and compositions of the original (2011) and the updated (2015) studies are listed in Table 47.

The pyrolysis product vapors and gases are cooled to recover bio-crude and extract energy. A two-stage product cooling philosophy is used. In the first heat exchanger, pyrolysis product

vapors are cooled down to 132°C by pre-heating boiler feed water (used in regenerator to produce steam). Pyrolysis product vapors are then sent to a spray column where circulating cooling liquid is used to cool the products down to 39°C. Approximately 80wt% of bio-oil is condensed in this step. Circulating cooling water, condensed bio-oil and water from pyrolysis product stream leave the spray column bottom. A portion of this liquid stream is used as cooling liquid in spray column and is cooled to 32°C using cooling water. The objective of the spray column is to cool the product vapors down to 38°C and coalesce aerosol droplets. The cooled pyrolysis product gas from the spray column is sent to an electrostatic precipitator (ESP) where it is assumed that the rest of the bio-crude and water are removed. Liquid streams from the spray column and ESP are combined and sent to a decanter vessel. The bio-oil separates from water by gravity and accumulates at the bottom of the decanter vessel. Water, which forms the top liquid fraction, is sent to wastewater treatment plant and bio-oil is sent to the hydrotreating section. Product gases from the ESP are sent to hydrogen production section.

The collected bio-crude contains 25 wt% of oxygen and the H:C ratio in bio-oil is 1.15. Thus, hydrotreating is used to remove oxygen from bio-crude and upgrade the H:C ratio to 2.1, similar to gasoline. It is assumed that all the oxygen in bio-crude can be removed during one-step hydrotreating resulting in production of gasoline which does not require additional upgrading or conditioning. The hydrotreater is operated at 740 psia and 350°C with a space velocity of 1.5 hr^{-1}.

Table 47. Product Yields and Compositions

	White Oak (2011)	Loblolly Pine (2015)
Material Balances (wt% biomass, dry basis)		
Bio-oil	29.2	19.2
Water	12.2	34.8
Gases	39.2	35.1
Char	13.9	7.7
Coke	5.6	3.2
Bio-crude properties		
water content	10 wt%	14.4 wt%
Specific gravity @ 25°C	1.1	0.82
Elemental Composition (wt%, dry)		
C	70.63	67.82
H	6.76	6.59
O	22.61	24.86
Pyrolysis gas composition (vol%)		
H_2	24.9	3.6
CO	23.5	22.8
CO_2	39.9	63.9
CH_4	8.6	5.9
C_2+	3.1	3.8

Hydrogen required for hydrotreating is produced by steam reforming the pyrolysis product gas. About 45% of the pyrolysis product gas from the ESP is recycled back as fluidization gas in pyrolysis reactor mixing zone, the remaining 55% of the gas is used for hydrogen production and methane is added to meet the overall hydrogen demand. This stream is first preheated to 746°F using steam generated in the regenerator. The stream reforming unit operates adiabatically where

70% methane conversion is achieved. The reformer outlet gas is mixed with steam from biomass dryer and is sent to shift reactor where 90% CO conversion is assumed. The shifted, hydrogen rich gas containing H_2 and CO_2 is sent to an amine plant where 95% of CO_2 is removed. The enriched hydrogen stream is then compressed to 765 psi in a 6-stage compressor with 5 intercoolers. Gas leaving the final compression stage is not cooled as it is to be heated prior to entering the hydrotreater. Concentration of hydrogen in the compressed stream is 87.5%.

The balance of plant includes the utilities required for the plant. Cooling water is made available at 80°F and 65 psia. The evaporative losses in the cooling tower and cooling water blowdown are matched by make-up cooling water at a rate of 30,559 gallons/hr. Steam is generated in the plant using boiler feed water at 1000 psia. After using it for heating, steam from high pressure header is expanded in a multi-stage turbine. About 89,000 lb/hr of steam at 400 psia and 526°F is removed from the turbine and is used for biomass drying. The remaining steam is further expanded down to 0.2 psia. During this process, the steam turbine generates 3 MW electricity. However, approximately 12 MW electricity is required to operate all the electrically powered equipment (chipper, compressors, blowers, pumps, ESP) so electricity is imported.

Wastewater is generated in the plant downstream of pyrolysis reactor, hydrotreater, shift reactor, amine plant steam condensate and during hydrogen compression. The total wastewater flow is 560 gpm.

Natural gas is used to operate process and gasoline loading flare. It is also used to make-up fuel demand in the thermal oxidizer used to heat steam reformer gas and steam mixture. The total natural gas demand is 60 MMBtu/hr.

Economic Analysis of Catalytic Biomass Pyrolysis Process

Heat and material balance data generated from Aspen Plus simulations were used for equipment sizing and equipment costs were estimated using Aspen Icarus. Installed costs were estimated using equipment type specific installation factors from industrial experience. The capital cost comparison is summarized in Table 48. The cost basis in the 2011 study was 2010 USD, while in the recent study, all the values are in 2014 USD. The capital cost in the recent study was estimated to be ~10% higher than the previous estimate.

The total installed cost of the plant for both the studies is almost twice that of the total equipment cost. Installed cost distribution includes: Equipment cost (51.1%); Electrical (12.0%); Piping (11.6%); I&C (6.0%); Civil (5.6%); Spares (3.4%); and Steel (2.6%).

The final project cost is calculated by including costs for engineering, permits, commissioning, contingencies, etc. These costs were estimated using factors generally accepted in industry and include: Contingencies (24.4%); Engineering (12.0%); Home office (3.8%); Commissioning (3.0%); Escalation (3.0%); Construction Management (2.8%); and First Fills, Insurance, Permits (2.9%). The total project cost is approximately $410,112,116.

The debt term for the project is assumed to be 20 years. This gives us an annualized capital cost of $22,667,958. It is assumed that 60% of the capital cost is leveraged and the total financed debt for the 2015 study is $ 282,423,565. Assuming the debt is made available at an interest rate of 7.5% paid over the debt term of 20 years, monthly payments on loan are $2,275,185.

The gasoline production rates and yields based on the earlier and the updated process analyses are presented in Table 48. A plant capacity factor of 80% for the first year, 85% for the second year, 90% for the third year and 95% for the rest of the 20 year term was assumed. Thus, the annualized gasoline production rate, an average of gasoline production rate over the 20 year term of plant, is 1,359,618 barrels per year.

Table 48. Summary of Economic Analysis of Catalytic Biomass Pyrolysis

	2011 Estimate white oak feedstock, $2010	**2015 Estimate loblolly pine feedstock, $2014**
Total Equipment Cost	$ 152,010,973	$ 165,007,124
Total Installed Cost	$ 298,550,400	$ 310,399,299
Final Project Cost	$ 410,112,116	$470,705,942
Gasoline Production (bbl/day)	3,985	3,791
Gasoline yield (gal/dry-ton biomass)	83.6	79.6

The plant operating expenses include biomass feedstock, make-up catalyst, waste (ash and wastewater) disposal, utilities (electricity, natural gas, make-up water, etc.), operating expenditure (maintenance, insurance, property tax, etc.) and personnel (wages, etc.). A summary of the flows, costs and expenses of these individual items is given in

Table 49. All the parameters are annualized which is an average over the 20-year plant term. Natural gas and electricity pricing forecast was obtained from US Energy Information Administration's (EIA) energy outlook. Make-up cooling and boiler feed water cost estimates are derived from industrial experience. Catalyst costs are assumed to be $15,000/ton (for comparison, price of fresh FCC catalyst is $3,000/ton). Catalyst loss rate for FCC material is usually around 50 lb/MMlb-circulated. A conservative make-up catalyst demand of 100 lb/MMlb-circulated was used in the model.

In addition to the operating expenses, the total annual cost also includes the payments made on loan and annualized capital cost. The annual payment on loan is $27,302,220 whereas the annualized capital cost is $25,902,816. Thus, the total annual cost is $145,817,456/yr resulting in a production cost of $2.68/gal of gasoline.

The annualized gasoline production rate, over the 20 year term of plant, is 1,294,565 barrels per year. To keep the comparison between the two studies on the same basis, production tax credit of $0.45/gal and blender credit of $0.46/gal were used. Thus, the total government subsidy was $1.01/gal. The IRR was calculated pre-tax and pre-depreciation and is estimated to be 16.6%. While the return is not promising, the analysis highlights the factors that have the most impact on the process economics. The relative importance of five different variables towards the IRR was studied using tornado diagram. It also indicates the parameters towards which the IRR is most sensitive. The tornado plot in Figure 81 clearly shows that gasoline price/ subsidy for biofuel production has the most impact on the process economics.

As shown in the previous study, it still holds true that a decrease of $1/gal in either the gasoline price or government subsidy decreases the IRR by ~10% points. However, an increase of $1/gal improves the profitability of the project by increasing the IRR by ~8% points. The next most sensitive variable is the capital cost investment. If the capital cost estimate is $100MM higher than anticipated, the IRR decreases from 16.6% to 12.4% whereas if the capital cost estimates are lower by $100MM, IRR increases by 5.7% points. Although feedstock cost is makes up 48% of the operating expenses, IRR is only marginally affected by change in feedstock price as a ±$10/dry ton variation in feedstock price changes the IRR by ±1% points. Similarly, a change in catalyst loss rate of ±50 lb/MMlb-circulated leads to a 0.9% points change in IRR.

Updating the economics and process heat and material balances, changed the return significantly. The previous IRR estimated in 2011 was 20.5 %, while in the updated study, an IRR of 16.6 % was determined. This is a direct result of a lower gasoline yield of 79 gal

gasoline/dry-ton of biomass compared to the 83.6 gal/dry-ton previously considered. However, gasoline price /subsidy on fuel production can change the economics significantly. As shown earlier, even a $1/gal increase in gasoline price or a subsidy of $1/gal of fuel produced yields a return of ~25%, which is very promising.

As shown in the previous study, it still holds true that a decrease of $1/gal in either the gasoline price or government subsidy decreases the IRR by ~10% points. However, an increase of $1/gal improves the profitability of the project by increasing the IRR by ~8% points. The next most sensitive variable is the capital cost investment. If the capital cost estimate is $100MM higher than anticipated, the IRR decreases from 16.6% to 12.4% whereas if the capital cost estimates are lower by $100MM, IRR increases by 5.7% points. Although feedstock cost is makes up 48% of the operating expenses, IRR is only marginally affected by change in feedstock price as a ±$10/dry ton variation in feedstock price changes the IRR by ±1% points. Similarly, a change in catalyst loss rate of ±50 lb/MMlb-circulated leads to a 0.9% points change in IRR.

Updating the economics and process heat and material balances, changed the return significantly. The previous IRR estimated in 2011 was 20.5 %, while in the updated study, an IRR of 16.6 % was determined. This is a direct result of a lower gasoline yield of 79 gal gasoline/dry-ton of biomass compared to the 83.6 gal/dry-ton previously considered. However, gasoline price /subsidy on fuel production can change the economics significantly. As shown earlier, even a $1/gal increase in gasoline price or a subsidy of $1/gal of fuel produced yields a return of ~25%, which is very promising.

Table 49. Summary of items included in production cost

			2011 Study		2015 Study	
	Unit	Annualized cost, $/unit	Annualized demand, units/yr	Annualized cost, $/yr	Annualized demand, units/yr	Annualized cost, $/yr
Biomass	dry tons	$65	682,550	$44,365,750	682,550	$44,365,750
Make-up catalyst	ton	$15,000	758	$11,375,832	758	$11,375,832
Electricity	kWh	$0.06	68,844,139	$4,130,648	70,476,828	$4,228,610
Ash disposal	ton	$25.00	159,719	$3,992,979	6,349	$158,736
Wastewater disposal	gal	$ 0.01	275,752,042	$2,894,535	275,843,027	$2,758,430
Natural gas	MMBtu	$5.25	491,436	$2,587,753	490,648	$2,575,900
Make-up cooling water	gal	$0.01	186,731,663	$259,529	250,427,449	$250,427
Make-up boiler feed water	gal	$0.02	3,456,344	$72,569	2,419,441	$48,389
Operating expenditure				$15,066,834		$18,603,331
Personnel				$7,835,873		$8,247,014
Total annualized operating expenses				$92,582,302		$92,612,419

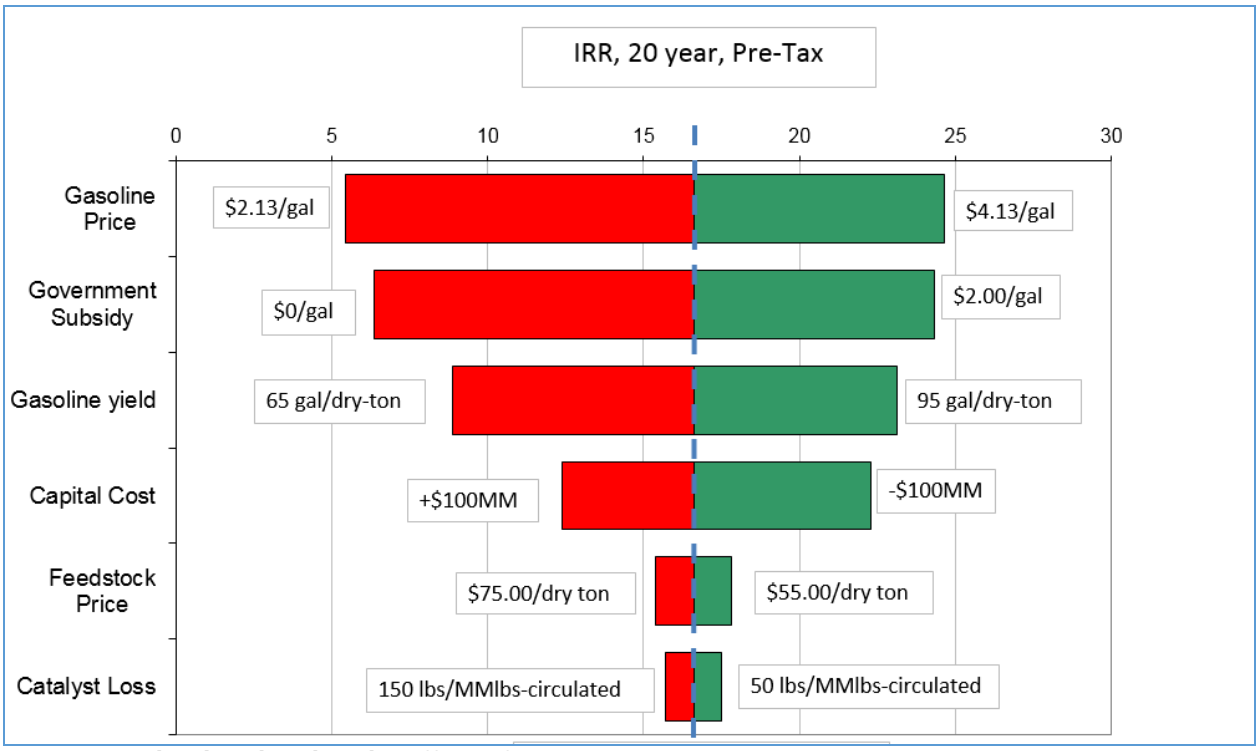

Figure 81: Tornado plot showing the effect of parameters on IRR

Summary

The goal of this project was to demonstrate a technology that integrates catalytic biomass pyrolysis with hydroprocessing to produce advanced hydrocarbon biofuels. The technical goals are to optimize the catalytic biomass pyrolysis process to produce a low oxygen-content, thermally-stable bio-crude intermediate and evaluate the impact of bio-crude quality on the hydroprocessing step.

A novel single-step catalytic biomass pyrolysis process to produce a hydrocarbon-rich bio-crude intermediate was developed. The design, construction, and commissioning of the 1 TPD catalytic biomass pyrolysis unit was completed in a previous DOE/ARPA-E funded project. As a continuation, this project supported the operation of the unit. Early experiments were hampered by fouling of a heat exchanger that was originally installed directly downstream of the spray quench. This design was not suitable for long-term operation so a new design was developed and modifications were implemented. The quench system modifications that are still in use today significantly improved system operability and led to the operational success of the unit.

Obtaining pilot-scale quantities of catalyst and feedstock posed a challenge for the project. Fortunately, sources of both catalyst and feedstock that met the needs of the project were identified. Feedstock was available from a previous DOE/BETO project (the National Advanced Bioenergy Consortium - NABC) and Idaho National Laboratory (INL) became a project partner after the first Go/No-Go decision point to provide additional feedstocks. Four tons of ground hybrid poplar were provided by INL; however, it did not successfully feed in the system. The bulk density was too low and the material bridged in the lower section of the feeder. Additioanl samples of prepared feedstocks were provided but the INL pilot-scale feedstock preparation unit proved too inflexible to significantly alter the physical properties of prepared biomass to be of use to the project. After unsuccessfully getting feedstock from INL, a local provider of loblolly pine sawdust was identified that had materails that was suitable for the 1TPD system. Additional red oak feedstock (3 tons) was procured from Iowa State University, the original source of the NABC feedstcoks that were successfully fed in the 1TPD system.

During the course of this project, different commercially available catalysts such as FCC and non-zeolite alumina catalysts were evaluated. Unfortunately, scaling up the catalyst identified and developed in the previous ARPA-E project proved difficult, but a commercially-available alumina catalyst that was available in sufficient quantities for the 1TPD system. Laboratory testing validated that the performance of the alumina catalyst was comparable to the previously developed catalyst. Bio-crude yield and quality (in terms of oxygen content) measured in laboratory-scale (1” and 3” diameter bubling fluidized bed reactors) systems were reproduced in a 1 TPD process. The reproducibility of the small-scale pyrolysis yields at the 1TPD scale is an achievement worth noting.

Typically, the ITPD unit was operated for 12 hours per experiment; but, extended studies for 20 and 30 hours were performed as well. Each experiment was used to optimize the system to increase operability, collect engineering data, and produce biocrude per the demand of the hydroprocessing studies. Material and carbon balances were typically between 80-100%. Steady-state bio-crude yields varied between 38 and 50 gallons/dry ton of biomass. Moderate temperatures (450 °C ≤ T < 500 °C) favored higher yields. In general, the bio-crude contained aromatic hydrocarbons and phenolic compounds. The deliverable with respect to biocrude production was a total of 75 gallons. A total of 230 gallons of bio-crude was produced for upgrading.

Detailed chemical characterization of bio-crude samples is very challenging due to the presence of many polar and non-volatile species; however, it is required for informing downstream processing to biofuels and biochemicals. Typically, a number of different techniques are used collectively to fully characterize bio-oils, bio-crudes, and upgraded bio-derived fuels and chemicals. In this project, existing and new analytical techniques were used to characterize the biocrudes and upgraded products. Comprehensive two-dimensional GC (GC×GC) was used to characterize phenols and alcohols. Supercritical fluid chromatography (SFC) was also used as a pre-fractionation step to improve the separation in GC×GC for the very complex mixture. In combination with negative electrospray ionization (ESI-) and high resolution mass spectrometry, this is a selective methods for identifying oxygen containing species, particularly hydroxylated and carboxylated compounds. Furthermore, for thermally-labile and/or non-volatile compounds (e.g., with low vapor pressures caused by a high polarity), derivatization was used to enhance GC analysis. Also, fourier transform ion cyclotron resonance mass spectrometry (FT-ICR/MS) is a form of high resolution mass spectrometry that yields great insight to the characterization of complex mixtures by providing a unique combination of ultrahigh resolving power (the ability to resolve mass spectral signals differing by < 1 mDa) and accurate mass determination (determination of molecular masses to ~5 decimal places).

The SFC-MS results showed clear chemical differences between the bio-crude feeds and that tentatively correlated with the oxygen content in the bio-crudes. FT-ICR/MS analysis showed that biocrude samples are enriched in oxygen-containing compounds and that $O_4 – O_6$ heteroatom compounds are present in the greatest relative abundance. Plots of double bond equivalents (DBE) versus carbon number provide useful insight into the structural complexity and trends within a select heteroatom class. Oxygen classes identified ranged from $O_2 – O_{13}$ with very little difference observed between samples. There is an observed increase in the maximum carbon number and DBE values with increasing oxygen content with and ions associated ~50 carbon atoms and DBE values of ~25. Compounds with oxygen numbers greater than ~3 and carbon numbers greater than ~ 30-40 are often times not observed by GC or GC x GC analyses, which lends FT-ICR MS as a complimentary approach to GC x GC MS especially for the molecular analysis of highly aromatic and polar oxygen-containing compounds.

A commercially scaleable hydroprocessing unit was designed, built, commissioned, and operated. This unit was successfully commissioned and system performance was validated by demonstrating hydroprocessing of vacuum gas oil. Haldor Topsøe developed a strategy for upgrading bio-crude intermediates based on extensive hydroprocessing catalyst and process development expertise. They preformed preliminary studies to identify an appropriate catalyst for bio-crude upgrading and to determine process conditions (temperature, pressure, and H_2/bio-crude ratio). A specific hydroprocessing catalyst was selected for bio-crude upgrading. Catalyst dilution strategies for heat management were implemented to maximize time on stream and hydroprocessing performance at selected process conditions. The hydroprocessing studies at RTI built upon these preliminary efforts and resulted in upgrading of pine and oakwood biocrudes for over 1500 hours. Several biocrudes with different oxygen contents and chemical compositions were evaluated at slightly different conditions and as such the hydrotreating performance varied; some runs lasted over 350 hours and others lasted less than 100 hours. For example, very little deactivation was observed over a period of 200 hours of operation for an experiment that was performed at lower space velocity and the oxygen content of the upgraded products collected within the time-on-stram of 165 hours was below 1 wt%. In general, steady state mass balances ranged between 91% and 98% and the carbon balances were from 83% to 98%. The liquid yield

for the HDT products were between 51 and 86 wt% and the liquid carbon recoveries ranged from 55% to 95%. Depending on the bio-crude feedstock, the hydrogen consumption varied between 0.01-0.07 g/g of biocrude; deep deoxygenation to achieve less than 2wt% O in HDT product consumes significant amount of hydrogen. Original upgrading targets for the project were a total of 2000 hours of bio-crude upgrading.

Integrating bio-crudes into an existing refinery and was investigated with the express purpose of defining the impact on the refinery operation. The high concentration of oxygen containing compounds makes bio-crude too polar to be blended with any standard refinery feedstock. A preliminary hydrotreating step can reduce the oxygen content to about 2-9 wt% and make the bio-crude miscible with straight run diesel. Since bio-crude contains a high concentration of aromatic compounds and nitrogen, co-processing partially upgraded bio-crude with straight diesel was compared to hydrotreating light cycle oil (LCO). LCO is a product from a fluid catalytic cracking unit which boils in the diesel range. The goal was to determine the impact of the bio-crude on hydrotreated product yields, product properties, hydrogen consumption and HDS/HDN activity.

No additional pressure drop was measured across the reactor when hydrotreating the partially upgraded bio-crude with a straight run diesel and the HDS activity was not negatively affected by the nitrogen containing compounds in the bio-crude. However, the yield of diesel is approximately 6 percentage points lower, partly due to the oxygen in the feed and partly due to the heavy fraction of the partially upgrade bio-crude that does not fall into the diesel range. The hydrogen consumption for hydrotreating the partially upgraded bio-crude/straight run diesel blend is lower compared to hydrotreating the same amount of LCO blended with straight run diesel. The co-processing studies at Haldor Topsoe were performed for over 1800 hours.

The Bioenergy Technologies Office has a cost target of $3/gallon gasoline equivalent (gge) to produce renewable hydrocarbon fuels from lignocellulosic biomass by 2022. A variety of biomass-to-liquid fuel technologies are being evaluated based on this target. This project specifically evaluated the integration of catalytic fast pyrolysis with hydroprocessing to produce advanced biofuels. The TEA completed in this project modelled a 2000 dry metric ton per day plant. The experimental yields obtained in this work was used in the TEA model. This project assumed the production of finished fuel like other TEAs published for biomass-fuel technology in the literature.

In summary, a lot of activity in this area occurred in the past 10-15 years with notable successes and failures; however, very little technical information is available in the open literature from pilot-scale studies such as those performed in this project. This project showed that it is technically feasible to consistently generate 20% O_2 pyrolysis liquids and that these liquids can be effectively hydrotreated into low oxygen fuel blendstocks. Also, the reproducibility of the small-scale pyrolysis yields at the 1TPD scale is an achievement worth noting. Furthermore, advanced analytical techniques were used to analyze bio-crude, particulary the oxygen-containing compounds. Insights into the impact of oxygen content and oxygen speciation on bio-crdue upgarading were sought. Clearly, more successful upgrading correlated with bio-crudes that had lower oxygen content. This was most evident when partially upgraded bio-crude with 55-90% less oxygen compared to the starting bio-crdue was blended with straight run diesel was hydrotreated without any noticeable increase in pressure drop across the reactor or any measureable loss of hydrodenitrification activity for over 1800 hours. Also, minimizing hydrogen demand while maximizing biofuels yield are the desired outcomes for the integrated process. Nevertheless, several technical challenges remain before catalytic biomass pyrolysis

becomes a commercial reality, most notably bio-crude yields and quality still need to be improved.

References

1. USDOE, *Biomass Multi-Year Program Plan*, D.o. Energy, Editor. 2011: Washington, DC. p. 1-200.
2. Venderbosch, R.H., et al., *Stabilization of biomass-derived pyrolysis oils.* Journal of Chemical Technology and Biotechnology, 2010. **85**(5): p. 674-686.
3. Wildschut, J., et al., *Hydrotreatment of Fast Pyrolysis Oil Using Heterogeneous Noble-Metal Catalysts.* Industrial & Engineering Chemistry Research, 2009. **48**(23): p. 10324-10334.
4. Elliott, D.C., *Historical developments in hydroprocessing bio-oils.* Energy & Fuels, 2007. **21**(3): p. 1792-1815.
5. French, R. and S. Czernik, *Catalytic pyrolysis of biomass for biofuels production.* Fuel Processing Technology, 2010. **91**(1): p. 25-32.
6. Yanik, S., et al., *Biomass Conversion Process*, U.S.P. Office, Editor. 2010, KiOR, Inc.: United States. p. 10.
7. Yanik, S., P. O'Connor, and R. Bartek, *Co-processing Solid Biomass in a Conventional Petroleum Refining Process Unit*, W.I.P. Organization, Editor. 2010, KiOR, Inc.: Unites States. p. 40.
8. Oasmaa, A. and S. Czernik, *Fuel oil quality of biomass pyrolysis oils - State of the art for the end user.* Energy & Fuels, 1999. **13**(4): p. 914-921.
9. Jones, S.B., et al., *Production of Gasoline and Diesel from Biomass via Fast Pyrolysis, Hydrotreating and Hydrocracking: A Design Case", , , operated for Battelle under the U.S. Department of Energy for Contract* 2009, Pacific Northwest National Laboratory: Richland, WA.
10. Marsman, J.H., et al., *Identification and classification of components in flash pyrolysis oil and hydrodeoxygenated oils by two-dimensional gas chromatography and time-of-flight mass spectrometry.* Journal of Chromatography A, 2008. **1188**(1): p. 17-25.
11. Novakova, L., et al., *Modern analytical supercritical fluid chromatography using columns packed with sub-2 mum particles: a tutorial.* Anal Chim Acta,, 2014. **824**: p. 18-35.
12. Holcapek, M., R. and M.L. Jirasko, *Basic rules for the interpretation of atmospheric pressure ionization mass spectra of small molecules.* J Chromatogr A, 2010. **1217**(25): p. 3908-3921.